The

Grand Unified Theory

of

Classical Physics

August 2010

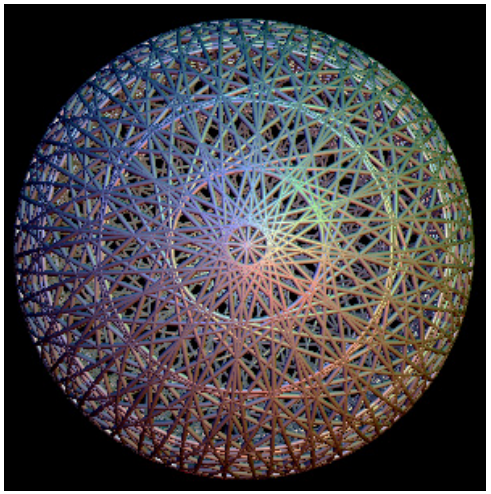

Dr. Randell L. Mills
BlackLight Power, Inc.
493 Old Trenton Road
Cranbury, NJ 08512
609-490-1090
rmills@blacklightpower.com

Part 1:

Atomic Physics

Review of Theory

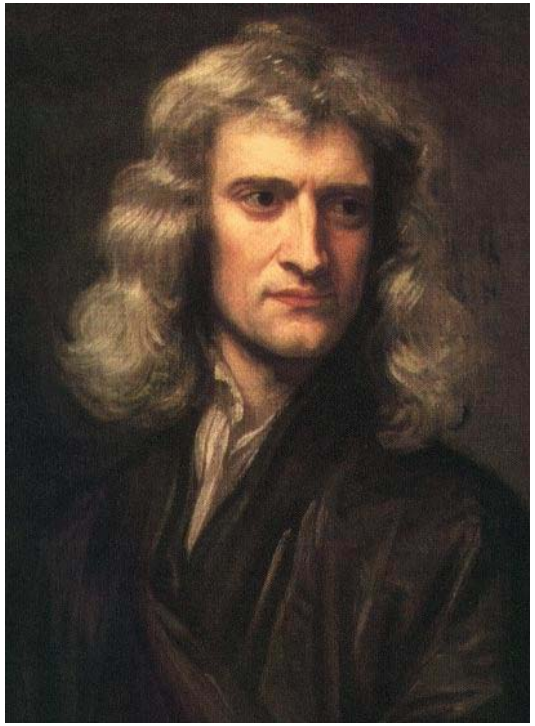

- Assume physical laws apply on all scales including the atomic scale

- Start with first principles
  - Conservation of mass-energy
  - Conservation of linear and angular momentum
  - Maxwell's Equations
  - Newton's Laws
  - Special Relativity

- **Highly predictive**– application of Maxwell's equations precisely predicts hundreds of fundamental spectral observations in exact equations with no adjustable parameters (fundamental constants only).

- In addition to first principles, the only assumptions needed to predict the Universe over 85 orders of magnitude of scale (Quarks to Cosmos):
  - Four-dimensional spacetime
  - The fundamental constants that comprise the fine structure constant
  - Fundamental particles including the photon have $\hbar$ of angular momentum
  - The Newtonian gravitational constant G
  - The spin of the electron neutrino

Electron as a Source Current: Maxwell's Equations Determines Its Structure

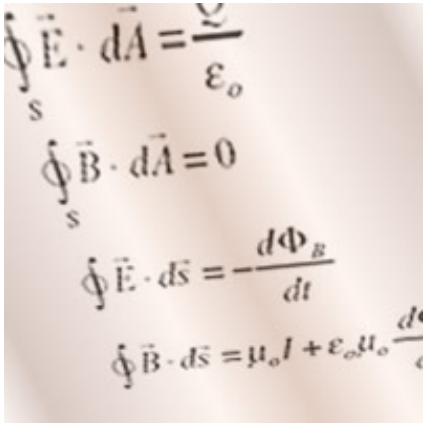

Using Maxwell's equations, the structure of the electron is derived as a boundary-value problem wherein the electron comprises the source current of time-varying electromagnetic fields during transitions with the constraint that the bound $n=1$ *state electron cannot radiate energy.*

Although it is well known that an **accelerated point particle** radiates, an *extended distribution* modeled as a superposition of accelerating charges comprising a current does not have to radiate. The physical boundary condition of nonradiation that was imposed on the bound electron follows from a derivation by Haus.

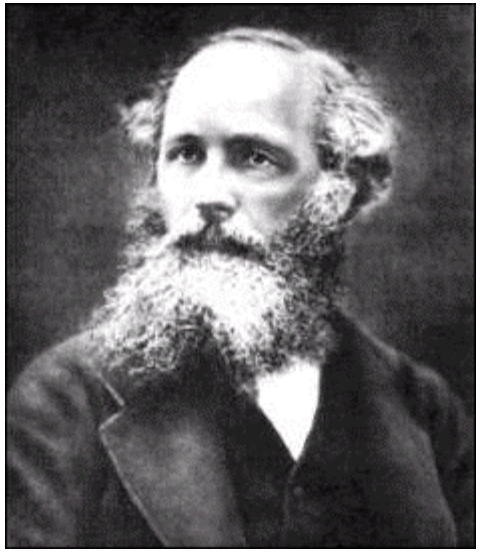

Boundary Constraint Derived from Maxwell's Equations

The function that describes the motion of the electron must not possess spacetime Fourier components that are synchronous with waves traveling at the speed of light. Similarly, nonradiation is demonstrated based on the electron's electromagnetic fields and the Poynting power vector.

H. A. Haus, Am. J. Phys., 54, 1126 (1986)
T. A. Abbott, D. J. Griffiths, Am. J. Phys., 53, 1203 (1985)
G. Goedecke, Phys. Rev. B, 135, 281 (1964)

Generalized Expansion in Vector Spherical Waves for Time-Varying Spherical Electromagnetic Fields for the Electron Transition as the Matching Source Current

The electron is considered a localized source distribution comprising harmonically varying sources of charge $\rho(\mathbf{x})e^{-i\omega t}$, current $\mathbf{J}(\mathbf{x})e^{-i\omega t}$, and intrinsic magnetization $\mathbf{M}(\mathbf{x})e^{-i\omega t}$ for multipole radiation.

Electromagnetic Waves

to solve the electron source current

The Green function $G(\mathbf{x}',\mathbf{x})$ which is appropriate to the equation

$$\left(\nabla^2 + k^2\right) G\left(\mathbf{x}',\mathbf{x}\right) = -\delta\left(\mathbf{x}'-\mathbf{x}\right)$$

in the infinite domain with the spherical wave expansion for the outgoing wave Green function is

$$G\left(\mathbf{x}',\mathbf{x}\right) = \frac{e^{-ik\left|\mathbf{x}-\mathbf{x}'\right|}}{4\pi\left|\mathbf{x}-\mathbf{x}'\right|} = ik\sum_{\ell=0}^{\infty} j_\ell\left(kr_<\right) h_\ell^{(1)}\left(kr_>\right) \sum_{m=-\ell}^{\ell} Y_{\ell,m}^*\left(\theta',\phi'\right) Y_{\ell,m}\left(\theta,\phi\right)$$

Electron Multipole Electromagnetic Fields

The general multipole field solution to Maxwell's equations in a source-free region of empty space with the assumption of a time dependence $e^{i\omega t}$ is

$$\mathbf{B} = \sum_{\ell,m} \left[a_E(\ell,m) f_\ell(kr) \mathbf{X}_{\ell,m} - \frac{i}{k} a_M(\ell,m) \nabla \times g_\ell(kr) \mathbf{X}_{\ell,m} \right]$$

$$\mathbf{E} = \sum_{\ell,m} \left[\frac{i}{k} a_E(\ell,m) \nabla \times f_\ell(kr) \mathbf{X}_{\ell,m} + a_M(\ell,m) g_\ell(kr) \mathbf{X}_{\ell,m} \right]$$

$\mathbf{X}_{\ell,m}$ is the vector spherical harmonic defined by

$$\mathbf{X}_{\ell,m}(\theta,\phi) = \frac{1}{\sqrt{\ell(\ell+1)}} \mathbf{L} Y_{\ell,m}(\theta,\phi)$$

where

$$\mathbf{L} = \frac{1}{i}(\mathbf{r} \times \nabla)$$

Electron Multipole Electromagnetic Fields

The electric and magnetic coefficients $a_E(\ell,m)$ and $a_M(\ell,m)$ specify the amounts of electric (ℓ,m) multipole and magnetic (ℓ,m) multipole fields, and are determined by sources and boundary conditions as are the relative proportions:

$$a_E(\ell,m)=\frac{4\pi k^2}{i\sqrt{\ell(\ell+1)}}\int Y_\ell^{m*}\left\{\rho\frac{\partial}{\partial r}\left[rj_\ell(kr)\right]+\frac{ik}{c}(\mathbf{r}\cdot\mathbf{J})j_\ell(kr)-ik\nabla\cdot(r\times\boldsymbol{M})j_\ell(kr)\right\}d^3x$$

and

$$a_M(\ell,m)=\frac{-4\pi k^2}{\sqrt{\ell(\ell+1)}}\int j_\ell(kr)Y_\ell^{m*}\mathbf{L}\cdot\left(\frac{\mathbf{J}}{c}+\nabla\times\boldsymbol{M}\right)d^3x$$

Additional Boundary Conditions Give the Constant Two-Dimensional Current $Y_0^0(\theta,\phi)$ Corresponding to Spin

The potential energy, $V(\mathbf{r})$, is an inverse-radius-squared relationship given by Gauss' law which for a point charge or a two-dimensional spherical shell at a distance r from the nucleus the potential is

$$V(r)=-\frac{e^2}{4\pi\varepsilon_0 r}$$

Thus, consideration of conservation of energy would require that the electron radius must be fixed.

Addition constraints requiring a two-dimensional source current of fixed radius are matching the delta function of the equation operating on the Green with no singularity, no time dependence and consequently no radiation, absence of self-interaction, and exact electroneutrality of the hydrogen atom wherein the electric field is given by

$$\mathbf{n}\bullet\left(\mathbf{E}_1-\mathbf{E}_2\right)=\frac{\sigma_s}{\varepsilon_0}$$

where $\mathbf{n}$ is the normal unit vector, $\mathbf{E}_1$ and $\mathbf{E}_2$ are the electric field vectors that are discontinuous at the opposite surfaces, σ_s is the discontinuous two-dimensional surface charge density, and $\mathbf{E}_2=0$.

Radial Electron Function

The solution for the radial function which satisfies the boundary conditions is a delta function in spherical coordinates—a spherical shell :

$$f(r) = \frac{1}{r^2}\,\delta(r - r_n)$$

where $r_n = nr_1$ is an allowed radius

This function defines the charge density on a spherical shell of a fixed radius, not yet determined, with the charge motion confined to the two-dimensional spherical surface. The integer subscript n is *determined during photon absorption* wherein the force balance between the electric fields of the electron and proton plus any resonantly absorbed photons gives the result that $r_n = nr_1$ wherein n is an integer in an excited state.

Electron Orbitsphere

Leptons such as the electron are indivisible, perfectly conducting, and possess an inalienable $\hbar$ of intrinsic angular momentum such that any inelastic perturbation involves the entire particle wherein the intrinsic angular momentum remains unchanged. Bound state transitions are allowed involving the exchange of photons between states, each having $\hbar$ of angular momentum in their fields.

The electron orbitsphere or spin function is a constant two-dimensional spherical surface of charge $-e$ and mass m_e with the Bohr radius of the hydrogen atom, $r=a_H$. It is a nonradiative, minimum-energy surface, that is absolutely stable except for quantized state changes with the corresponding balanced forces in the $n=1$ state providing a pressure equivalent of twenty million atmospheres.

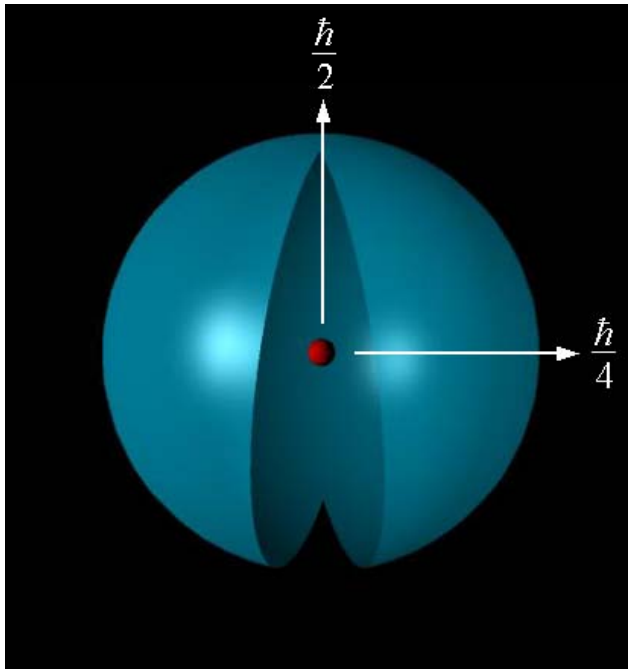

The corresponding uniform current-density function having intrinsic angular momentum components of $\mathbf{L}_{xy}=\frac{\hbar}{4}$ and $\mathbf{L}_z=\frac{\hbar}{2}$ following Larmor excitation in a magnetic field give rise to the phenomenon of electron spin.

The orbitsphere has a thickness of the Schwarzschild radius:

$$r_g=\frac{2Gm_e}{c^2}=1.3525\times10^{-57}\,m.$$

de Broglie Relationship from the Angular Momentum

Given time harmonic motion and a radial delta function, the relationship between an allowed radius and the electron wavelength is given by

$$2\pi r_n = \lambda_n$$

The magnitude of the velocity and the angular frequency for *every* point on the surface of the bound electron and their relationships with the wavelengths and r_n are

$$v_n = \frac{\hbar}{m_e r_n} = \frac{h}{m_e \lambda_n} = \frac{h}{m_e 2\pi r_n}$$

$$\omega_n = \frac{\hbar}{m_e r_n^2}$$

where the velocity and angular frequency are determined by the boundary conditions that the angular momentum density at each point on the surface is constant and the magnitude of the total angular momentum of the orbitsphere $\mathbf{L}$ must also be constant.

de Broglie Relationship from the Angular Momentum cont'd

The constant total is $\hbar$ given by the integral

$$\begin{aligned}\mathbf{m} &= \int \frac{1}{4\pi r^2} \left| \mathbf{r} \times m_e \mathbf{v} \right| \delta\left(r - r_n\right) dx^3 \\ &= m_e r_n \frac{\hbar}{m_e r_n} \\ &= \hbar\end{aligned}$$

The integral of the magnitude of the angular momentum of the electron is $\hbar$ in any inertial frame and is ***relativistically invariant (Lorentz scalar)***.

The relationship between wavelength and velocity gives the ***de Broglie relationship***:

$$\lambda_n = \frac{h}{p_n} = \frac{h}{m_e v_n}$$

Angular Functions

Spherical and Time-Harmonic Two-Dimensional Currents: match the time-varying spherical electromagnetic fields during transitions between states with the further constraint that the electron is nonradiative in a state defined as the $n=1$ state.

To further match the required multipole electromagnetic fields between transitions of states, the trial nonradiative source current functions are time and spherical harmonics, each having an exact radius and an exact energy.

Angular Functions cont'd

Then, each allowed electron charge-density (mass-density) function is the product of a radial delta function $\left(f(r)=\frac{1}{r^2}\delta(r-r_n)\right)$, two angular functions (spherical harmonic functions $Y_\ell^m(\theta,\phi)=P_\ell^m(\cos\theta)e^{im\phi}$), and a time-harmonic function $\left(e^{i\omega_n t}\right)$.

The spherical harmonic $Y_0^0(\theta,\phi)=1$ is also an allowed solution that is in fact required in order for the electron charge and mass densities to be positive definite and to give rise to the phenomena of electron spin.

The form of the angular solution must be a superposition:

$$Y_0^{\,0}(\theta,\phi)+Y_\ell^{\,m}(\theta,\phi)$$

The current is constant at every point on the surface for the s orbital corresponding to $Y_0^0(\theta,\phi)$.

Charge-Density Functions

The quantum numbers of the spherical harmonic currents can be related to the observed electron orbital angular momentum states. The currents corresponding to s, p, d, f, etc. orbitals are

$\ell = 0$

$$\rho(r,\theta,\phi,t) = \frac{e}{8\pi r^2}[\delta(r-r_n)]\left[Y_0^0(\theta,\phi) + Y_\ell^m(\theta,\phi)\right]$$

$\ell \neq 0$

$$\rho(r,\theta,\phi,t) = \frac{e}{4\pi r^2}[\delta(r-r_n)]\left[Y_0^0(\theta,\phi) + \mathrm{Re}\left\{Y_\ell^m(\theta,\phi)e^{im\omega_n t}\right\}\right]$$

where $Y_\ell^m(\theta,\phi)$ are the spherical harmonic functions that spin about the z-axis with angular frequency ω_n with $Y_0^0(\theta,\phi)$ the constant function and

$$\mathrm{Re}\left\{Y_\ell^m(\theta,\phi)e^{im\omega_n t}\right\} = P_\ell^m(\cos\theta)\cos(m\phi + m\omega_n t)$$

Spin and Orbital Parameters

- The constant spin function is modulated by a time and spherical harmonic function.
- The modulation or traveling charge density wave corresponds to an orbital angular momentum in addition to a spin angular momentum.
- These states are typically referred to as p, d, f, etc. states or orbitals and correspond to an ℓ quantum number not equal to zero.

Orbital and Spin Functions

The orbital function modulates the constant (spin) function. (shown for t=0; three-dimensional view)

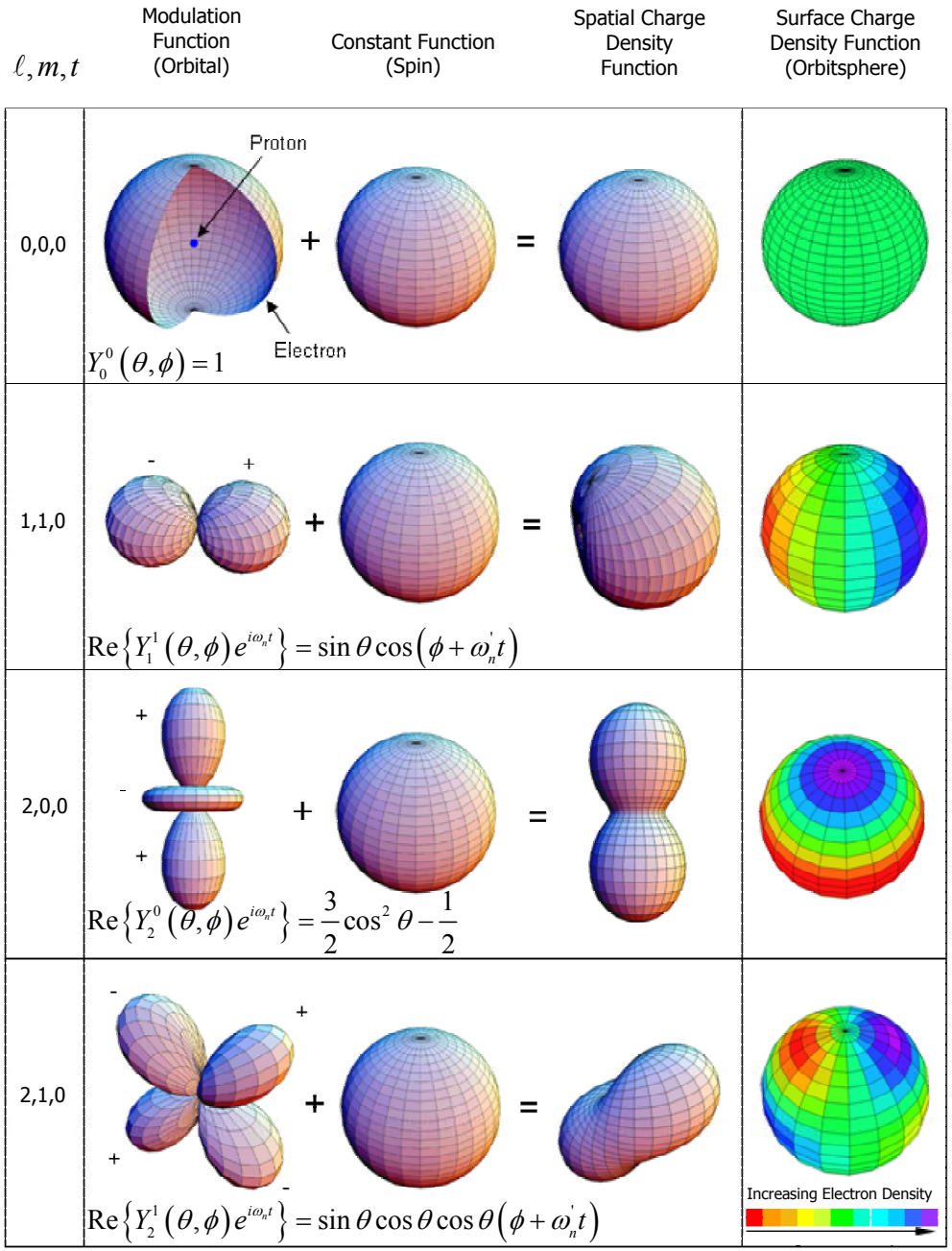

Charge Density Wave Moves on the Surface About the Z-Axis

Charge Density Wave Moves on the Surface About the Z-Axis

Intrinsic Spin Angular Momentum and Rotational Energy

$$\ell = 0$$

$$I_z = I_{spin} = \frac{m_e r_n^{\,2}}{2}$$

$$L_z = I\omega \mathbf{i}_z = \pm\frac{\hbar}{2}$$

$$E_{rotational} = E_{rotational,\,spin} = \frac{1}{2}\left[I_{spin}\left(\frac{\hbar}{m_e r_n^{\,2}}\right)^2\right] = \frac{1}{2}\left[\frac{m_e r_n^{\,2}}{2}\left(\frac{\hbar}{m_e r_n^{\,2}}\right)^2\right] = \frac{1}{4}\left[\frac{\hbar^2}{2I_{spin}}\right]$$

$$T = \frac{\hbar^2}{2m_e r_n^2}$$

Orbital Angular Momentum and Rotational Energies

The mechanics of the electron is solved from the two-dimensional wave equation plus time in the form of an energy equation wherein it provides for conservation of energy and angular momentum.

$$-\frac{\hbar^2}{2I}\left[\frac{1}{\sin\theta}\frac{\partial}{\partial\theta}\left(\sin\theta\frac{\partial}{\partial\theta}\right)_{r,\phi}+\frac{1}{\sin^2\theta}\left(\frac{\partial^2}{\partial\phi^2}\right)_{r,\theta}\right]Y(\theta,\phi)=E_{rot}Y(\theta,\phi)$$

Orbital Angular Momentum and Rotational Energies cont'd

$$\ell \neq 0$$

$$I_{orbital} = m_e r_n^{\,2} \sqrt{\frac{\ell}{\ell+1}}$$

$$\mathbf{L}_{orbital} = \hbar \sqrt{\frac{\ell}{\ell+1}} \mathbf{i}_z$$

$$E_{rotational,\,orbital} = \frac{\hbar^2}{2m_e r_n^2} \frac{\ell}{\ell+1}$$

$$\left\langle L_{z\ orbital} \right\rangle = 0$$

relativistically invariant (Lorentz scalar)

$$\left\langle E_{rotational,\,orbital} \right\rangle = 0$$

Required degeneracy with B=0 from spherical wave motion

Special Relativistic Correction to the Electron Radius

The relationship between the electron wavelength and its radius is given by

$2\pi r = \lambda$ where λ is the de Broglie wavelength.

The distance along each great circle in the direction of instantaneous motion undergoes length contraction and time dilation. Using a phase matching condition, the wavelengths of the electron and laboratory inertial frames are equated, and the corrected radius is given by

$$r_n = r_n^{'}\left[\sqrt{1-\left(\frac{v}{c}\right)^2}\,\sin\left[\frac{\pi}{2}\left(1-\left(\frac{v}{c}\right)^2\right)^{3/2}\right]+\frac{1}{2\pi}\cos\left[\frac{\pi}{2}\left(1-\left(\frac{v}{c}\right)^2\right)^{3/2}\right]\right]$$

where the electron velocity is given by

$$v_n = \frac{\hbar}{m_e r_n}$$

$\frac{e}{m_e}$ of the electron, the electron angular momentum of $\hbar$, and μ_B are invariant, but the mass and charge densities increase in the laboratory frame due to the relativistically contracted electron radius. As $v \to c$, $r / r' \to \frac{1}{2\pi}$ and r = λ.

The Normalized Radius as a Function of the Velocity Due to Relativistic Contraction

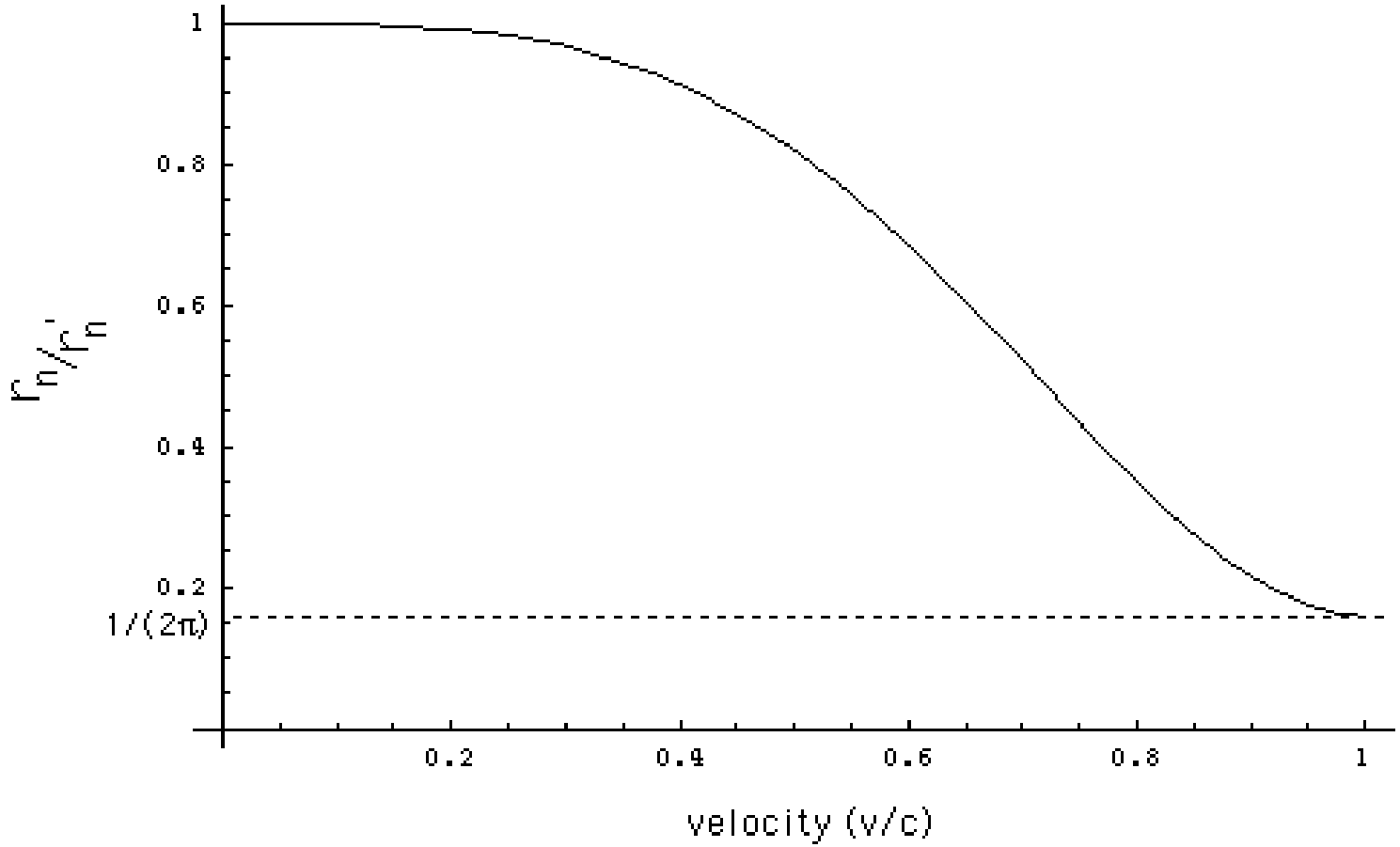

Nonradiation Condition
(Acceleration Without Radiation)

$$K_\ell^{m_\ell}(s,\Theta,\Phi,\omega) = 4\pi\omega_n \frac{\sin(2sr_n)}{2sr_n} \otimes G_\ell^{m_\ell}(s,\Theta) \otimes H_\ell^{m_\ell}(s,\Theta,\Phi) \otimes \frac{1}{4\pi}[\delta(\omega-\omega_n)+\delta(\omega+\omega_n)]$$

wherein $G_\ell^{m_\ell}(s,\Theta)$ and $H_\ell^{m_\ell}(s,\Theta,\Phi)$ are the spherical−coordinate Fourier transforms of $N_{\ell,m}P_\ell^m\left(\cos\theta\right)$and, $e^{im\phi}$ respectively.

$$\mathbf{s}_n \bullet \mathbf{v}_n = \mathbf{s}_n \bullet \mathbf{c} = \omega_n$$

$$r_n = \lambda_n$$

Radiation of the bound electron requires an excited state wherein a potentially emitted photon circulates along the orbitsphere at light speed. Spacetime harmonics

of $\frac{\omega_n}{c} = k$ or $\frac{\omega_n}{c}\sqrt{\frac{\varepsilon}{\varepsilon_0}} = k$ for which the Fourier transform of the lightlike current-density function is nonzero do not exist. Radiation due to charge motion does not occur in any medium when this boundary condition is met.

Nonradiation Based on the Electron Electromagnetic Fields and the Poynting Power Vector

The general multipole field solution to Maxwell's equations in a source-free region of empty space with the assumption of a time dependence $e^{i\omega t}$ is

$$\mathbf{B} = \sum_{\ell,m}\left[a_E(\ell,m) f_\ell(kr)\mathbf{X}_{\ell,m} - \frac{i}{k} a_M(\ell,m)\nabla\times g_\ell(kr)\mathbf{X}_{\ell,m}\right]$$
$$\mathbf{E} = \sum_{\ell,m}\left[\frac{i}{k} a_E(\ell,m)\nabla\times f_\ell(kr)\mathbf{X}_{\ell,m} + a_M(\ell,m) g_\ell(kr)\mathbf{X}_{\ell,m}\right] \qquad (1)$$

Nonradiation Based on the Electron Electromagnetic Fields and the Poynting Power Vector cont'd

For the electron source current comprising a multipole of order (ℓ, m), the far fields are given by

$$\mathbf{B} = -\frac{i}{k} a_M(\ell, m) \nabla \times g_\ell(kr) \mathbf{X}_{\ell,m}$$
$$\mathbf{E} = a_M(\ell, m) g_\ell(kr) \mathbf{X}_{\ell,m} \tag{2}$$

and the time-averaged power radiated per solid angle $\frac{dP(\ell, m)}{d\Omega}$ is

$$\frac{dP(\ell, m)}{d\Omega} = \frac{c}{8\pi k^2} \left| a_M(\ell, m) \right|^2 \left| \mathbf{X}_{\ell,m} \right|^2 \tag{3}$$

where is $a_M(\ell, m)$

$$a_M(\ell, m) = \frac{-ek^2}{c\sqrt{\ell(\ell+1)}} \frac{\omega_n}{2\pi} N j_\ell(kr_n) \Theta \sin(ks) \tag{4}$$

In the case that k is the lightlike k^0, then $k = \omega_n / c$ regarding a potentially emitted photon, in Eq. (4), and Eqs. (2-3) vanishes for

$$s = vT_n = R = r_n = \lambda_n \tag{5}$$

There is no radiation.

Spin Function

The spin function comprises a constant charge (current) density function with moving charge confined to a two-dimensional spherical shell and comprises a uniform complete coverage.

The uniform magnetostatic current-density function $Y_0^0(\theta,\phi)$ of the orbitsphere spin function comprises a continuum of correlated orthogonal great-circle current loops wherein each point charge(current) density-element moves time harmonically with constant angular velocity, ω_n , and velocity, v_n , in the direction of the current.

The current-density is generated from *orthogonal great-circle current-density elements (one dimensional "current loops")* that serve as basis elements to form two distributions of an infinite number of great circles wherein each covers one-half of a two-dimensional spherical shell and is defined as a basis element current vector field ("BECVF") and an orbitsphere current-vector field ("OCVF").

Spin Function Cont'd.

Then, the *continuous* uniform electron current density function $Y_0^0(\theta,\phi)$ that covers the entire spherical surface as a distribution of an infinite number of great circles is generated using the CVFs.

First, the generation of the BECVF is achieved by rotation of two great circle basis elements, one in the x'z'-plane and the other in the y'z'-plane, about the ($-i_x$, i_y, $0i_z$)-axis by an infinite set of infinitesimal increments of the rotational angle over a π span wherein the current direction is such that the resultant angular momentum vector of the basis elements of $\frac{\hbar}{2\sqrt{2}}$ is stationary on this axis.

Spin Function Cont'd.

The generation of the OCVF is achieved by rotation of two great circle basis elements, one in the x'y'-plane and the other in the plane that bisects the x'y'-quadrant and is parallel to the z'-axis, about the $\left(-\frac{1}{\sqrt{2}}\mathbf{i}_x, \frac{1}{\sqrt{2}}\mathbf{i}_y, \mathbf{i}_z\right)$ -axis by an infinite set of infinitesimal increments of the rotational angle over a π span wherein the current direction is such that the resultant angular momentum vector of the basis elements of $\frac{\hbar}{2}$ having components of $\mathbf{L}_{xy} = \frac{\hbar}{2\sqrt{2}}$ and $\mathbf{L}_z = \frac{\hbar}{2\sqrt{2}}$ is stationary on this axis.

Spin Function Cont'd.

Then, a uniform great-circle distribution $Y_0^0(\theta,\phi)$ is exactly generated from the CVFs by the convolution of the BECVF with the OCVF that results in the placement of a BECVF at each great circle of the OCVF followed by density normalization.

Since the angular momentum vector of the BECVF matches that of the replaced great circle basis elements and is unaffected by normalization, the resultant angular momentum of the distribution is the same as that of the OCVF, except that coverage of the spherical surface is complete and uniform.

Generation of the BECVF

The BECVF is generated from two orthogonal great-circle current loops that serve as basis elements. The current on the great circle in the y'z'-plane moves clockwise and the current on the great circle in the x'z'-plane moves counter clockwise (arrows). Each point or coordinate position on the continuous two-dimensional BECVF defines an infinitesimal charge(mass)-density element, which moves along a geodesic orbit comprising a great circle. Two such infinitesimal charges (masses) are shown at point one, moving clockwise on the great circle in the y'z'-plane, and at point two moving counter clockwise on the great circle in the x'z'-plane. The xyz-system is the laboratory frame, and the orthogonal-current-loop basis set is rigid with respect to the x'y'z'-system that rotates about the $(-i_x, i_y, 0i_z)$- axis by π radians to generate the elements of the BECVF. The resultant angular momentum vector of the orthogonal great-circle current loops that is stationary in the xy-plane that is evenly distributed over the half-surface is $\frac{\hbar}{2\sqrt{2}}$ in the direction of $(-i_x, i_y, 0i_z)$.

Generation of the BECVF cont'd.

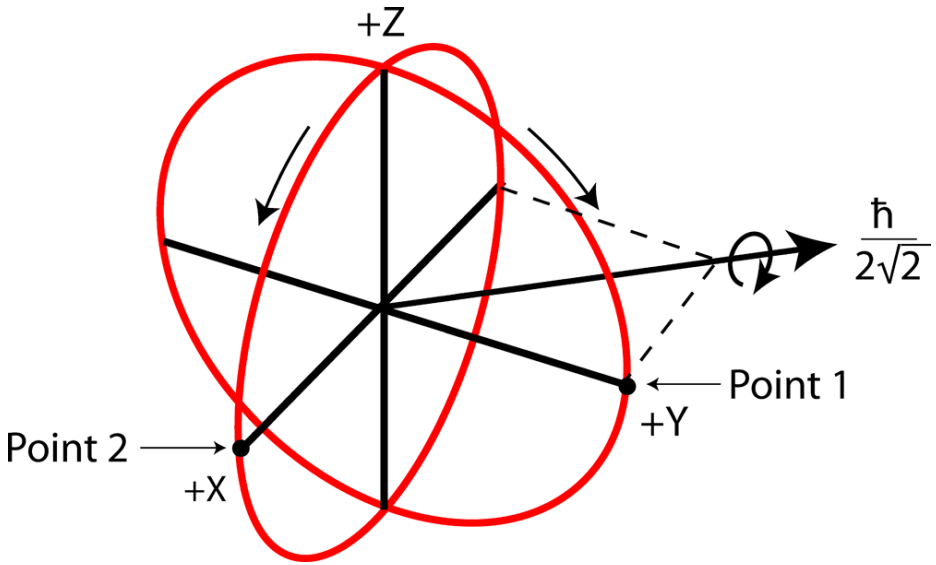

The rotational matrix about the ($-i_x$, i_y, $0i_z$)-axis by θ, $R_{(-\mathbf{i_x},\mathbf{i_y},0\mathbf{i_z})}(\theta)$,

is $R_{(-\mathbf{i_x},\mathbf{i_y},0\mathbf{i_z})}(\theta) = R_z\left(\frac{\pi}{4}\right) R_x(-\theta) R_z\left(\frac{-\pi}{4}\right)$

Generation of the BECVF cont'd.

BECVF Matrices ($R_{(-\mathbf{i_x},\mathbf{i_y},0\mathbf{i_z})}(\theta)$)

$$\begin{bmatrix} x' \\ y' \\ z' \end{bmatrix} = \begin{bmatrix} \frac{1}{2}+\frac{\cos\theta}{2} & -\frac{1}{2}+\frac{\cos\theta}{2} & -\frac{\sin\theta}{\sqrt{2}} \\ -\frac{1}{2}+\frac{\cos\theta}{2} & \frac{1}{2}+\frac{\cos\theta}{2} & -\frac{\sin\theta}{\sqrt{2}} \\ \frac{\sin\theta}{\sqrt{2}} & \frac{\sin\theta}{\sqrt{2}} & \cos\theta \end{bmatrix} \bullet \left(\begin{bmatrix} 0 \\ r_n\cos\phi \\ -r_n\sin\phi \end{bmatrix} + \begin{bmatrix} r_n\cos\phi \\ 0 \\ -r_n\sin\phi \end{bmatrix} \right)$$

Generation of the BECVF cont'd.

The infinite sum of great circles that constitute the BECVF:

$$BECVF = \lim_{\Delta\theta \to 0} \sum_{m=1}^{m=\frac{\pi}{|\Delta\theta|}} \left[\left(R_{\left(-\mathbf{i}_x, \mathbf{i}_y, 0\mathbf{i}_z\right)} \left(m\Delta\theta_M \right) \bullet \left(GC^{basis}_{\left(0\mathbf{i}_x, \mathbf{i}_y, \mathbf{i}_z\right)} + GC^{basis}_{\left(\mathbf{i}_x, 0\mathbf{i}_y, \mathbf{i}_z\right)} \right) \right) \right]$$

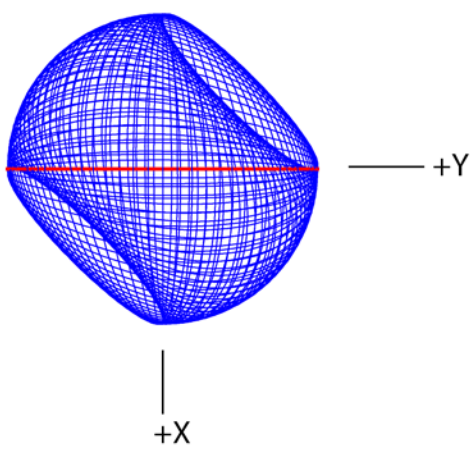

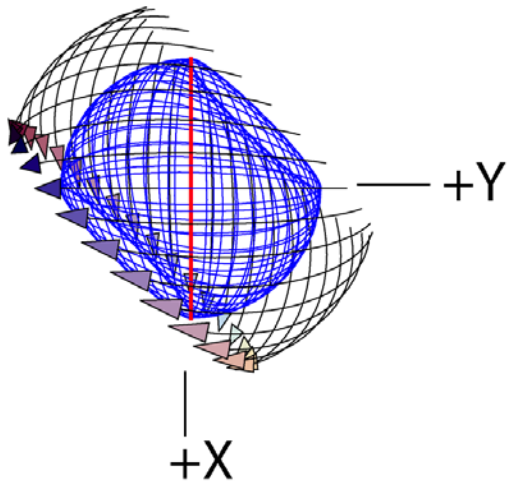

Algorithm of the Current Loops

3D View of the Resultant BECVF Semi-Sphere

BECVF:

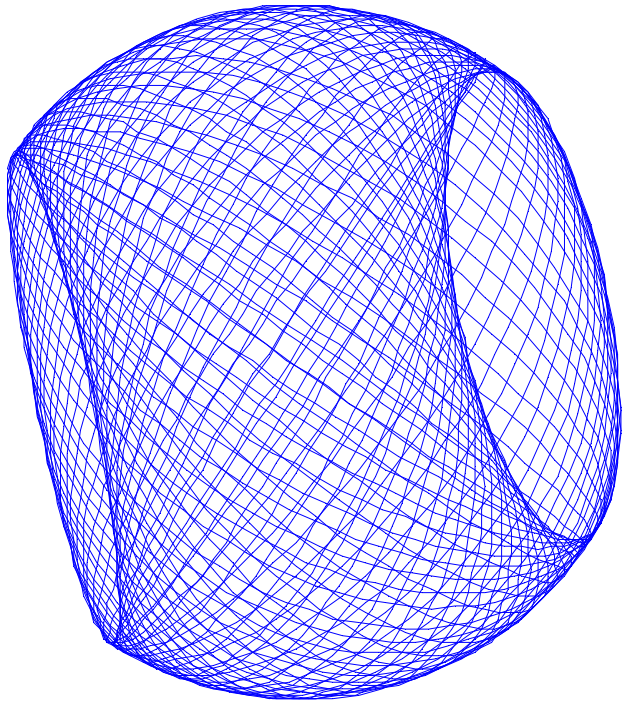

Generation of the OCVF

In the generation of the OCVF, the current on the great circle in the plane that bisects the x'y'-quadrant and is parallel to the z'-axis moves clockwise, and the current on the great circle in the x'y'-plane moves counter clockwise. Rotation of the great circles about the $\left(-\frac{1}{\sqrt{2}}\mathbf{i}_x, \frac{1}{\sqrt{2}}\mathbf{i}_y, \mathbf{i}_z\right)$-axis by π radians generates the elements of the OCVF. The stationary resultant angular momentum vector of the orthogonal great-circle current loops along the $\left(-\frac{1}{\sqrt{2}}\mathbf{i}_x, \frac{1}{\sqrt{2}}\mathbf{i}_y, \mathbf{i}_z\right)$-axis is $\frac{\hbar}{2}$ corresponding to each of the z and -xy-components of magnitude $\frac{\hbar}{2\sqrt{2}}$.

Generation of the OCVF cont'd.

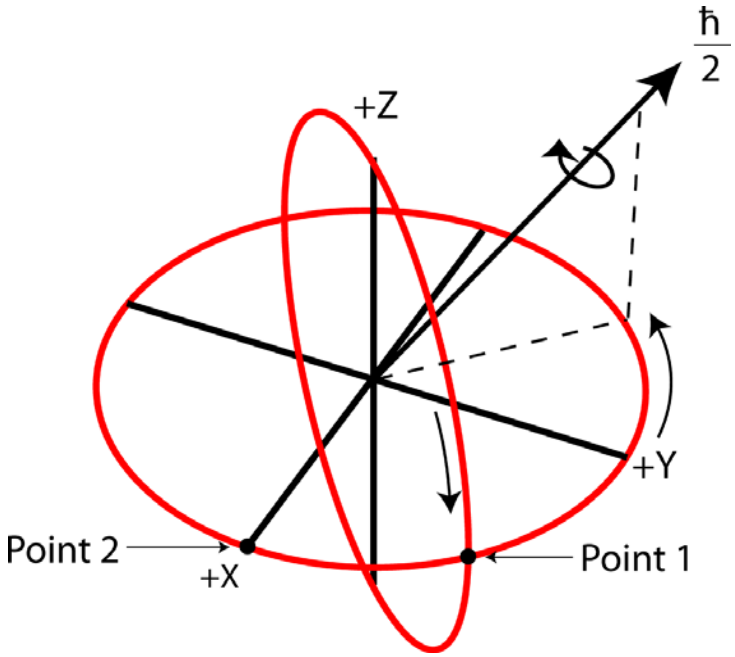

The rotation about the $\left(-\frac{1}{\sqrt{2}}\mathbf{i}_x, \frac{1}{\sqrt{2}}\mathbf{i}_y, \mathbf{i}_z\right)$ -axis by θ, $R_{\left(-\frac{1}{\sqrt{2}}\mathbf{i}_x, \frac{1}{\sqrt{2}}\mathbf{i}_y, \mathbf{i}_z\right)}(\theta)$, is given by

$$R_{\left(-\frac{1}{\sqrt{2}}\mathbf{i}_x, \frac{1}{\sqrt{2}}\mathbf{i}_y, \mathbf{i}_z\right)}(\theta) = R_z\left(\frac{\pi}{4}\right) R_y\left(\frac{\pi}{4}\right) R_z(\theta) R_y\left(\frac{-\pi}{4}\right) R_z\left(-\frac{\pi}{4}\right) = R_z\left(\frac{\pi}{4}\right) R_{(-\mathbf{i}_x, \mathbf{i}_y, 0\mathbf{i}_z)}(\theta) R_z\left(-\frac{\pi}{4}\right)$$

Generation of the OCVF cont'd.

OCVF Matrices ($R_{\left(-\frac{1}{\sqrt{2}}\mathbf{i_x},\frac{1}{\sqrt{2}}\mathbf{i_y},\mathbf{i_z}\right)}(\theta)$)

$$\begin{bmatrix} x' \\ y' \\ z' \end{bmatrix} = \begin{bmatrix} \frac{1}{4}(1+3\cos\theta) & \frac{1}{4}(-1+\cos\theta+2\sqrt{2}\sin\theta) & \frac{1}{4}(-\sqrt{2}+\sqrt{2}\cos\theta-2\sin\theta) \\ \frac{1}{4}(-1+\cos\theta-2\sqrt{2}\sin\theta) & \frac{1}{4}(1+3\cos\theta) & \frac{1}{4}(\sqrt{2}-\sqrt{2}\cos\theta-2\sin\theta) \\ \frac{1}{2}\left(\frac{-1+\cos\theta}{\sqrt{2}}+\sin\theta\right) & \frac{1}{4}(\sqrt{2}-\sqrt{2}\cos\theta+2\sin\theta) & \cos^2\frac{\theta}{2} \end{bmatrix} \bullet \left(\begin{bmatrix} \frac{r_n\cos\phi}{\sqrt{2}} \\ \frac{r_n\cos\phi}{\sqrt{2}} \\ -r_n\sin\phi \end{bmatrix} + \begin{bmatrix} r_n\cos\phi \\ r_n\sin\phi \\ 0 \end{bmatrix} \right)$$

Generation of the OCVF cont'd.

The infinite sum of great circles that constitute the OCVF:

$$OCVF = \lim_{\Delta\theta \to 0} \sum_{m=1}^{m=\frac{\pi}{|\Delta\theta|}} \left[\left(R_{\left(-\frac{1}{\sqrt{2}}\mathbf{i}_x, \frac{1}{\sqrt{2}}\mathbf{i}_y, \mathbf{i}_z\right)} \left(m\Delta\theta_M\right) \bullet \left(GC^{basis}_{\left(\frac{1}{\sqrt{2}}\mathbf{i}_x, \frac{1}{\sqrt{2}}\mathbf{i}_y, 0\mathbf{i}_z\right)} + GC^{basis}_{\left(\mathbf{i}_x, \mathbf{i}_y, 0\mathbf{i}_z\right)} \right) \right) \right]$$

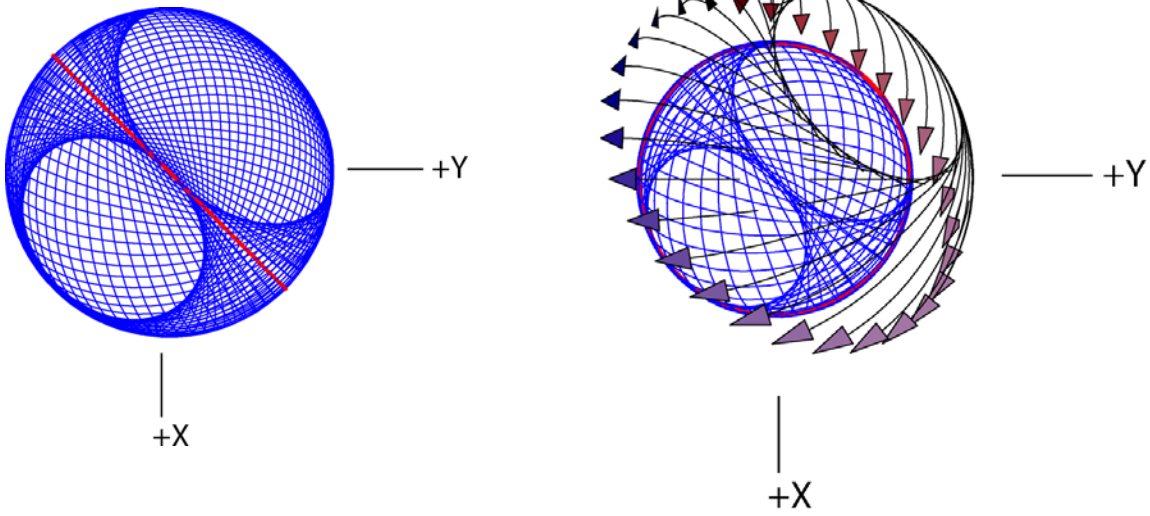

Algorithm of the Current Loops

3D View of the Resultant OCVF Semi-Sphere

OCVF:

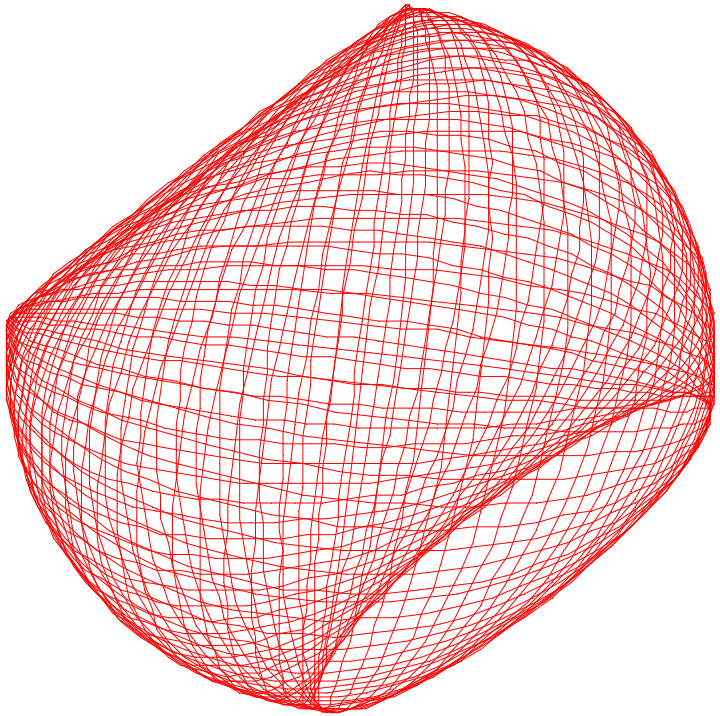

Generation of $Y_0^0(\theta,\phi)$

The further constraint that the current density is uniform such that the charge density is uniform, corresponding to an equipotential, minimum energy surface is satisfied by using the CVFs to generate the uniform great-circle distribution $Y_0^0(\theta,\phi)$ by the convolution of the BECVF with the OCVF followed by density normalization.

The convolution operator treats each CVF independently and results in the placement of a BECVF at each great circle of the OCVF such that the resultant angular momentum of the distribution is the same as that of the OCVF.

This is achieved by rotating the orientation, phase, and vector-matched basis-element, the BECVF, about the same axis as that which generated the OCVF.

Generation of $Y_0^0(\theta,\phi)$ cont'd

Then, $Y_0^0(\theta,\phi)$ is generated by rotation of the BECVF, about the $\left(-\frac{1}{\sqrt{2}}\mathbf{i}_x,\frac{1}{\sqrt{2}}\mathbf{i}_y,\mathbf{i}_z\right)$-axis by an infinite set of infinitesimal increments of the rotational angle.

The current direction is such that the resultant angular momentum vector of the BECVF basis element rotated over the 2π span is equivalent that of the OCVF great circle basis elements, $\frac{\hbar}{2}$ having components of $\mathbf{L}_{xy}=\frac{\hbar}{2\sqrt{2}}$ and $\mathbf{L}_z=\frac{\hbar}{2\sqrt{2}}$ that is stationary on the $\left(-\frac{1}{\sqrt{2}}\mathbf{i}_x,\frac{1}{\sqrt{2}}\mathbf{i}_y,\mathbf{i}_z\right)$ -axis.

Since the resultant angular momentum vector of the BECVF over the 2π span matches that of the replaced great circle basis elements and is stationary on the rotational axis as in the case of the OCVF, the resultant angular momentum of the distribution is the same as that of the OCVF, except that coverage of the spherical surface is complete.

Generation of $Y_0^{\,0}(\theta,\phi)$ cont'd

The infinite double sum of great circles that constitute $Y_0^{\,0}(\theta,\phi)$:

$$Y_0^{\,0}(\theta,\phi) = \lim_{\Delta\theta\to 0}\sum_{m=1}^{m=\frac{2\pi}{|\Delta\theta|}}\left[R_{\left(-\frac{1}{\sqrt{2}}\mathbf{i}_x,\frac{1}{\sqrt{2}}\mathbf{i}_y,\mathbf{i}_z\right)}\left(m\Delta\theta_M^{OCVF}\right)\cdot\lim_{\Delta\theta\to 0}\sum_{n=1}^{n=\frac{2\pi}{|\Delta\theta|}}\left[R_{(-\mathbf{i}_x,\mathbf{i}_y,0\mathbf{i}_z)}\left(n\Delta\theta_N^{BECVF}\right)\bullet GC^{basis}_{(0\mathbf{i}_x,\mathbf{i}_y,\mathbf{i}_z)}\right]\right]$$

A discrete representation of the current distribution $Y_0^{\,0}(\theta,\phi)$ can be generated from the continuous convolution of the BECVF with the OCVF as a superposition of *M* discrete incremental rotations of the position of the BECVF comprising *N* great circles about the $\left(-\frac{1}{\sqrt{2}}\mathbf{i}_x,\frac{1}{\sqrt{2}}\mathbf{i}_y,\mathbf{i}_z\right)$-axis such that the number of convolved BECVF elements is *M*.

Generation of $Y_0^0(\theta,\phi)$ cont'd

$$\begin{bmatrix} x' \\ y' \\ z' \end{bmatrix} = \sum_{m=1}^{m=M} \begin{bmatrix} \frac{1}{4}\left(1+3\cos\left(\frac{m2\pi}{M}\right)\right) & \frac{1}{4}\left(-1+\cos\left(\frac{m2\pi}{M}\right)+2\sqrt{2}\sin\left(\frac{m2\pi}{M}\right)\right) & \frac{1}{4}\left(-\sqrt{2}+\sqrt{2}\cos\left(\frac{m2\pi}{M}\right)-2\sin\left(\frac{m2\pi}{M}\right)\right) \\ \frac{1}{4}\left(-1+\cos\left(\frac{m2\pi}{M}\right)-2\sqrt{2}\sin\left(\frac{m2\pi}{M}\right)\right) & \frac{1}{4}\left(1+3\cos\left(\frac{m2\pi}{M}\right)\right) & \frac{1}{4}\left(\sqrt{2}-\sqrt{2}\cos\left(\frac{m2\pi}{M}\right)-2\sin\left(\frac{m2\pi}{M}\right)\right) \\ \frac{1}{2}\left(\frac{-1+\cos\left(\frac{m2\pi}{M}\right)}{\sqrt{2}}+\sin\left(\frac{m2\pi}{M}\right)\right) & \frac{1}{4}\left(\sqrt{2}-\sqrt{2}\cos\left(\frac{m2\pi}{M}\right)+2\sin\left(\frac{m2\pi}{M}\right)\right) & \cos^2\frac{\left(\frac{m2\pi}{M}\right)}{2} \end{bmatrix}$$

$$\bullet \sum_{n=1}^{n=N} \begin{bmatrix} \frac{1}{2}+\frac{\cos\left(\frac{n2\pi}{N}\right)}{2} & -\frac{1}{2}+\frac{\cos\left(\frac{n2\pi}{N}\right)}{2} & -\frac{\sin\left(\frac{n2\pi}{N}\right)}{\sqrt{2}} \\ -\frac{1}{2}+\frac{\cos\left(\frac{n2\pi}{N}\right)}{2} & \frac{1}{2}+\frac{\cos\left(\frac{n2\pi}{N}\right)}{2} & -\frac{\sin\left(\frac{n2\pi}{N}\right)}{\sqrt{2}} \\ \frac{\sin\left(\frac{n2\pi}{N}\right)}{\sqrt{2}} & \frac{\sin\left(\frac{n2\pi}{N}\right)}{\sqrt{2}} & \cos\left(\frac{n2\pi}{N}\right) \end{bmatrix} \begin{bmatrix} 0 \\ r_n\cos\phi \\ -r_n\sin\phi \end{bmatrix}$$

Generation of $Y_0^0(\theta,\phi)$ cont'd

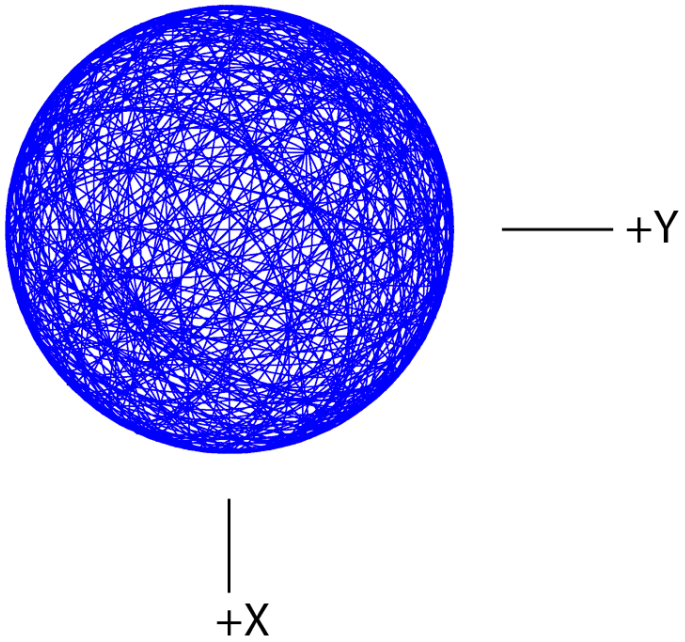

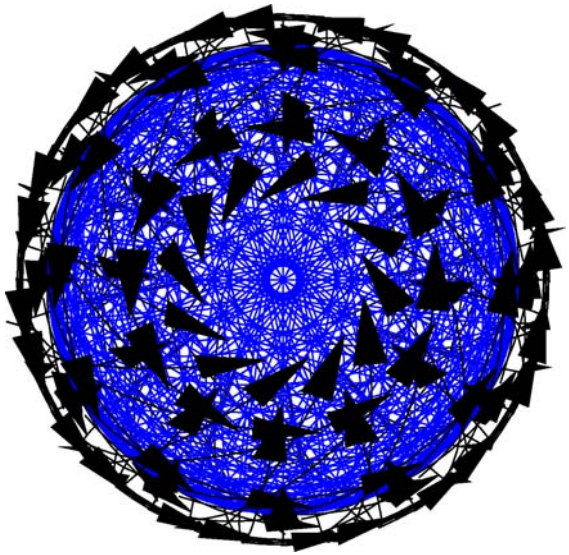

Discrete representations of the current distribution $Y_0^0(\theta,\phi)$

(30 degree increments, $N = M = 12$) viewed along the z-axis and along the $\left(-\frac{1}{\sqrt{2}}\mathbf{i}_x, \frac{1}{\sqrt{2}}\mathbf{i}_y, \mathbf{i}_z\right)$-axis with current vectors superimposed. Normalization gives the uniform distribution without changing the angular momentum.

3-D View of $Y_0^0(\theta,\phi)$

Generation of $Y_0^0(\theta,\phi)$ cont'd

The bound electron exists as a spherical two-dimensional supercurrent (electron *orbitsphere*), an extended distribution of charge and current completely surrounding the nucleus. Unlike a spinning sphere, there is a complex pattern of motion on its surface (indicated by vectors) that generate two orthogonal components of angular momentum that give rise to the phenomenon of electron spin. A representation of the $\left(-\frac{1}{\sqrt{2}}\mathbf{i}_x,\frac{1}{\sqrt{2}}\mathbf{i}_y,\mathbf{i}_z\right)$ -axis view of the total uniform supercurrent-density pattern of the orbitsphere with 144 vectors overlaid on the continuous bound-electron current density giving the direction of the current of each great circle element (nucleus not to scale) is shown.

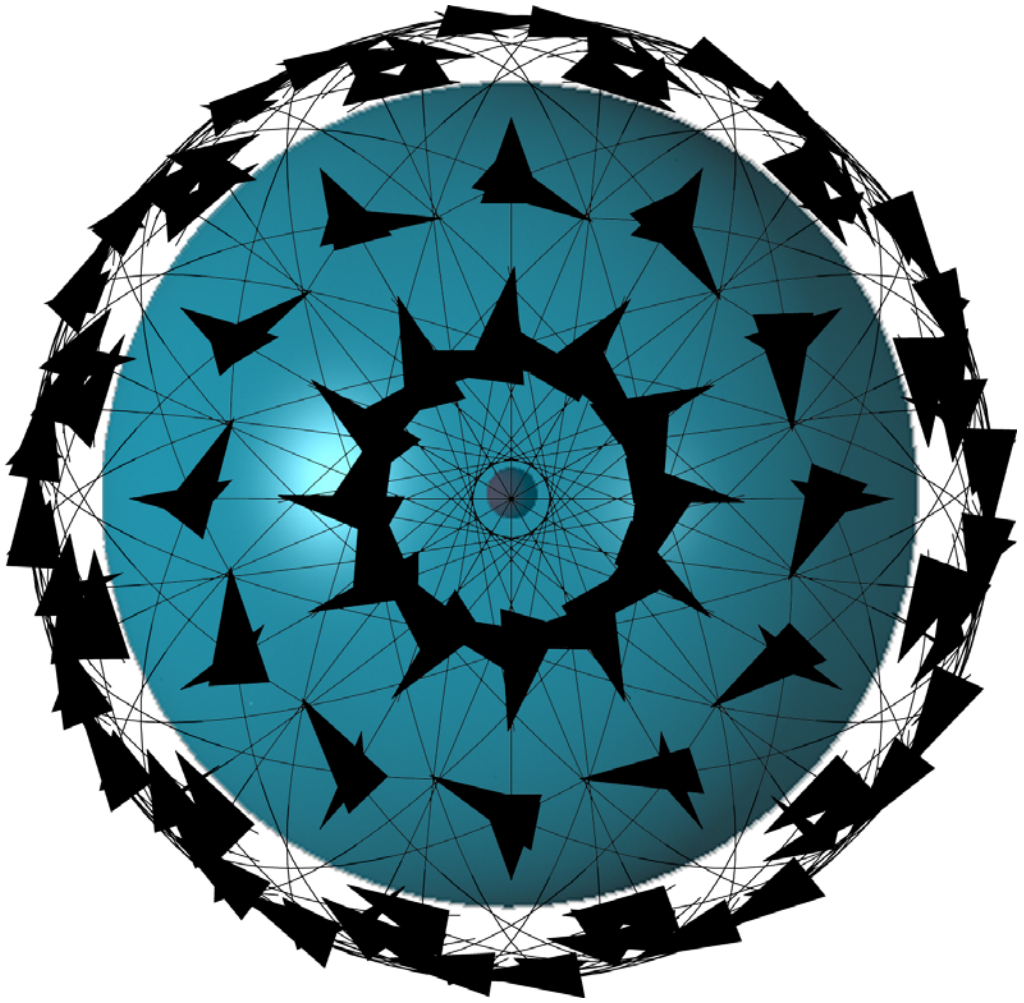

Spin Angular Momentum of $Y_0^0(\theta,\phi)$

During the generation of the BECVF, the orthogonal great-circle basis set is rotated about the ($-i_x$, i_y, $0i_z$)-axis.

The resultant angular momentum vector is along this axis. Thus, the resultant angular momentum vector of magnitude $\frac{\hbar}{2\sqrt{2}}$ is stationary throughout the rotations.

The convolution operation of the BECVF with the OCVF is also about the resultant angular momentum axis, the $\left(-\frac{1}{\sqrt{2}}\mathbf{i}_x, \frac{1}{\sqrt{2}}\mathbf{i}_y, \mathbf{i}_z\right)$-axis.

Here, the resultant angular momentum vector of twice the BECVF of $\frac{\hbar}{2\sqrt{2}}$ in the direction of ($-i_x$, i_y, $0i_z$) is matched to and replaces that of the basis element great circles.

Spin Angular Momentum of $Y_0^0(\theta,\phi)$ cont'd

This current vector distribution is normalized by scaling the constant current of each great circle element resulting in the exact uniformity of the distribution independent of time since $\nabla \cdot K = 0$ along each great circle.

There is no alteration of the angular momentum with normalization since it only affects the density parallel to the angular momentum axis of the distribution, the $\left(-\frac{1}{\sqrt{2}}\mathbf{i}_x, \frac{1}{\sqrt{2}}\mathbf{i}_y, \mathbf{i}_z\right)$ -axis.

This was proven by numerical integration of the normalized distribution.

Spin Angular Momentum of $Y_0^0(\theta,\phi)$ cont'd

Then, the boundary condition of $Y_0^0(\theta,\phi)$ having the desired angular momentum components, coverage, element motion, and uniformity are shown to be achieved by designating the $\left(-\frac{1}{\sqrt{2}}\mathbf{i}_x,\frac{1}{\sqrt{2}}\mathbf{i}_y,\mathbf{i}_z\right)$ -axis as the z-axis.

Specifically, this uniform spherical shell of current meets the boundary conditions of having an angular velocity magnitude at each point on the surface of ω_n and three angular momentum projections of $\mathbf{L}_{xy}=+/-\frac{\hbar}{4}$ and $\mathbf{L}_z=\frac{\hbar}{2}$ that give rise to the Stern Gerlach experiment and the phenomenon corresponding to the spin quantum number.

Spin Angular Momentum of $Y_0^0(\theta,\phi)$ cont'd

With the application of a magnetic field, the magnetic moment corresponding to the intrinsic angular momentum of the electron of $\frac{\hbar}{2}$ aligns with the applied field direction designated the z-axis. Thus, the resultant angular momentum initially along the $\left(-\frac{1}{\sqrt{2}}\mathbf{i}_x,\frac{1}{\sqrt{2}}\mathbf{i}_y,\mathbf{i}_z\right)$-axis aligns with the z-axis. The new projections relative to the Cartesian coordinates are shown.

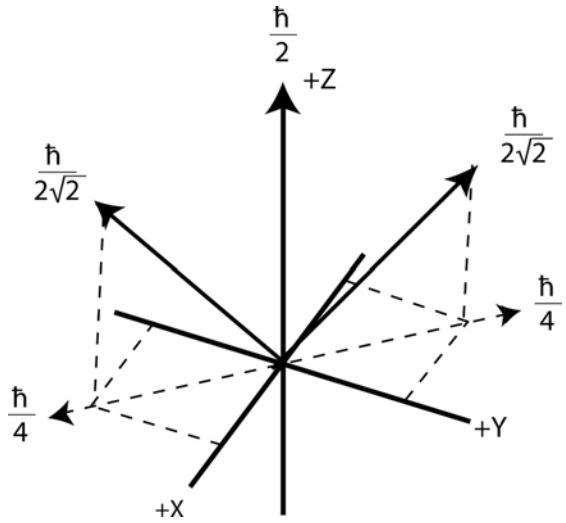

The vector projections of the angular momentum that are Zeeman-splitting active whereby they give rise to the Stern Gerlach phenomenon and other aspects of spin are those components that are onto the xy-plane and the z-axis.

Zeeman L Components

$$\mathbf{L}_{xy} = +/-\frac{\hbar}{4}$$

$$\mathbf{L}_z = \frac{\hbar}{2}$$

Spin Angular Momentum of $Y_0^0(\theta,\phi)$ cont'd

The charge, current, mass, and angular momentum distributions of $Y_0^0(\theta,\phi)$ are uniform.

The electron charge, current, mass, and angular momentum density are given by equating the surface area integral to $-e$, $-e\omega_n$, m_e , and $\hbar$, respectively.

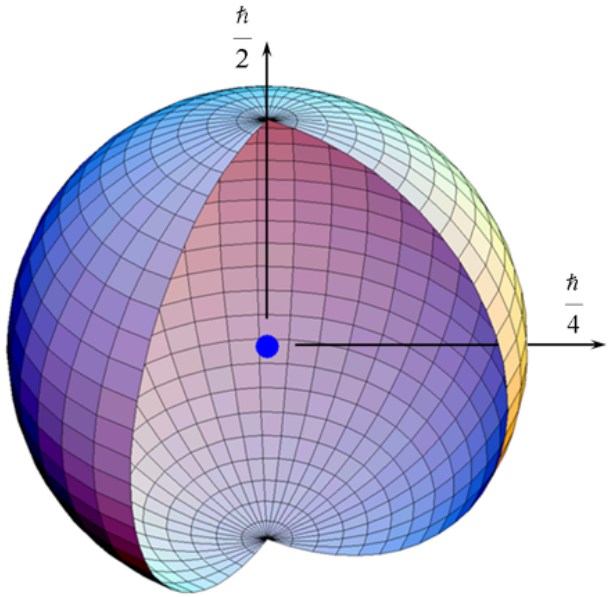

The orbitsphere is a uniform two dimensional spherical shell of zero thickness with the Bohr radius of the hydrogen atom, $r = a_H$, having intrinsic angular momentum components of $\mathbf{L}_{xy} = \frac{\hbar}{4}$ and $\mathbf{L}_z = \frac{\hbar}{2}$ following Larmor excitation in a magnetic field.

Stern-Gerlach Experiment

The Stern-Gerlach experiment implies a magnetic moment of one Bohr magneton and an associated angular momentum quantum number of 1/2. Historically, this quantum number is called the spin quantum number, s ($s = \frac{1}{2}; m_s = \pm\frac{1}{2}$).

The superposition of the vector projection of the orbitsphere angular momentum on the z-axis is $\frac{\hbar}{2}$ with one of the orthogonal components of $\frac{\hbar}{4}$ being Zeeman active depending on the handedness of the Larmor frequency photon.

Excitation of a resonant Larmor precession gives rise to $\hbar$ on an axis **S** that precesses about the z-axis called the spin axis at the Larmor frequency at an angle of $\theta = \frac{\pi}{3}$.

The projections of the precessing components are:

$$\mathbf{S}_{\perp} = \pm\hbar \sin\frac{\pi}{3} = \pm\sqrt{\frac{3}{4}}\hbar\ \mathbf{i}_{Y_R}$$

$$\mathbf{S}_{\parallel} = \pm\hbar \cos\frac{\pi}{3} = \pm\frac{\hbar}{2}\mathbf{i}_{Z_R}$$

Stern-Gerlach Experiment cont'd

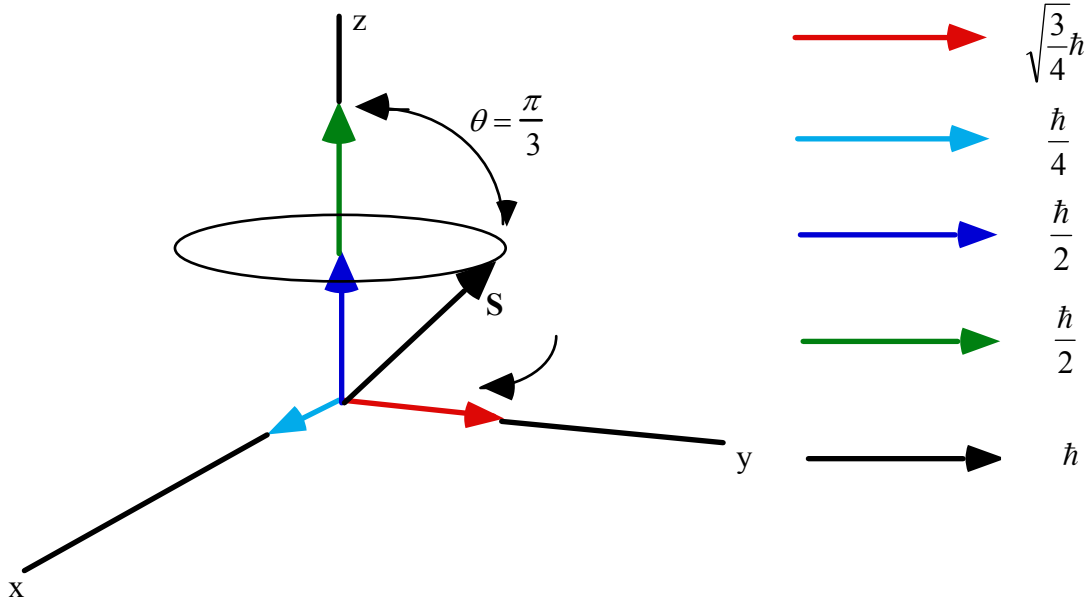

Animation of Larmor Precession

The intrinsic angular momentum is on the z-axis is $\frac{\hbar}{2}$, but the excitation of the precessing **S** component gives $\hbar$—twice the angular momentum on the z-axis due to the contribution from the precessing vector **S**.

The superposition of the $\frac{\hbar}{2}$ z-axis component of the orbitsphere angular momentum and the $\frac{\hbar}{2}$ z-axis component of **S** gives $\hbar$ corresponding to the observed Zeeman splitting due to an electron magnetic moment of a Bohr magneton, $\mu_B = \frac{e\hbar}{2m_e}$.

Electron g Factor

Conservation of angular momentum of the orbitsphere permits a discrete change of its "kinetic angular momentum" $(\mathbf{r} \times m\mathbf{v})$ by the applied magnetic field of $\frac{\hbar}{2}$, and concomitantly the "potential angular momentum" $(\mathbf{r} \times e\mathbf{A})$ must change by $-\frac{\hbar}{2}$.

$$\Delta \mathbf{L} = \frac{\hbar}{2} - \mathbf{r} \times e\mathbf{A}$$
$$= \left[\frac{\hbar}{2} - \frac{e\phi}{2\pi} \right] \hat{z}$$

In order that the change of angular momentum, $\Delta \mathbf{L}$, equals zero, ϕ must be $\Phi_0 = \frac{h}{2e}$, the magnetic flux quantum.

The magnetic moment of the electron is parallel or antiparallel to the applied field only.

Electron g Factor cont'd

Power flow during the spin-flip transition is governed by the Poynting power theorem,

$$\nabla \bullet \left(\mathrm{E} \times \mathrm{H} \right) = -\frac{\partial}{\partial t}\left[\frac{1}{2}\mu_0 \mathrm{H} \bullet \mathrm{H} \right] - \frac{\partial}{\partial t}\left[\frac{1}{2}\varepsilon_0 \mathrm{E} \bullet \mathrm{E} \right] - \mathrm{J} \bullet \mathrm{E}$$

The total energy of the flip transition is the sum of the energy of reorientation of the magnetic moment, the magnetic energy, the electric energy, and the dissipated energy of a fluxon treading the orbitsphere, respectively.

$$\Delta E_{mag}^{spin} = 2\left(1 + \frac{\alpha}{2\pi} + \frac{2}{3}\alpha^2 \left(\frac{\alpha}{2\pi} \right) - \frac{4}{3}\left(\frac{\alpha}{2\pi} \right)^2 \right) \mu_B \mathrm{B}$$

$$\Delta E_{mag}^{spin} = g\mu_B \mathrm{B}$$

Where the stored magnetic energy corresponding to the $\frac{\partial}{\partial t}\left[\frac{1}{2}\mu_0 \mathrm{H} \bullet \mathrm{H} \right]$ term increases, the stored electric energy corresponding to the $\frac{\partial}{\partial t}\left[\frac{1}{2}\varepsilon_0 \mathrm{E} \bullet \mathrm{E} \right]$ term increases, and the $\mathrm{J} \bullet \mathrm{E}$ term is dissipative.

The spin-flip transition can be considered as involving a magnetic moment of g times that of a Bohr magneton. The calculated value of the $\frac{g}{2}$ factor is 1.001 159 652 137. The experimental value of $\frac{g}{2}$ is 1.001 159 652 188(4).

Magnetic Field of the Electron

$$\mathbf{H} = \frac{e\hbar}{m_e r_n^3}(\mathbf{i}_r \cos\theta - \mathbf{i}_\theta \sin\theta)$$

for $r < r_n$

$$\mathbf{H} = \frac{e\hbar}{2m_e r^3}(\mathbf{i}_r 2\cos\theta + \mathbf{i}_\theta \sin\theta)$$

for $r > r_n$

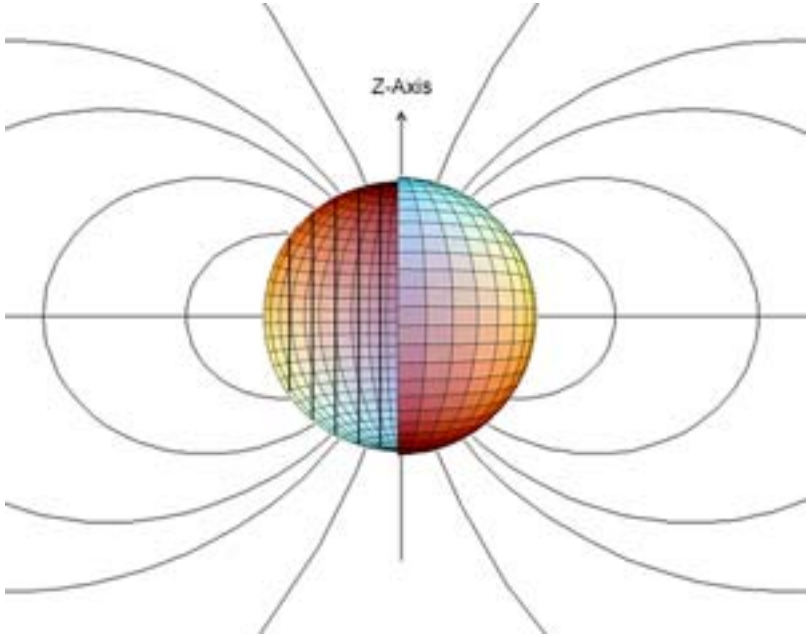

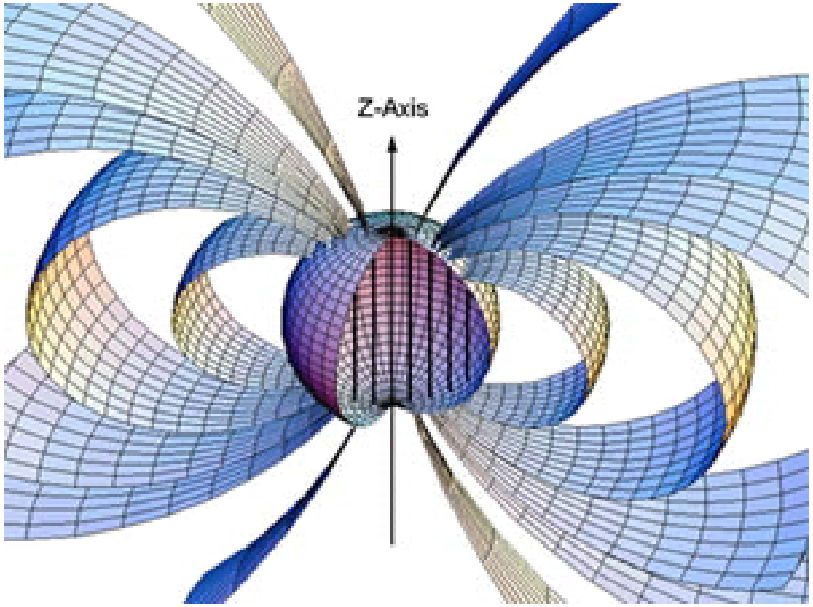

Derivation of the Magnetic Energy

The energy stored in the magnetic field of the electron is

$$E_{mag} = \frac{1}{2}\mu_0 \int_0^{2\pi}\int_0^{\pi}\int_0^{\infty} H^2 r^2 \sin\theta \, dr \, d\theta \, d\Phi$$

$$E_{mag\ \text{total}} = \frac{\pi \mu_0 e^2 \hbar^2}{m_e{}^2 r_1{}^3}$$

Electric Fields of Proton, Electron, and Hydrogen Atom

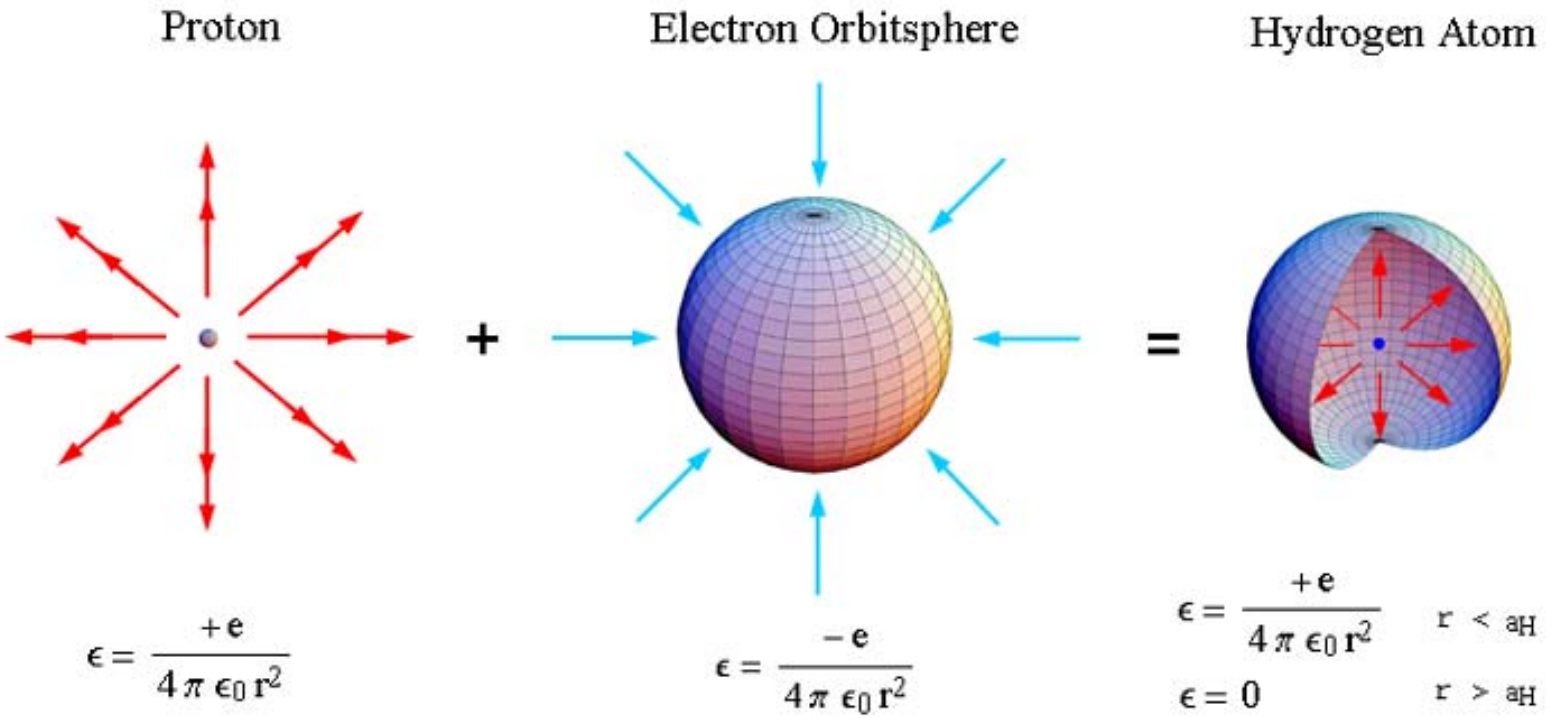

Force Balance Equation

$$\frac{m_e}{4\pi r_1^2}\frac{v_1^2}{r_1} = \frac{e}{4\pi r_1^2}\frac{Ze}{4\pi\varepsilon_0 r_1^2} - \frac{1}{4\pi r_1^2}\frac{\hbar^2}{m r_1^3}$$

$$r_1 = \frac{a_H}{Z}$$

Energy Calculations

- Potential Energy

$$V = \frac{-Ze^2}{4\pi\varepsilon_0 r_1} = \frac{-Z^2e^2}{4\pi\varepsilon_0 a_H} = -Z^2\ X\ 4.3675\ X\ 10^{-18}\ J = -Z^2\ X\ 27.2\ eV$$

- Kinetic Energy

$$T = \frac{Z^2e^2}{8\pi\varepsilon_0 a_H} = Z^2\ X\ 13.59\ eV \qquad T = E_{ele} = -\frac{1}{2}\varepsilon_0 \int_{\infty}^{r_1} \mathbf{E}^2 dv$$

where $\mathbf{E} = -\frac{Ze}{4\pi\varepsilon_0 r^2}$

- Electric Energy

$$E_{ele} = -\frac{Z^2e^2}{8\pi\varepsilon_0 a_H} = -Z^2\ X\ 2.1786\ X\ 10^{-18}\ J = -Z^2\ X\ 13.598\ eV$$

Relativistic Ionization Energies

The electron motion is perpendicular to the radius; thus, the radius is invariant to length contraction, the charge is invariant, and only the dependency of the radius on the relativistic mass needs to be considered.

Using the relativistic velocity with $m_e = m_e(v)$, the relativistic electron mass, and the radius from the force balance equation, the relativistic parameter β is

$$\beta = \frac{v}{c} = \frac{\hbar}{m_e c r} = \frac{\hbar}{m_e c \frac{a_0}{Z}\frac{m_{e0}}{m_e}\left(1+\frac{m_e}{m_p A}\right)} = \frac{\hbar}{m_{e0} c \frac{a_0}{Z}\left(1+\frac{m_e}{m_p A}\right)} = \frac{\alpha Z}{\left(1+\frac{m_{e0}}{2m_p A}\right)} \tag{1}$$

where Z is the nuclear charge and $m = Am_p$ is the nuclear mass with A being the atomic mass number.

Then, the relativistic radius of the bound electron is given by

$$r = \frac{a_0}{Z}\left(\sqrt{1-\frac{v^2}{c^2}}+\frac{m_{e0}}{m_p A}\right) = \frac{a_0}{Z}\left(\sqrt{1-\left(\frac{\alpha Z}{\left(1+\frac{m_{e0}}{2m_p A}\right)}\right)^2}+\frac{m_{e0}}{m_p A}\right) \tag{2}$$

The binding energy E_B is given by the negative of the sum of the relativistic potential V and kinetic energies T:

$$E_B = -(V+T) \tag{3}$$

In the case that the electron spin-nuclear interaction is negligible, E_B reduces to

$$E_B = m_{e0}c^2\left(1-\sqrt{1-(\alpha Z)^2}\right) \tag{4}$$

Some Calculated Parameters for the Hydrogen Atom (n=1)

radius	$r_1=a_{\mathrm{H}}$	5.2918×10^{-11} m
potential energy	$V=\frac{-e^2}{4\pi\varepsilon_o a_H}$	-27.196 eV
kinetic energy	$T=\frac{e^2}{8\pi\varepsilon_0 a_H}$	13.598 eV
angular velocity (spin)	$\omega_1=\frac{\hbar}{m_e r_1^2}$	4.13×10^{16} rads^{-1}
linear velocity	$v_1=r_1\omega_1$	2.19×10^{6} ms^{-1}
wavelength	$\lambda_1=2\pi r_1$	3.325×10^{-10} m
spin quantum number	$s=\frac{1}{2}$	$\frac{1}{2}$
moment of inertia	$I=\frac{m_e r_1^2}{2}$	1.277×10^{-51} kgm^2
angular kinetic energy	$E_{angular}=\frac{1}{2}I\omega_1^2$	6.795 eV

Some Calculated Parameters for the Hydrogen Atom (n=1) cont'd

magnitude of the angular momentum	$\hbar$	$1.0545\ X\ 10^{-34}\ Js$
projection of the angular momentum onto the transverse-axis	$\frac{\hbar}{4}$	$2.636\ X\ 10^{-35}\ Js$
projection of the angular momentum onto the z -axis	$S_z = \frac{\hbar}{2}$	$5.273\ X\ 10^{-35}\ Js$
mass density	$\frac{m_e}{4\pi r_1^2}$	$2.589\ X\ 10^{-11}\ kgm^{-2}$
charge -density	$\frac{e}{4\pi r_1^2}$	$4.553\ Cm^{-2}$

Relativistic ionization energies for some one-electron atoms

One e Atom	Z	β (Eq. (1.267) of Ref. [7])	Theoretical Ionization Energies (eV) (Eq. (1.272) of Ref. [7])	Experimental Ionization Energies (eV) [a]	Relative Difference between Experimental and Calculated [b]
H	1	0.00730	13.59847	13.59844	-0.000002
He^{+}	2	0.01459	54.41826	54.41778	-0.000009
Li^{2+}	3	0.02189	122.45637	122.45429	-0.000017
Be^{3+}	4	0.02919	217.72427	217.71865	-0.000026
Be^{4+}	5	0.03649	340.23871	340.2258	-0.000038
C^{5+}	6	0.04378	490.01759	489.99334	-0.000049
N^{6+}	7	0.05108	667.08834	667.046	-0.000063
O^{7+}	8	0.05838	871.47768	871.4101	-0.000078
F^{8+}	9	0.06568	1103.220	1103.1176	-0.000093
Ne^{9+}	10	0.07297	1362.348	1362.1995	-0.000109
Na^{10+}	11	0.08027	1648.910	1648.702	-0.000126
Mg^{11+}	12	0.08757	1962.945	1962.665	-0.000143
Al^{12+}	13	0.09486	2304.512	2304.141	-0.000161

[a] From theoretical calculations, interpolation of H isoelectronic and Rydberg series, and experimental data [35-38].

[b] (Experimental-theoretical)/experimental.

Relativistic ionization energies for some one-electron atoms cont'd

One e Atom	Z	β (Eq. (1.267) of Ref. [7])	Theoretical Ionization Energies (eV) (Eq. (1.272) of Ref. [7])	Experimental Ionization Energies (eV) [a]	Relative Difference between Experimental and Calculated [b]
Si^{13+}	14	0.10216	2673.658	2673.182	-0.000178
P^{14+}	15	0.10946	3070.451	3069.842	-0.000198
S^{15+}	16	0.11676	3494.949	3494.1892	-0.000217
Cl^{16+}	17	0.12405	3947.228	3946.296	-0.000236
Ar^{17+}	18	0.13135	4427.363	4426.2296	-0.000256
K^{18+}	19	0.13865	4935.419	4934.046	-0.000278
Ca^{19+}	20	0.14595	5471.494	5469.864	-0.000298
Sc^{20+}	21	0.15324	6035.681	6033.712	-0.000326
Ti^{21+}	22	0.16054	6628.064	6625.82	-0.000339
V^{22+}	23	0.16784	7248.745	7246.12	-0.000362
Cr^{23+}	24	0.17514	7897.827	7894.81	-0.000382
Mn^{24+}	25	0.18243	8575.426	8571.94	-0.000407
Fe^{25+}	26	0.18973	9281.650	9277.69	-0.000427

[a] From theoretical calculations, interpolation of H isoelectronic and Rydberg series, and experimental data [35-38].

[b] (Experimental-theoretical)/experimental.

Relativistic ionization energies for some one-electron atoms cont'd

One e Atom	Z	β (Eq. (1.267) of Ref. [7])	Theoretical Ionization Energies (eV) (Eq. (1.272) of Ref. [7])	Experimental Ionization Energies (eV) [a]	Relative Difference between Experimental and Calculated [b]
Co^{26+}	27	0.19703	10016.63	10012.12	-0.000450
Ni^{27+}	28	0.20432	10780.48	10775.4	-0.000471
Cu^{28+}	29	0.21162	11573.34	11567.617	-0.000495
Zn^{29+}	30	0.21892	12395.35	12388.93	-0.000518
Ga^{30+}	31	0.22622	13246.66	13239.49	-0.000542
Ge^{31+}	32	0.23351	14127.41	14119.43	-0.000565
As^{32+}	33	0.24081	15037.75	15028.62	-0.000608
Se^{33+}	34	0.24811	15977.86	15967.68	-0.000638
Kr^{35+}	36	0.26270	17948.05	17936.21	-0.000660
Rb^{36+}	37	0.27000	18978.49	18964.99	-0.000712
Mo^{41+}	42	0.30649	24592.04	24572.22	-0.000807
Xe^{53+}	54	0.39406	41346.76	41299.7	-0.001140
U^{91+}	92	0.67136	132279.32	131848.5	-0.003268

[a] From theoretical calculations, interpolation of H isoelectronic and Rydberg series, and experimental data [35-38].

[b] (Experimental-theoretical)/experimental.

Excited States

•The discretization of the angular momentum of the electron and the photon gives rise to quantized electron radii and energy levels.

•Transitions occur in integer units of the electron's inalienable intrinsic angular momentum of $\hbar$ wherein the exciting photons carry an integer multiple of $\hbar$.

• Thus, for $\mathbf{r} \times m_e \mathbf{v}_e = \mathbf{p}$ to be constant, the velocity of the electron source current decreases by a factor of the integer and the radius increases by the factor of the integer.

• Concomitantly, the photon field superposes that of the proton causing a resultant central field of a reciprocal integer that establishes the force balance at the excited state radius.

Excited States cont'd

- This quantization condition is equivalent to that of Bohr except that the electron angular momentum is $\hbar$, the angular momentum of one or more photons that give to an excited state is $n\hbar$, and the photon field changes the central force balance.

- Also, the standing wave regards the photon field and not the electron that comprises an extended current and is not a wave function. Thus, the quantization condition can also be considered as arising from the discretization of the photon standing wave including the integer spherical periodicity of the spherical harmonics of the exited state of the bound electron as a spherical cavity.

Excited States cont'd

- The orbitsphere is a dynamic spherical resonator cavity which traps photons of discrete frequencies.
- The relationship between an allowed radius and the "photon standing wave" wavelength is $2\pi r = n\lambda$
  where n is an integer.
- The relationship between an allowed radius and the electron wavelength is $2\pi r = n\lambda$
  where n=1,2,3,4,...
- The radius of an orbitsphere increases with the absorption of electromagnetic energy.
- The solutions to Maxwell's equations for modes that can be excited in the orbitsphere resonator cavity give rise to four quantum numbers, and the energies of the modes are the experimentally known hydrogen spectrum.

Excited States cont'd

The relationship between the electric field equation and the "trapped photon" source charge-density function is given by Maxwell's equation in two dimensions

$$\mathbf{n} \bullet \left(\mathbf{E}_1 - \mathbf{E}_2 \right) = \frac{\sigma}{\varepsilon_0}$$

The photon standing electromagnetic wave is phase matched to with the electron

$$\mathbf{E}_{r\,photon\;\; n,\ell,m} = \frac{e\left(na_H\right)^{\ell}}{4\pi\varepsilon_0}\frac{1}{r^{(\ell+2)}}\left[-Y_0^0\left(\theta,\phi\right)+\frac{1}{n}\left[Y_0^0\left(\theta,\phi\right)+\mathrm{Re}\left\{Y_\ell^m\left(\theta,\phi\right)e^{im\omega_n t}\right\}\right]\right]\delta(r-r_n)$$

$$n = 1,2,3,4,\ldots \qquad \ell = 1,2,\ldots,n-1 \qquad m=-\ell,-\ell+1,\ldots,0,\ldots,+\ell$$

$$\mathbf{E}_{r\,total} = \frac{e}{4\pi\varepsilon_0 r^2} + \frac{e\left(na_H\right)^{\ell}}{4\pi\varepsilon_0}\frac{1}{r^{(\ell+2)}}\left[-Y_0^0\left(\theta,\phi\right)+\frac{1}{n}\left[Y_0^0\left(\theta,\phi\right)+\mathrm{Re}\left\{Y_\ell^m\left(\theta,\phi\right)e^{im\omega_n t}\right\}\right]\right]\delta\left(r-r_n\right)$$

For $r=na_H$ and $m=0$, the total radial electric field is

$$\mathbf{E}_{r\,total} = \frac{1}{n}\frac{e}{4\pi\varepsilon_0\left(na_H\right)^2}$$

Photon Absorption

- The energy of the photon which excites a mode in the electron spherical resonator cavity from radius a_H to radius na_H is

$$E_{photon} = \frac{e^2}{8\pi\varepsilon_0 a_H}\left[1-\frac{1}{n^2}\right] = h\nu = \hbar\omega$$

- The change in angular velocity of the orbitsphere for an excitation from n=1 to n=n is

$$\Delta\omega = \frac{\hbar}{m_e\left(a_H\right)^2} - \frac{\hbar}{m_e\left(na_H\right)^2} = \frac{\hbar}{m_e\left(a_H\right)^2}\left[1-\frac{1}{n^2}\right]$$

- The kinetic energy change of the transition is

$$\frac{1}{2}m_e(\Delta v)^2 = \frac{e^2}{8\pi\varepsilon_0 a_H}\left[1-\frac{1}{n^2}\right] = \hbar\omega$$

  - The change in angular velocity of the electron orbitsphere is identical to the angular velocity of the photon necessary for the excitation, ω_{photon}
  - The **correspondence principle holds**

Source Current of Excited States Gives the Excited State Lifetimes and Transition Rates

In a nonradiative state, there is no emission or absorption of radiation corresponding to the absence of radial motion wherein the electric coefficient a_E is zero since $\mathbf{r} \cdot \mathbf{J} = 0$.

The physical characteristics of the photon and the electron are the basis of physically solving for excited states according to Maxwell's equations.

The vector potential of the current that connects the initial and final states of a transition is

$$\mathbf{A}(r) = \frac{\mu_0}{2\pi} \frac{e\hbar}{m_e} \frac{1}{r_{n_i} - r_{n_f}} \frac{e^{-jk_r}}{4\pi r} \mathbf{i}_z \qquad (1)$$

The magnetic and electric fields are derived from the vector potential and are used in the Poynting power vector to give the power.

The transition probability or Einstein coefficient A_{ki} for intial state n_i and final state n_f of atomic hydrogen given by the power divided by the energy of the transition is

$$\frac{1}{\tau} = \frac{1}{m_e c^2} \frac{\eta}{24\pi} \left(\frac{e\hbar}{m_e a_0^2} \right)^2 \frac{1}{\left(n_f n_i \right)^2} = 2.67 \times 10^9 \frac{1}{\left(n_f n_i \right)^2} s^{-1} \qquad (2)$$

which matches the NIST values for all transitions extremely well.

Orbital and Spin Splitting

The ratio of the square of the angular momentum, M^2, to the squre of the energy, U^2, for a pure (l, m) multipole

$$\frac{M^2}{U^2} = \frac{m^2}{\omega^2}$$

The magnetic moment is defined as $\mu = \dfrac{\text{charge x angular momentum}}{2 \text{ x mass}}$

The radiation of a mulipole of order (ℓ, m) carries $m\hbar$ units of the z component of angular momentum per photon of energy $\hbar\omega$. Thus, the z component of the angular momentum of the corresponding excited state electron oribitsphere is $L_z = m\hbar$.

Therefore,

$$\mu_z = \frac{em\hbar}{2m_e} = m\mu_B$$

where μ_B is the Bohr magnton.

The orbital splitting energy is

$$E_{mag}^{orb} = m\mu_B \mathbf{B}$$

Orbital and Spin Splitting cont'd

The spin and orbital splitting energies superimpose; thus, the principal excited state energy levels of the hydrogen atom are split by the energy $E_{mag}^{spin/orb}$

$$E_{mag}^{spin/orb} = m\frac{e\hbar}{2m_e}\mathbf{B} + m_s g\frac{e\hbar}{m_e}\mathbf{B}$$

where

$$n = 2,3,4,...$$
$$\ell = 1,2,...,n-1$$
$$m = -\ell,-\ell+1,...,0,...,+\ell$$
$$m_s = \pm\frac{1}{2}$$

Selection Rules for the Electric Dipole Transition

$$\Delta m = 0,\pm 1$$
$$\Delta m_s = 0$$

Resonant Line Shape

$$\frac{1}{\tau} = \frac{power}{energy} = \frac{1}{m_e c^2}\frac{\eta}{24\pi}\left(\frac{e\hbar}{m_e a_0^2}\right)^2\left[\frac{1}{n_i - n_f}\left(\frac{1}{n_f} - \frac{1}{n_i}\right)\right]^2$$

$$= 2.678\times 10^9 \Re s^{-1}$$

where $\Re$ is defined as $\Re = \left[\frac{1}{n_i - n_f}\left(\frac{1}{n_f} - \frac{1}{n_i}\right)\right]^2$

$$\mathbf{E}(\omega) \propto \int_0^\infty e^{-\alpha t} e^{-i\omega t} dt = \frac{1}{\alpha - i\omega}$$

The relationship between the rise-time and the band-width for exponential decay is

$$\tau\Gamma = \frac{1}{\pi}$$

The energy radiated per unit frequency interval is

$$\frac{dI(\omega)}{d\omega} = I_0 \frac{\Gamma}{2\pi}\frac{1}{(\omega - \omega_0 - \Delta\omega)^2 + (\Gamma/2)^2}$$

Broadening of the Spectral Line and the Radiative Reaction

Broadening of the spectral line due to the rise-time and shifting of the spectral line due to the radiative reaction. The resonant line shape has width Γ. The level shift is $\Delta\omega$.

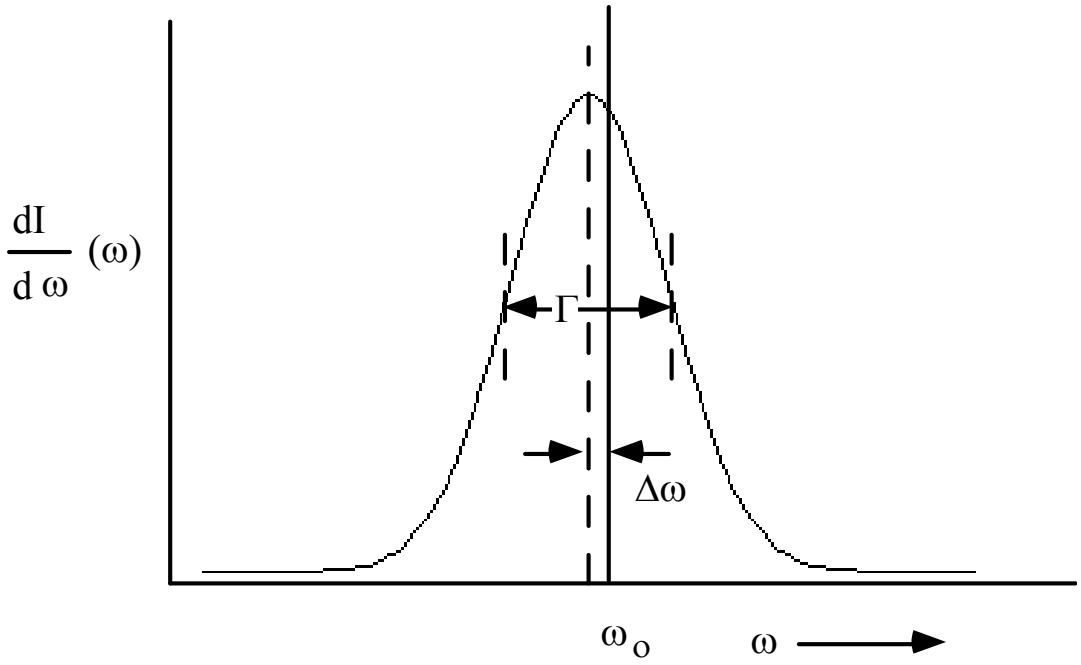

Hydrogen Lamb Shift

The hydrogen Lamb Shift corresponding to the transition energy of ${}^2P_{1/2} \rightarrow {}^2S_{1/2}$ is due to the radiation reaction force between the electron and the photon and conservation of energy and linear momentum involving recoil during emission.

The radiation reaction force shifts the H radius from $r_0 = 2a_H$ to

$$r = 2a_H - (2\pi\alpha)^2 \frac{\hbar}{6m_e c} = 1.99999744 a_H$$

The change in energy $\Delta E_{total}^{H\ Lamb}$ is given as the sum of the electric and magnetic energy changes and photon recoil energy:

$$\Delta E_{total}^{H\ Lamb} = \frac{-0.5e^2}{8\pi\varepsilon_o}\left[\frac{1}{r_0} - \frac{1}{r_-}\right] + 4\pi\mu_0\mu_B^2\left(\frac{1}{r_0^3} - \frac{1}{r_-^3}\right) + \frac{\left(-13.5983\ eV\left(1 - \frac{1}{2^2}\right)\right)^2}{2m_H c^2}$$

$$\begin{aligned}\Delta E_{total}^{H\ Lamb} &= 6.95953\ X\ 10^{-25}\ J - 4.38449\ X\ 10^{-27}\ J + 8.87591\ X\ 10^{-27}\ J \\ &= 7.00445\ X\ 10^{-25}\ J\end{aligned}$$

The Lamb shift energy expressed in terms of frequency:

$$\Delta f_{total}^{H\ Lamb} = 1057.09\ MHz$$

The experimental Lamb shift:

$$\Delta f_{total}^{H\ Lamb}(\text{experimental}) = 1057.845\ MHz$$

Given the 100 MHz natural linewidth of the $2P$ state, the 0.07% relative difference is within measurement error and the propagated errors in the fundamental constants of the equations.

Muonic Hydrogen Lamb Shift

The muonic hydrogen Lamb shift corresponding to the transition energy of $^2P_{1/2} \rightarrow {}^2S_{1/2}$ is also due to the radiation reaction force between the electron and the photon and conservation of energy and linear momentum involving recoil during emission wherein the muon, and also the tau, is a resonant particle production state of an electron.

The radiation reaction force shifts the muonic H radius from

$r_0 = 2a_{\mu p} = 9.6728246\ X\ 10^{-3} a_H$ ($a_{\mu p}$ is defined as $a_H \frac{m_e}{m_\mu}$) to

$$r = 2a_H \frac{m_e}{m_\mu} + \left[\left(2\pi\alpha\right)^2 + 2\left(2\pi\alpha\right)^3 - 3\left(2\pi\alpha\right)^4 \right] \frac{\hbar}{6 m_e c} = 2.0005735 a_{\mu p} = 9.6755983\ X\ 10^{-3} a_H$$

The change in energy $\Delta E_{total}^{\mu p\ Lamb}$ is given as the sum of the electric and magnetic energy changes and photon recoil energy:

$$\Delta E_{total}^{\mu p\ Lamb} = \frac{-0.5 e^2}{8\pi\varepsilon_0}\left[\frac{1}{r_0} - \frac{1}{r_+}\right] + 4\pi\mu_0 \mu_{B_\mu}^2 \left(\frac{1}{r_0^3} - \frac{1}{r_+^3}\right) + \frac{\left(-13.5983 \frac{m_\mu}{m_e}\ eV\left(1 - \frac{1}{2^2}\right)\right)^2}{2 m_{\mu p} c^2}$$

$$\begin{aligned} \Delta E_{total}^{\mu p\ Lamb} &= -3.22846\ X\ 10^{-20}\ J + 2.03334\ X\ 10^{-22}\ J - 3.41241\ X\ 10^{-22}\ J \\ &= -3.24225\ X\ 10^{-20}\ J \end{aligned}$$

The magnitude of the muonic H Lamb shift energy expressed in terms of frequency:

$$\Delta f_{total}^{\mu p\ Lamb} = 48{,}931.0\ GHz$$

Muonic Hydrogen Lamb Shift Cont'd

Using the literature values for $E_{2P_{3/2}^{F=2}\rightarrow 2P_{1/2}}$, the $^2P_{3/2}^{F=2}$ level shift with respect to the unperturbed $^2P_{1/2}$ level, and $E_{2S_{1/2}^{F=1}}$, the $^2S_{1/2}^{F=1}$ level shift with respect to the unperturbed $^2S_{1/2}$ level, $\Delta E_{total}^{\mu p\ Lamb}$ can be compared to the total energy of the muonic hydrogen Lamb shift corresponding to the transition $^2P_{3/2}F=2 \rightarrow {}^2S_{1/2}F=1$;

$$\begin{aligned}\Delta E_{total}^{\mu p\ Lamb\,^2P_{3/2}\ F=2\rightarrow {}^2S_{1/2}\ F=1} &= \Delta E_{total}^{\mu p\ Lamb} - E_{2P_{3/2}^{F=2}\rightarrow 2P_{1/2}} + E_{2S_{1/2}^{F=1}} \\ &= -3.24225\ X\ 10^{-20}\ J - 1.54199\ X\ 10^{-21}\ J + 9.13841\ X\ 10^{-22}\ J \\ &= -3.30507\ X\ 10^{-20}\ J\end{aligned}$$

The magnitude of the $^2P_{3/2}F=2 \rightarrow {}^2S_{1/2}\ F=1$ muonic hydrogen Lamb shift energy expressed in terms of frequency:

$$\Delta f_{total}^{\mu p\ Lamb\,^2P_{3/2}\ F=2\rightarrow {}^2S_{1/2}\ F=1} = 49{,}879.0\ GHz$$

The magnitude of the experimental muonic hydrogen Lamb shift matching the $^2S_{1/2}$ state lower than the $^2P_{1/2}$ state:

$$\Delta f_{total}^{\mu p\ Lamb\,^2P_{3/2}\ F=2\rightarrow {}^2S_{1/2}\ F=1}\left(\text{experimental}\right) = 49{,}881.88\ GHz$$

Given the 18.6 GHz natural linewidth of the $2P$ state, the 0.0058% relative difference is within the measurement error and the propagated errors in the fundamental constants of the equations. For example, the relative difference is 0.0025% using the 2002 CODATA constants.

Fine Structure Spin-Orbital Coupling

The energy of the $2P$ level is split by a relativistic interaction between the spin and orbital angular momentum as well as the corresponding radiation reaction force.

The corresponding energy $\Delta E_{total}^{H\ FS}$ and frequency $\Delta f_{total}^{H\ FS}$ for the transition ${}^2P_{1/2} \rightarrow {}^2P_{3/2}$ is known as the hydrogen fine structure and is given by the sum of the spin-orbital coupling energy

$$E_{s/o} = \frac{\alpha^5 (2\pi)^2}{8} m_e c^2 \sqrt{\frac{3}{4}} = 7.24043\ X\ 10^{-24}\ J$$

and the radiation reaction force that shifts the H radius from $r_0 = 2a_H$ to

$$r = 2a_H - (2\pi\alpha)^3 \frac{\hbar}{6m_e c} \sqrt{\frac{3}{4}} = 1.99999990 a_H$$

The radiation reaction energy of the hydrogen fine structure $\Delta E_{RRtotal}^{H\ FS}$ is given as the sum of the electric and magnetic energy changes:

$$\Delta E_{RRtotal}^{H\ FS} = \frac{-0.5e^2}{8\pi\varepsilon_0}\left[\frac{1}{r_0} - \frac{1}{r_-}\right] + 4\pi\mu_0\mu_B^2\left(\frac{1}{r_0^3} - \frac{1}{r_-^3}\right) = 2.76347\ X\ 10^{-26}\ J - 1.74098\ X\ 10^{-28}\ J$$

$$= 2.74606\ X\ 10^{-26}\ J$$

Then, the total energy of the hydrogen fine structure is given by the sum:

$$\Delta E_{total}^{H\ FS} = E_{s/o} + \Delta E_{RRtotal}^{H\ FS} = 7.24043\ X\ 10^{-24}\ J + 2.74606\ X\ 10^{-26}\ J = 7.26789\ X\ 10^{-24}\ J$$

The fine structure energy expressed in terms of frequency:

$$\Delta f_{total}^{H\ FS} = 10{,}968.46\ MHz$$

The experimental hydrogen fine structure:

$$\Delta f_{total}^{H\ FS}(\text{experimental}) = 10{,}969.05\ MHz$$

Given the large natural linewidth of the $2P$ state, the 0.005% relative difference is within the measurement error and propagated errors in the fundamental constants of the equations.

Hyperfine Structure

The hyperfine structure of the hydrogen atom is calculated from the force balance contribution between the electron and the proton.

The energy corresponds to the Stern-Gerlach and electric and magnetic energy changes.

The total energy of the transition from antiparallel to parallel alignment, $\Delta E_{total}^{S/N}$, is given as the sum:

$$\Delta E_{total}^{S/N} = -\mu_0 \mu_B \mu_P \sqrt{\frac{3}{4}} \left(\frac{1}{r_+^3} + \frac{1}{r_-^3} \right) + \frac{-e^2}{8\pi\varepsilon_0} \left[\frac{1}{r_+} - \frac{1}{r_-} \right] + \left(-1 - \left(\frac{2}{3} \right)^2 - \frac{\alpha}{4} \right) 4\pi\mu_o \mu_B^2 \left(\frac{1}{r_+^3} - \frac{1}{r_-^3} \right)$$

$$= -1.918365 \times 10^{-24} J + 9.597048 \times 10^{-25} J + 1.748861 * 10^{-26} J$$

$$= -9.411714 \times 10^{-25} J$$

where

$$r = a_H \pm \frac{2\pi\alpha \, \mu_P}{ec} \sqrt{\frac{3}{4}}$$

The energy is expressed in terms of wavelength using the Planck relationship:

$$\lambda = \frac{hc}{\Delta E_{total}^{S/N}} = 21.10610 \text{ cm}$$

The experimental value from the hydrogen maser is 21.10611 cm.

Muonium Hyperfine Structure Interval

The hyperfine structure of muonium is calculated from the force balance contribution between the electron and the muon.

The energy corresponds to the Stern-Gerlach and electric and magnetic energy changes.

The energy of the ground state ($1^2S_{1/2}$) hyperfine structure interval of muonium, $\Delta E\left(\Delta\nu_{Mu}\right)$

is given as the sum:

$$\Delta E\left(\Delta\nu_{Mu}\right) = -\mu_0\mu_B\mu_\mu\sqrt{\frac{3}{4}}\left(\frac{1}{r_{2+}^3}+\frac{1}{r_{2-}^3}\right)+\frac{-e^2}{8\pi\varepsilon_o}\left[\frac{1}{r_{2+}}-\frac{1}{r_{2-}}\right]$$

$$+4\pi\mu_0\left(-1-\left(\frac{2}{3}\cos\frac{\pi}{3}\right)^2-\alpha\right)\left(\mu_B^2\left(\frac{1}{r_{2+}^3}-\frac{1}{r_{2-}^3}\right)+\mu_{B,\mu}^2\left(\frac{1}{r_{1+}^3}-\frac{1}{r_{1-}^3}\right)\right)$$

$$= -6.02890320\times10^{-24}\,J + 3.02903048\times10^{-24}\,J + 4.23209178\times10^{-26}\,J + 1.36122030\times10^{-28}\,J$$

$$= -2.95741568\times10^{-24}\,J$$

where $r_2 = a_\mu \pm \dfrac{2\pi\alpha\ \mu_\mu}{ec}\sqrt{\dfrac{3}{4}}$ and $r_1 = \dfrac{a_\mu \pm \dfrac{2\pi\alpha\ \mu_\mu}{ec}\sqrt{\dfrac{3}{4}}}{\left(\dfrac{m_\mu}{m_e}\pm\dfrac{m_\mu e\alpha c}{2\hbar^2}\mu_0\ \mu_\mu\sqrt{\dfrac{3}{4}}\right)^{1/3}}$

Muonium Hyperfine Structure Interval cont'd

Using Planck's equation, the interval frequency, $\Delta\lambda_{Mu}$, and wavelength, $\Delta\nu_{Mu}$, are

$$\Delta\nu_{Mu} = 4.46330328 \text{ GHz}$$

$$\Delta\lambda_{Mu} = 6.71682919 \text{ cm}$$

The experimental hyperfine structure interval of muonium is

$$\Delta E(\Delta\nu_{Mu}) = -2.957415336 \times 10^{-24} \ J$$

$$\Delta\nu_{Mu} = 4.463302765(53)\text{GHz}\,(12\text{ppm})$$

$$\Delta\lambda_{Mu} = 6.71682998 \text{ cm}$$

Positronium Hyperfine Structure

The leptons are at the same radius, and the positronium hyperfine interval is given by the sum of the Stern-Gerlach, $\Delta E_{\text{spin-spin}}$, and spin-orbital coupling, $\Delta E_{s/o}({}^3S_1 \rightarrow {}^1S_0)$, energies.

The hyperfine structure interval of positronium (${}^3S_1 \rightarrow {}^1S_0$) is given by the sum:

$$\begin{aligned}
\Delta E_{\text{Ps hyperfine}} &= \Delta E_{\text{spin-spin}} + \Delta E_{s/o}({}^3S_1 \rightarrow {}^1S_0) \\
&= \frac{g\mu_0 e^2 \hbar^2}{8m_e^2 (2a_0)^3} + \frac{3g\alpha^5 (2\pi)^2}{8} m_e c^2 \sqrt{\frac{3}{4}} \\
&= \frac{g\alpha^5 (2\pi)^2}{8} m_e c^2 \left(\frac{1}{8\pi\alpha} + \frac{3\sqrt{3}}{2} \right) \\
&= 8.41155110 \times 10^{-4} \text{ eV}
\end{aligned}$$

Using Planck's equation, the interval in frequency, $\Delta\upsilon$, is

$$\Delta\upsilon = 203.39041 \text{ GHz}$$

The experimental ground-state hyperfine structure interval is

$$\Delta E_{\text{Ps hyperfine}}(\text{experimental}) = 8.41143 \times 10^{-4} \text{ eV}$$

$$\Delta\upsilon(\text{experimental}) = 203.38910(74) \text{ GHz} (3.6\text{ppm})$$

Excited States of Helium

The orbitsphere is a resonator cavity which traps single photons of discrete frequencies.

In the ground state of the helium atom, both electrons are at $r_1 = r_2 = 0.567a_0$.

When a photon is absorbed, one of the initially indistinguishable electrons called electron 1 moves to a smaller radius, and the other called electron 2 moves to a greater radius.

The radii of electron 2 are determined from the force balance of the electric, magnetic, and centrifugal forces that corresponds to the minimum of energy of the system.

The excited-state energies are then given by the electric energies at these radii.

Exemplary color scale, translucent views of the charge-densities of the inner and outer electrons of helium excited states. The spherical harmonic modulation functions propagate about the z-axis as spatially and temporally harmonic charge-density waves. The corresponding orbital function of the outer-electron modulates the time-constant (spin) function, (shown for t = 0; three-dimensional view). The inner electron is essentially that of He^+ (nuclei red, not to scale).

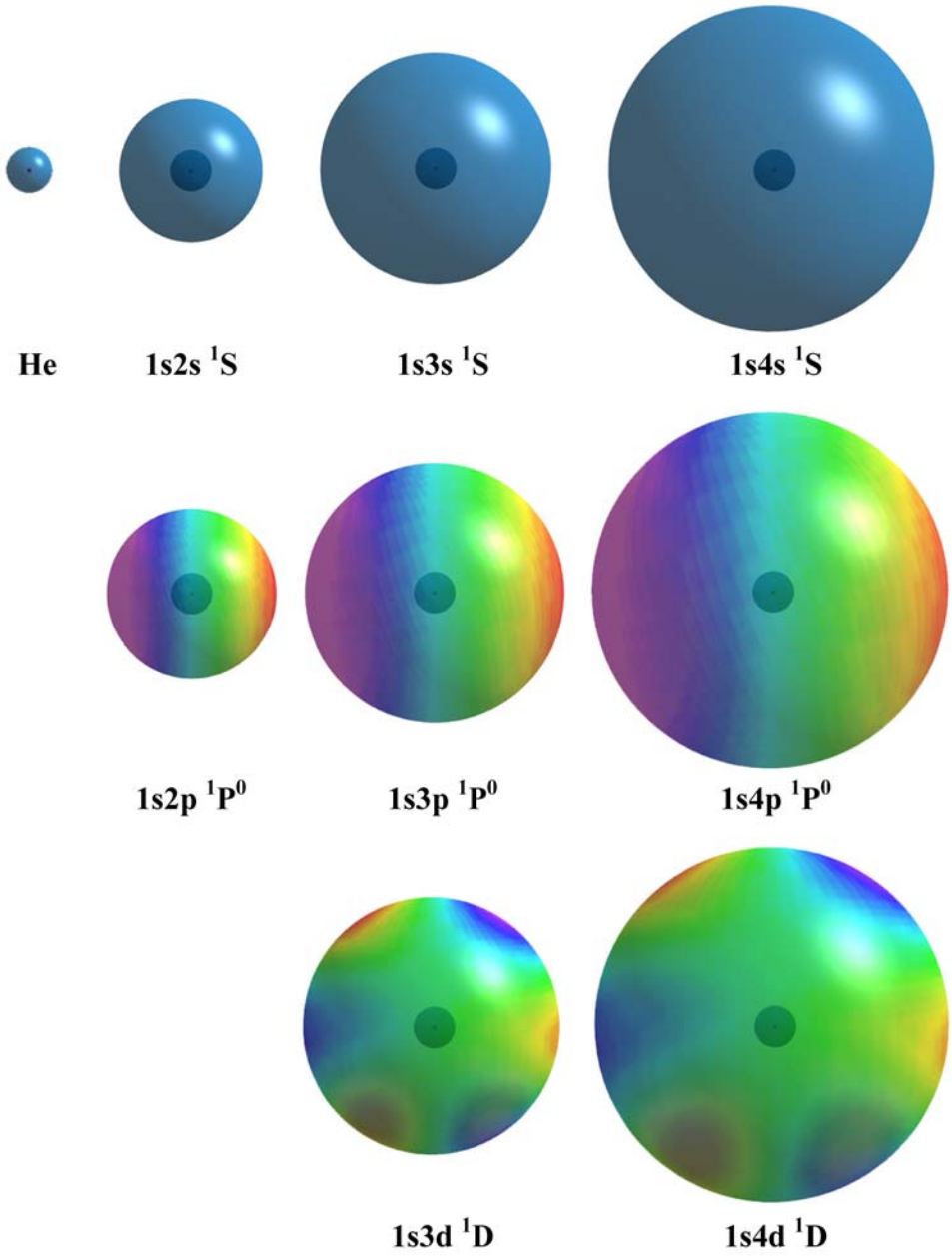

Excited States of Helium cont'd

Singlet Excited States with $\ell = 0$ ($1s^2 \rightarrow 1s^1(ns)^1$)

Force Balance Equation

$$\frac{m_e v^2}{r_2} = \frac{\hbar^2}{m_e r_2^3} = \frac{1}{n}\frac{e^2}{4\pi\varepsilon_0 r_2^2} + \frac{2}{3}\frac{1}{n}\frac{\hbar^2}{2m_e r_2^3}\sqrt{s(s+1)}$$

Radius of electron 2

$$r_2 = \left[n - \frac{\sqrt{\frac{3}{4}}}{3} \right] a_{He} \qquad n = 2,3,4,\ldots$$

The excited-state energy is the energy stored in the electric field, E_{ele}, which is the energy of electron 2 relative to the ionized electron at rest having zero energy:

$$E_{ele} = -\frac{1}{n}\frac{e^2}{8\pi\varepsilon_0 r_2}$$

Excited States of Helium cont'd

Triplet Excited States with $\ell = 0$ ($1s^2 \rightarrow 1s^1(ns)^1$)

Force Balance Equation

$$\frac{m_e v^2}{r_2} = \frac{\hbar^2}{m_e r_2^3} = \frac{1}{n}\frac{e^2}{4\pi\varepsilon_0 r_2^2} + 2\frac{2}{3}\frac{1}{n}\frac{\hbar^2}{2m_e r_2^3}\sqrt{s(s+1)}$$

Radius of electron 2

$$r_2 = \left[n - \frac{2\sqrt{\frac{3}{4}}}{3} \right] a_{He} \qquad n = 2,3,4,\ldots$$

Excited States of Helium cont'd

Singlet Excited States with $\ell \neq 0$

Force Balance Equation

$$\frac{m_e v^2}{r_2} = \frac{\hbar^2}{m_e r_2^3} = \frac{1}{n}\frac{e^2}{4\pi\varepsilon_0 r_2^2} - \frac{1}{n}\frac{\frac{3}{2}}{(2\ell+1)!!}\left(\frac{\ell+1}{\ell}\right)^{1/2}\frac{1}{\ell+2}\frac{1}{2}\frac{\hbar^2}{m_e r^3}\left(\sqrt{s(s+1)} - \sqrt{\frac{\ell}{\ell+1}}\right)$$

Radius of electron 2

$$r_2 = \left[n + \frac{\frac{3}{4}}{(2\ell+1)!!}\frac{1}{\ell+2}\left(\frac{\ell+1}{\ell}\right)^{1/2}\left(\sqrt{\frac{3}{4}} - \sqrt{\frac{\ell}{\ell+1}}\right)\right] a_{He} \qquad n = 2,3,4,\ldots$$

Excited States of Helium cont'd

Triplet Excited States with $\ell \neq 0$

Force Balance Equation

$$\frac{m_e v^2}{r_2} = \frac{\hbar^2}{m_e r_2^3} = \frac{1}{n}\frac{e^2}{4\pi\varepsilon_0 r_2^2} + \frac{1}{n}\frac{\frac{3}{2}}{(2\ell+1)!!}\left(\frac{\ell+1}{\ell}\right)^{1/2}\frac{1}{\ell+2}\frac{1}{2}\frac{\hbar^2}{m_e r^3}\left(2\sqrt{s(s+1)} - \sqrt{\frac{\ell}{\ell+1}}\right)$$

Radius of electron 2

$$r_2 = \left[n - \frac{\frac{3}{4}}{(2\ell+1)!!}\frac{1}{\ell+2}\left(\frac{\ell+1}{\ell}\right)^{1/2}\left(2\sqrt{\frac{3}{4}} - \sqrt{\frac{\ell}{\ell+1}}\right)\right]a_{He} \qquad n = 2,3,4,\ldots$$

Excited States of Helium cont'd

For over 100 states, the r-squared value is 0.999994, and the typical average relative difference is about 5 significant figures which is within the error of the experimental data.

Calculated and experimental energies of states of helium.

n	ℓ	r_1 (a_{He}) [a]	r_2 (a_{He}) [b]	**Term Symbol**	E_{ele} CP He I Energy Levels [c] (eV)	NIST He I Energy Levels [d] (eV)	Difference CP-NIST (eV)	Relative Difference [e] (CP-NIST)
1	0	0.56699	0.566987	$1s^2\ ^1S$	-24.58750	-24.58741	-0.000092	0.0000038
2	0	0.506514	1.42265	$1s2s\ ^3S$	-4.78116	-4.76777	-0.0133929	0.0028090
2	0	0.501820	1.71132	$1s2s\ ^1S$	-3.97465	-3.97161	-0.0030416	0.0007658
2	1	0.500571	1.87921	$1s2p\ ^3P^0_2$	-3.61957	-3.6233	0.0037349	-0.0010308
2	1	0.500571	1.87921	$1s2p\ ^3P^0_1$	-3.61957	-3.62329	0.0037249	-0.0010280
2	1	0.500571	1.87921	$1s2p\ ^3P^0_0$	-3.61957	-3.62317	0.0036049	-0.0009949
2	1	0.499929	2.01873	$1s2p\ ^1P^0$	-3.36941	-3.36936	-0.0000477	0.0000141

Excited States of Helium cont'd

n	ℓ	r_1 (a_{He}) [a]	r_2 (a_{He}) [b]	**Term Symbol**	E_{ele} CP He I Energy Levels [c] (eV)	NIST He I Energy Levels [d] (eV)	Difference CP-NIST (eV)	Relative Difference [e] (CP-NIST)
3	0	0.500850	2.42265	$1s3s\ ^3S$	-1.87176	-1.86892	-0.0028377	0.0015184
3	0	0.500302	2.71132	$1s3s\ ^1S$	-1.67247	-1.66707	-0.0054014	0.0032401
3	1	0.500105	2.87921	$1s3p\ ^3P^0_2$	-1.57495	-1.58031	0.0053590	-0.0033911
3	1	0.500105	2.87921	$1s3p\ ^3P^0_1$	-1.57495	-1.58031	0.0053590	-0.0033911
3	1	0.500105	2.87921	$1s3p\ ^3P^0_0$	-1.57495	-1.58027	0.0053190	-0.0033659
3	2	0.500011	2.98598	$1s3d\ ^3D_3$	-1.51863	-1.51373	-0.0049031	0.0032391
3	2	0.500011	2.98598	$1s3d\ ^3D_2$	-1.51863	-1.51373	-0.0049031	0.0032391
3	2	0.500011	2.98598	$1s3d\ ^3D_1$	-1.51863	-1.51373	-0.0049031	0.0032391
3	2	0.499999	3.00076	$1s3d\ ^1D$	-1.51116	-1.51331	0.0021542	-0.0014235
3	1	0.499986	3.01873	$1s3p\ ^1P^0$	-1.50216	-1.50036	-0.0017999	0.0011997
4	0	0.500225	3.42265	$1s4s\ ^3S$	-0.99366	-0.99342	-0.0002429	0.0002445
4	0	0.500088	3.71132	$1s4s\ ^1S$	-0.91637	-0.91381	-0.0025636	0.0028054
4	1	0.500032	3.87921	$1s4p\ ^3P^0_2$	-0.87671	-0.87949	0.0027752	-0.0031555
4	1	0.500032	3.87921	$1s4p\ ^3P^0_1$	-0.87671	-0.87949	0.0027752	-0.0031555
4	1	0.500032	3.87921	$1s4p\ ^3P^0_0$	-0.87671	-0.87948	0.0027652	-0.0031442
4	2	0.500003	3.98598	$1s4d\ ^3D_3$	-0.85323	-0.85129	-0.0019398	0.0022787
4	2	0.500003	3.98598	$1s4d\ ^3D_2$	-0.85323	-0.85129	-0.0019398	0.0022787
4	2	0.500003	3.98598	$1s4d\ ^3D_1$	-0.85323	-0.85129	-0.0019398	0.0022787

Excited States of Helium cont'd

n	ℓ	r_1 (a_{He}) a	r_2 (a_{He}) b	**Term Symbol**	E_{ele} CP He I Energy Levels c (eV)	NIST He I Energy Levels d (eV)	Difference CP-NIST (eV)	Relative Difference e (CP-NIST)
4	2	0.500000	4.00076	$1s4d\ ^1D$	-0.85008	-0.85105	0.0009711	-0.0011411
4	3	0.500000	3.99857	$1s4f\ ^3F^0_3$	-0.85054	-0.85038	-0.0001638	0.0001926
4	3	0.500000	3.99857	$1s4f\ ^3F^0_4$	-0.85054	-0.85038	-0.0001638	0.0001926
4	3	0.500000	3.99857	$1s4f\ ^3F^0_2$	-0.85054	-0.85038	-0.0001638	0.0001926
4	3	0.500000	4.00000	$1s4f\ ^1F^0$	-0.85024	-0.85037	0.0001300	-0.0001529
4	1	0.499995	4.01873	$1s4p\ ^1P^0$	-0.84628	-0.84531	-0.0009676	0.0011446
5	0	0.500083	4.42265	$1s5s\ ^3S$	-0.61519	-0.61541	0.0002204	-0.0003582
5	0	0.500035	4.71132	$1s5s\ ^1S$	-0.57750	-0.57617	-0.0013253	0.0023002
5	1	0.500013	4.87921	$1s5p\ ^3P^0_2$	-0.55762	-0.55916	0.0015352	-0.0027456
5	1	0.500013	4.87921	$1s5p\ ^3P^0_1$	-0.55762	-0.55916	0.0015352	-0.0027456
5	1	0.500013	4.87921	$1s5p\ ^3P^0_0$	-0.55762	-0.55915	0.0015252	-0.0027277
5	2	0.500001	4.98598	$1s5d\ ^3D_3$	-0.54568	-0.54472	-0.0009633	0.0017685
5	2	0.500001	4.98598	$1s5d\ ^3D_2$	-0.54568	-0.54472	-0.0009633	0.0017685
5	2	0.500001	4.98598	$1s5d\ ^3D_1$	-0.54568	-0.54472	-0.0009633	0.0017685
5	2	0.500000	5.00076	$1s5d\ ^1D$	-0.54407	-0.54458	0.0005089	-0.0009345
5	3	0.500000	4.99857	$1s5f\ ^3F^0_3$	-0.54431	-0.54423	-0.0000791	0.0001454
5	3	0.500000	4.99857	$1s5f\ ^3F^0_4$	-0.54431	-0.54423	-0.0000791	0.0001454
5	3	0.500000	4.99857	$1s5f\ ^3F^0_2$	-0.54431	-0.54423	-0.0000791	0.0001454
5	3	0.500000	5.00000	$1s5f\ ^1F^0$	-0.54415	-0.54423	0.0000764	-0.0001404

Excited States of Helium cont'd

n	ℓ	r_1 (a_{He}) [a]	r_2 (a_{He}) [b]	**Term Symbol**	E_{ele} CP He I Energy Levels [c] (eV)	NIST He I Energy Levels [d] (eV)	Difference CP-NIST (eV)	Relative Difference [e] (CP-NIST)
5	4	0.500000	4.99988	$1s5g\ ^3G_4$	-0.54417	-0.54417	0.0000029	-0.0000054
5	4	0.500000	4.99988	$1s5g\ ^3G_5$	-0.54417	-0.54417	0.0000029	-0.0000054
5	4	0.500000	4.99988	$1s5g\ ^3G_3$	-0.54417	-0.54417	0.0000029	-0.0000054
5	4	0.500000	5.00000	$1s5g\ ^1G$	-0.54415	-0.54417	0.0000159	-0.0000293
5	1	0.499998	5.01873	$1s5p\ ^1P^0$	-0.54212	-0.54158	-0.0005429	0.0010025
6	0	0.500038	5.42265	$1s6s\ ^3S$	-0.41812	-0.41838	0.0002621	-0.0006266
6	0	0.500016	5.71132	$1s6s\ ^1S$	-0.39698	-0.39622	-0.0007644	0.0019291
6	1	0.500006	5.87921	$1s6p\ ^3P^0_2$	-0.38565	-0.38657	0.0009218	-0.0023845
6	1	0.500006	5.87921	$1s6p\ ^3P^0_1$	-0.38565	-0.38657	0.0009218	-0.0023845
6	1	0.500006	5.87921	$1s6p\ ^3P^0_0$	-0.38565	-0.38657	0.0009218	-0.0023845
6	2	0.500001	5.98598	$1s6d\ ^3D_3$	-0.37877	-0.37822	-0.0005493	0.0014523
6	2	0.500001	5.98598	$1s6d\ ^3D_2$	-0.37877	-0.37822	-0.0005493	0.0014523
6	2	0.500001	5.98598	$1s6d\ ^3D_1$	-0.37877	-0.37822	-0.0005493	0.0014523
6	2	0.500000	6.00076	$1s6d\ ^1D$	-0.37784	-0.37813	0.0002933	-0.0007757
6	3	0.500000	5.99857	$1s6f\ ^3F^0_3$	-0.37797	-0.37793	-0.0000444	0.0001176
6	3	0.500000	5.99857	$1s6f\ ^3F^0_4$	-0.37797	-0.37793	-0.0000444	0.0001176
6	3	0.500000	5.99857	$1s6f\ ^3F^0_2$	-0.37797	-0.37793	-0.0000444	0.0001176
6	3	0.500000	6.00000	$1s6f\ ^1F^0$	-0.37788	-0.37793	0.0000456	-0.0001205

Excited States of Helium cont'd

n	ℓ	r_1 (a_{He}) [a]	r_2 (a_{He}) [b]	**Term Symbol**	E_{ele} CP He I Energy Levels [c] (eV)	NIST He I Energy Levels [d] (eV)	Difference CP-NIST (eV)	Relative Difference [e] (CP-NIST)
6	4	0.500000	5.99988	$1s6g\ ^3G_4$	-0.37789	-0.37789	-0.0000023	0.0000060
6	4	0.500000	5.99988	$1s6g\ ^3G_5$	-0.37789	-0.37789	-0.0000023	0.0000060
6	4	0.500000	5.99988	$1s6g\ ^3G_3$	-0.37789	-0.37789	-0.0000023	0.0000060
6	4	0.500000	6.00000	$1s6g\ ^1G$	-0.37788	-0.37789	0.0000053	-0.0000140
6	5	0.500000	5.99999	$1s6h\ ^3H^0_4$	-0.37789	-0.37788	-0.0000050	0.0000133
6	5	0.500000	5.99999	$1s6h\ ^3H^0_5$	-0.37789	-0.37788	-0.0000050	0.0000133
6	5	0.500000	5.99999	$1s6h\ ^3H^0_6$	-0.37789	-0.37788	-0.0000050	0.0000133
6	5	0.500000	6.00000	$1s6h\ ^1H^0$	-0.37788	-0.37788	-0.0000045	0.0000119
6	1	0.499999	6.01873	$1s6p\ ^1P^0$	-0.37671	-0.37638	-0.0003286	0.0008730
7	0	0.500019	6.42265	$1s7s\ ^3S$	-0.30259	-0.30282	0.0002337	-0.0007718
7	0	0.500009	6.71132	$1s7s\ ^1S$	-0.28957	-0.2891	-0.0004711	0.0016295
7	1	0.500003	6.87921	$1s7p\ ^3P^0_2$	-0.28250	-0.28309	0.0005858	-0.0020692
7	1	0.500003	6.87921	$1s7p\ ^3P^0_1$	-0.28250	-0.28309	0.0005858	-0.0020692
7	1	0.500003	6.87921	$1s7p\ ^3P^0_0$	-0.28250	-0.28309	0.0005858	-0.0020692
7	2	0.500000	6.98598	$1s7d\ ^3D_3$	-0.27819	-0.27784	-0.0003464	0.0012468
7	2	0.500000	6.98598	$1s7d\ ^3D_2$	-0.27819	-0.27784	-0.0003464	0.0012468
7	2	0.500000	6.98598	$1s7d\ ^3D_1$	-0.27819	-0.27784	-0.0003464	0.0012468
7	2	0.500000	7.00076	$1s7d\ ^1D$	-0.27760	-0.27779	0.0001907	-0.0006864

Excited States of Helium cont'd

n	ℓ	r_1 (a_{He}) a	r_2 (a_{He}) b	**Term Symbol**	E_{ele} CP He I Energy Levels c (eV)	NIST He I Energy Levels d (eV)	Difference CP-NIST (eV)	Relative Difference e (CP-NIST)
7	3	0.500000	6.99857	$1s7f\ ^3F^0_3$	-0.27769	-0.27766	-0.0000261	0.0000939
7	3	0.500000	6.99857	$1s7f\ ^3F^0_4$	-0.27769	-0.27766	-0.0000261	0.0000939
7	3	0.500000	6.99857	$1s7f\ ^3F^0_2$	-0.27769	-0.27766	-0.0000261	0.0000939
7	3	0.500000	7.00000	$1s7f\ ^1F^0$	-0.27763	-0.27766	0.0000306	-0.0001102
7	4	0.500000	6.99988	$1s7g\ ^3G_4$	-0.27763	-0.27763	-0.0000043	0.0000155
7	4	0.500000	6.99988	$1s7g\ ^3G_5$	-0.27763	-0.27763	-0.0000043	0.0000155
7	4	0.500000	6.99988	$1s7g\ ^3G_3$	-0.27763	-0.27763	-0.0000043	0.0000155
7	4	0.500000	7.00000	$1s7g\ ^1G$	-0.27763	-0.27763	0.0000004	-0.0000016
7	5	0.500000	6.99999	$1s7h\ ^3H^0_5$	-0.27763	-0.27763	0.0000002	-0.0000009
7	5	0.500000	6.99999	$1s7h\ ^3H^0_6$	-0.27763	-0.27763	0.0000002	-0.0000009
7	5	0.500000	6.99999	$1s7h\ ^3H^0_4$	-0.27763	-0.27763	0.0000002	-0.0000009
7	5	0.500000	7.00000	$1s7h\ ^1H^0$	-0.27763	-0.27763	0.0000006	-0.0000021
7	6	0.500000	7.00000	$1s7\ i^3I_5$	-0.27763	-0.27762	-0.0000094	0.0000339
7	6	0.500000	7.00000	$1s7i\ ^3I6$	-0.27763	-0.27762	-0.0000094	0.0000339
7	6	0.500000	6.78349	$1s7i\ ^3I_7$	-0.27763	-0.27762	-0.0000094	0.0000339
7	6	0.500000	7.00000	$1s7i\ ^1I$	-0.27763	-0.27762	-0.0000094	0.0000338
7	1	0.500000	7.01873	$1s7p\ ^1P^0$	-0.27689	-0.27667	-0.0002186	0.0007900

Excited States of Helium cont'd

n	ℓ	r_1 (a_{He}) a	r_2 (a_{He}) b	**Term Symbol**	E_{ele} CP He I Energy Levels c (eV)	NIST He I Energy Levels d (eV)	Difference CP-NIST (eV)	Relative Difference e (CP-NIST)
8	0	0.500011	7.42265	$1s8s\ ^3S$	-0.22909	-0.22928	0.0001866	-0.0008139
8	0	0.500005	7.71132	$1s8s\ ^1S$	-0.22052	-0.2202	-0.0003172	0.0014407
9	0	0.500007	8.42265	$1s9s\ ^3S$	-0.17946	-0.17961	0.0001489	-0.0008291
9	0	0.500003	8.71132	$1s9s\ ^1S$	-0.17351	-0.1733	-0.0002141	0.0012355
10	0	0.500004	9.42265	$1s10s\ ^3S$	-0.14437	-0.1445	0.0001262	-0.0008732
10	0	0.500002	9.71132	$1s10s\ ^1S$	-0.14008	-0.13992	-0.0001622	0.0011594
11	0	0.500003	10.42265	$1s11s\ ^3S$	-0.11866	-0.11876	0.0001037	-0.0008734
11	0	0.500001	10.71132	$1s11s\ ^1S$	-0.11546	-0.11534	-0.0001184	0.0010268
						Avg.	**-0.000112**	**0.0000386**

Instability of Excited States

The relationship between the electric field equation and the "trapped photon" source charge-density function is given by Maxwell's equation in two dimensions

$$\mathbf{n} \bullet \left(\mathbf{E}_1 - \mathbf{E}_2\right) = \frac{\sigma}{\varepsilon_0}$$

$$n = 2,3,4,\ldots,$$

$$\sigma_{photon} = \frac{e}{4\pi r_n^2}\left[Y_0^0\left(\theta,\phi\right) - \frac{1}{n}\left[Y_0^0\left(\theta,\phi\right) + \mathrm{Re}\left\{ Y_\ell^m\left(\theta,\phi\right) e^{im\omega_n t} \right\} \right] \right] \delta(r - r_n)$$

$$\sigma_{electron} = \frac{-e}{4\pi r_n^2}\left[Y_0^0\left(\theta,\phi\right) + \mathrm{Re}\left\{ Y_\ell^m\left(\theta,\phi\right) e^{im\omega_n t} \right\} \right] \delta(r - r_n)$$

$$\sigma_{photon} + \sigma_{electron} = \frac{e}{4\pi (r_n)^2}$$

$$\left[Y_0^0(\theta,\phi)\dot{\delta}(r - r_n) - \frac{1}{n} Y_0^0(\theta,\phi)\delta(r - r_n) - \left(1 + \frac{1}{n}\right)\left[\mathrm{Re}\left\{ Y_\ell^m\left(\theta,\phi\right) e^{i\omega_n t} \right\} \right] \delta(r - r_n) \right]$$

Excited states are radiative since spacetime harmonics of $\frac{\omega_n}{c} = k$ or $\frac{\omega_n}{c}\sqrt{\frac{\varepsilon}{\varepsilon_0}} = k$ do exist for which the spacetime Fourier transform of the current density function is nonzero.

Stability of "Ground" and Hydrino States

$$\sigma_{photon} = \frac{e}{4\pi (r_n)^2}\left[Y_0^0(\theta,\phi) - \frac{1}{n}\left[Y_0^0(\theta,\phi) + \mathrm{Re}\left\{Y_\ell^m(\theta,\phi)e^{i\omega_n t}\right\}\right]\right]\delta(r-r_n) \qquad n = 1, \frac{1}{2}, \frac{1}{3}, \frac{1}{4}, \ldots,$$

$$\sigma_{electron} = \frac{-e}{4\pi (r_n)^2}\left[Y_0^0(\theta,\phi) + \mathrm{Re}\left\{Y_\ell^m(\theta,\phi)e^{i\omega_n t}\right\}\right]\delta(r-r_n) \qquad n = 1, \frac{1}{2}, \frac{1}{3}, \frac{1}{4}, \ldots,$$

$$\sigma_{photon} + \sigma_{electron} = \frac{-e}{4\pi r_n^2}\left[\frac{1}{n}Y_0^0(\theta,\phi) + \left(1+\frac{1}{n}\right)\mathrm{Re}\left\{Y_\ell^m(\theta,\phi)e^{im\omega_n t}\right\}\right]\delta(r-r_n)$$

These states are nonradiative since spacetime harmonics of $\frac{\omega_n}{c} = k$ or $\frac{\omega_n}{c}\sqrt{\frac{\varepsilon}{\varepsilon_o}} = k$ for which the Fourier transform of the current-density function is nonzero do not exist.

Photon Equations

The angular-momentum density, $\mathbf{m}$, of the emitted photon is

$$\mathbf{m} = \int \frac{1}{8\pi c} \mathrm{Re}\left[\mathbf{r} \times (\mathbf{E} \times \mathbf{B}^*)\right] dx^4 = \hbar$$

The Cartesian coordinate system x'y'z' wherein the first great circle magnetic field line lies in the x'z'-plane, and the second great circle electric field line lies in the y'z'-plane.

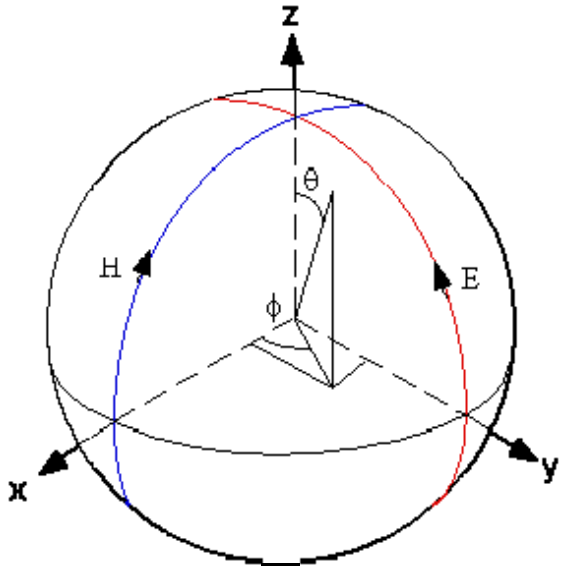

The Field-Line Pattern of the Right-Handed Circularly Polarized Photon is Generated by a Rotation of the Orthogonal Great Circle Electric and Magnetic Field Lines

The right-handed-circularly-polarized photon electric and magnetic vector field (RHCP photon-e&mvf) is generated by the rotation of the basis elements comprising the great circle magnetic field line in the xz-plane and the great circle electric field line in the yz-plane about the (i_x, i_y, $0i_z$)-axis by $\frac{\pi}{2}$:

E FIELD and H FIELD:

$$\begin{bmatrix} x' \\ y' \\ z' \end{bmatrix} = \begin{bmatrix} \frac{1}{2}+\frac{\cos\theta}{2} & \frac{1}{2}-\frac{\cos\theta}{2} & -\frac{\sin\theta}{\sqrt{2}} \\ \frac{1}{2}-\frac{\cos\theta}{2} & \frac{1}{2}+\frac{\cos\theta}{2} & \frac{\sin\theta}{\sqrt{2}} \\ \frac{\sin\theta}{\sqrt{2}} & -\frac{\sin\theta}{\sqrt{2}} & \cos\theta \end{bmatrix} \bullet \left(\begin{bmatrix} 0 \\ r_n\cos\phi \\ r_n\sin\phi \end{bmatrix}_{\text{Red}} + \begin{bmatrix} r_n\cos\phi \\ 0 \\ r_n\sin\phi \end{bmatrix}_{\text{Blue}} \right)$$

The Field-Line Pattern of a Right-Handed Circularly-Polarized Photon

Electric field lines red --- Magnetic field lines blue

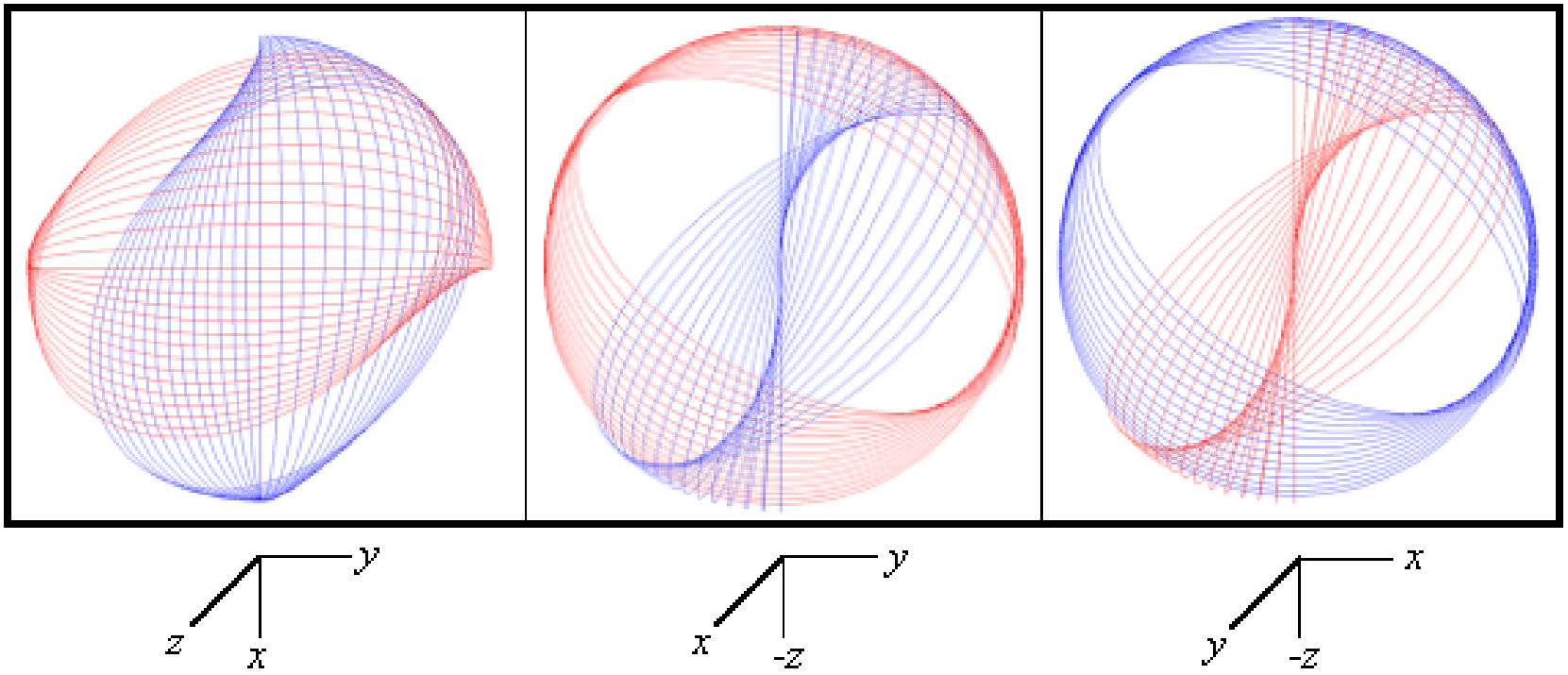

The Field-Line Pattern of the Left-Handed Circularly Polarized Photon is Generated by a Rotation of the Orthogonal Great Circle Electric and Magnetic Field Lines

The left-handed-circularly-polarized photon electric and magnetic vector field (LHCP photon-e&mvf) is generated by the rotation of the basis elements comprising the great circle magnetic field line in the xz-plane and the great circle electric field line in the yz-plane about the (i_x, $-i_y$, $0i_z$)-axis by $\frac{\pi}{2}$:

E FIELD and H FIELD:

$$\begin{bmatrix} x' \\ y' \\ z' \end{bmatrix} = \begin{bmatrix} \frac{1}{2}+\frac{\cos\theta}{2} & -\frac{1}{2}+\frac{\cos\theta}{2} & \frac{\sin\theta}{\sqrt{2}} \\ -\frac{1}{2}+\frac{\cos\theta}{2} & \frac{1}{2}+\frac{\cos\theta}{2} & \frac{\sin\theta}{\sqrt{2}} \\ -\frac{\sin\theta}{\sqrt{2}} & -\frac{\sin\theta}{\sqrt{2}} & \cos\theta \end{bmatrix} \bullet \left(\begin{bmatrix} 0 \\ r_n \cos\phi \\ r_n \sin\phi \end{bmatrix}_{\text{Red}} + \begin{bmatrix} r_n \cos\phi \\ 0 \\ r_n \sin\phi \end{bmatrix}_{\text{Blue}} \right)$$

The Field-Line Pattern of a Left-Handed Circularly Polarized Photon

Electric field lines red --- Magnetic field lines blue

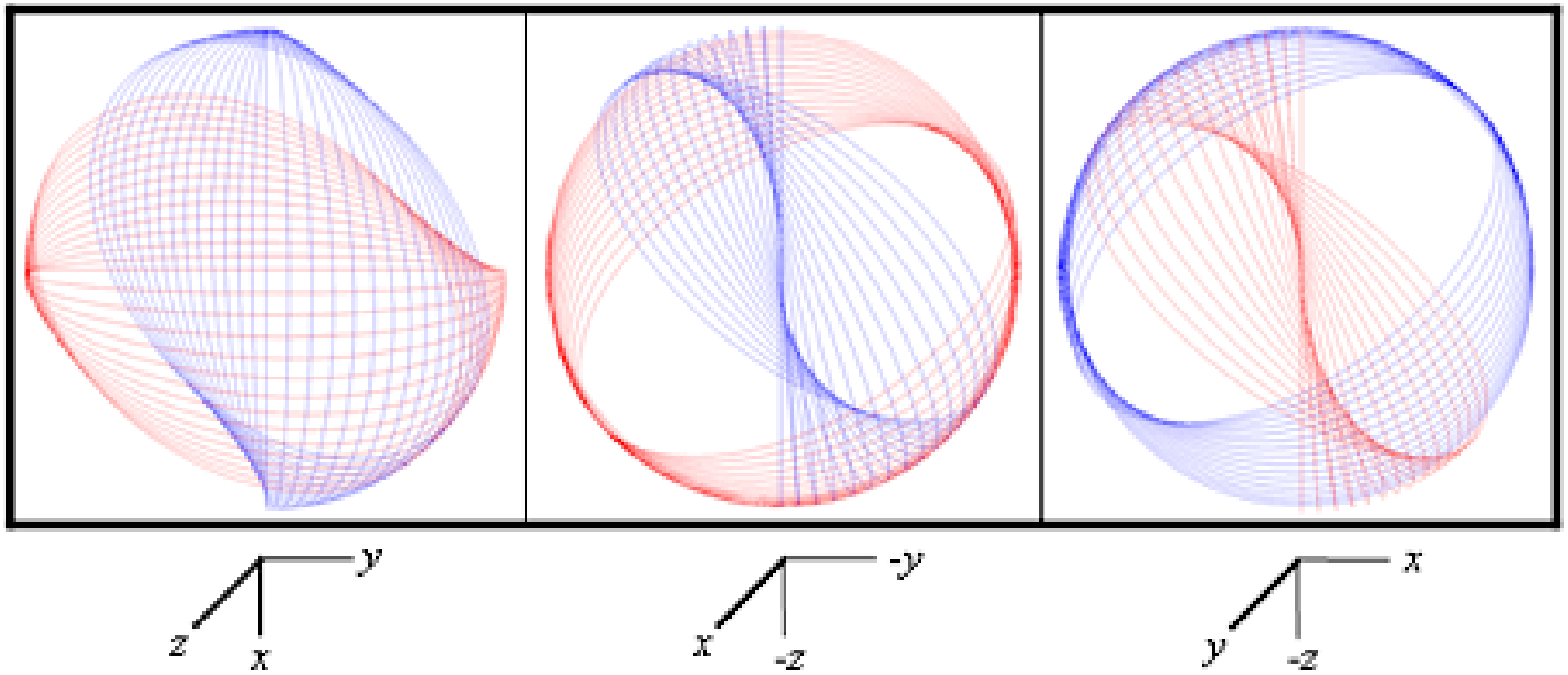

The Field-Line Pattern of a Linearly Polarized Photon

The linearly polarized (LP) photon-e&mvf is generated by the superposition of the RHCP photon-e&mvf and the LHCP photon-e&mvf:

Electric field lines red --- Magnetic field lines blue

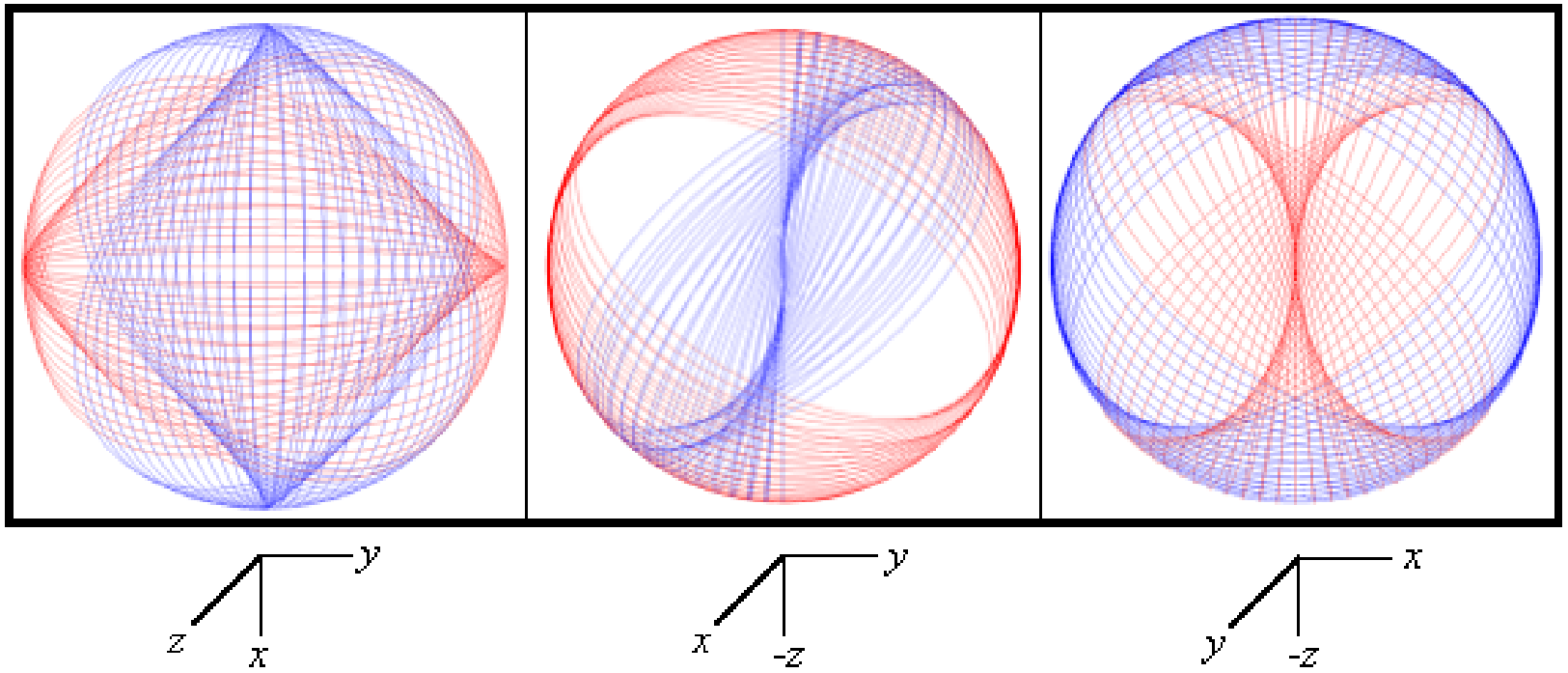

The Field of the Photon Observed from the Laboratory Frame

Consider an observer at the origin of his frame with the photon-e&mvf stationary in its own frame propagating at light-speed *c* relative to the observer along its z-axis ($z_{photon\text{-}e\&mvf}$) that is collinear to the z-axis of the observer, $z_{laboratory}$. Electric field lines red, magnetic field lines blue.

RHCP photon in its own reference frame

RHCP photon in the lab reference frame as it passes a fixed point over time.

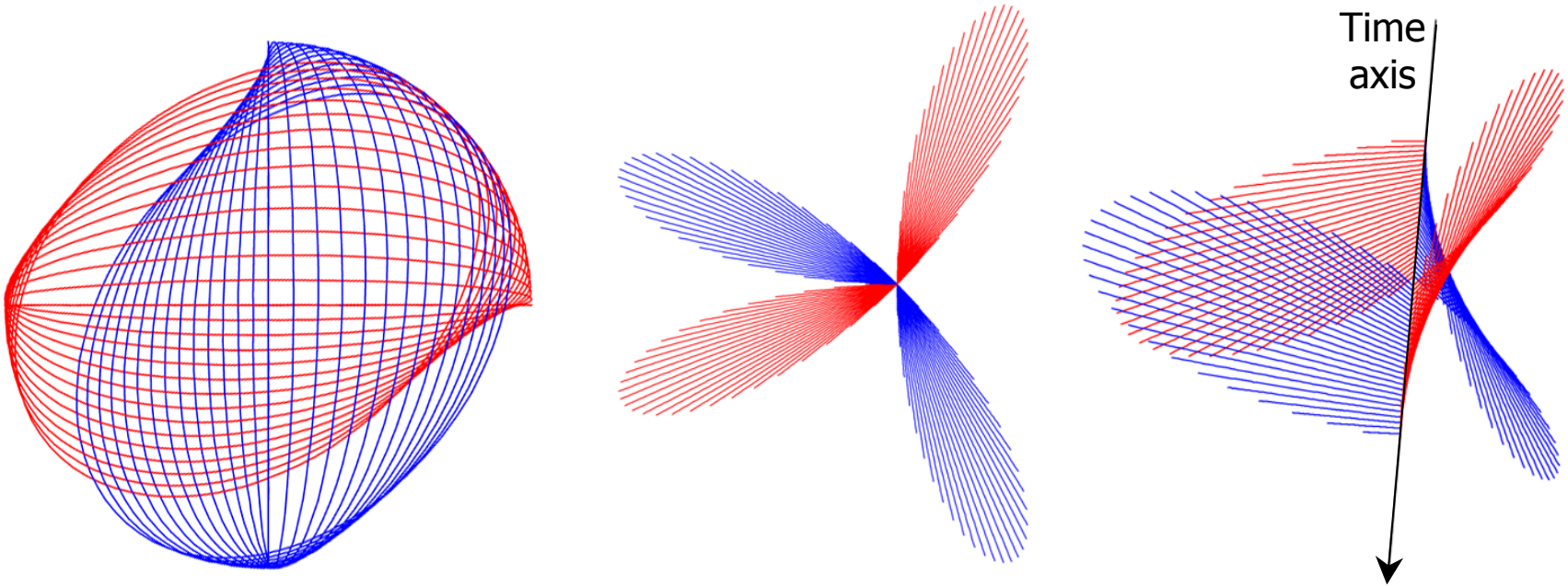

Electric Field of a Moving Point Charge $v = {}^{1}/_{3}c$

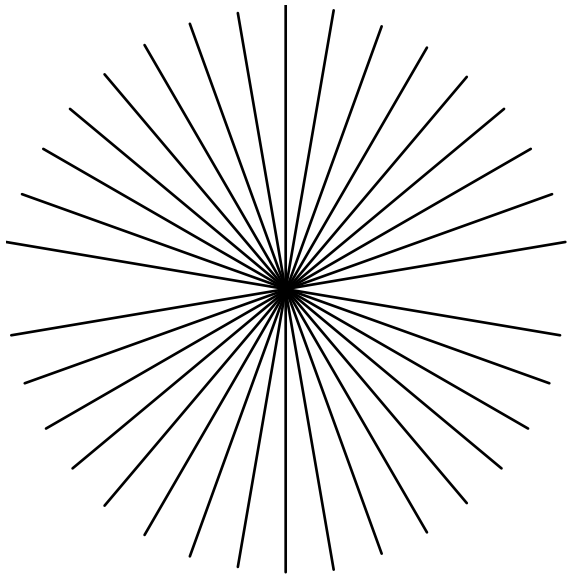

Electric Field of a Moving Point Charge $v = {}^{4}/_{5}c$

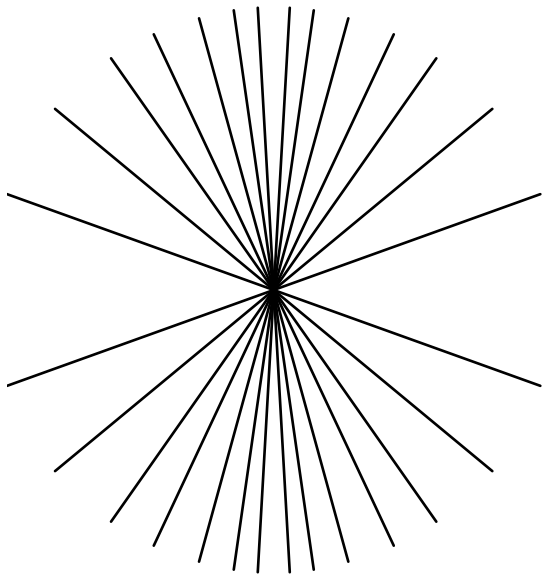

The Photon Equation in the Lab Frame of a Right-Handed Circularly-Polarized Photon Orbitsphere

$$\mathbf{E} = \mathbf{E}_0 \left[\mathbf{x} + i\mathbf{y} \right] e^{-jk_z z} e^{-j\omega t}$$

$$\mathbf{H} = \left(\frac{\mathbf{E}_0}{\eta} \right) \left[\mathbf{y} - i\mathbf{x} \right] e^{-jk_z z} e^{-j\omega t} = \mathbf{E}_0 \sqrt{\frac{\varepsilon}{\mu}} \left[\mathbf{y} - i\mathbf{x} \right] e^{-jk_z z} e^{-j\omega t}$$

with a wavelength of $\lambda = 2\pi \frac{c}{\omega}$

The relationship between the photon e&mvf radius and wavelength is $2r_0 = \lambda_0$

The Electric Field Lines of a Right-Handed Circularly-Polarized Photon E&MVF

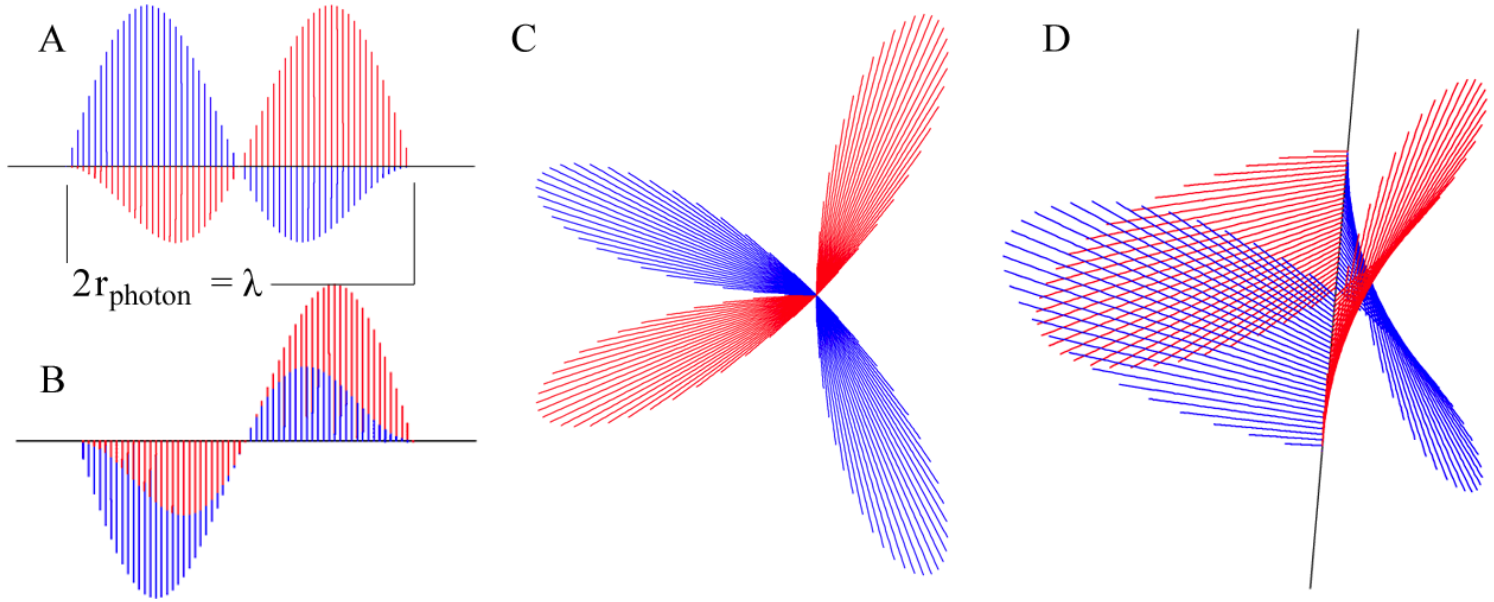

The electric (red) and magnetic (blue) field lines of a right-handed circularly polarized photon-e&mvf as seen in the lab inertial reference frame at a fixed time. A and B. Views transverse to the axis of propagation, the z-axis, wherein $2r_{photon} = \lambda$. C and D. Off z-axis views showing field aspects both along and transverse to the axis of propagation.

The Electric Field Rotation

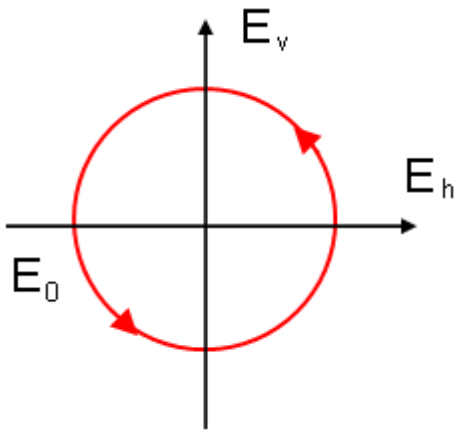

The rotation of the electric field rotation of a right-handed circularly polarized photon e&mvf as seen transverse to the axis of propagation in the lab inertial reference frame as it passes a fixed point.

Elliptically Polarized Photons

Magnitude of the magnetic and electric field lines vary as a function of angular position (θ,φ) on the spherical e&mvf.

$$\mathbf{E}_{\phi,\theta}=\frac{e}{4\pi\varepsilon_0 r_n^2}\left(-1+\frac{1}{n}\left[Y_0^0(\theta,\phi)+\mathrm{Re}\left\{Y_\ell^m(\theta,\phi)e^{im\omega_n t}\right\}\right]\right)\delta\left(r-\frac{\lambda}{2\pi}\right)$$

A photon is emitted when an electron is bound. Relations between the free-space photon wavelength, radius, and velocity and the corresponding parameters of a free electron as it is bound are:

- $r_{n,photon}$, the radius of the photon e&mvf, is equal to $r\pi_n\frac{c}{v_n}=na\pi_H\frac{c}{v_n}$, the electron orbitsphere radius times the product of π and the ratio of the speed of light c and v_n, the velocity of the orbitsphere.
- λ, the photon wavelength, is equal to $\lambda_n\frac{c}{v_n}$, where λ_n is the orbitsphere de Broglie wavelength.
- $\omega=\frac{2\pi c}{\lambda}$, the photon angular velocity, is equal to ω_n, the orbitsphere angular velocity.

Spherical Wave

Photons superimpose, and the amplitude due to N photons is

$$\mathbf{E}_{total} = \sum_{n=1}^{N} \frac{e^{-ik_r|\mathbf{r}-\mathbf{r}'|}}{4\pi|\mathbf{r}-\mathbf{r}'|} f(\theta,\varphi)$$

In the far field, the emitted wave is a spherical wave

$$\mathbf{E}_{total} = E_0 \frac{e^{-ikr}}{r}$$

- The Green Function is given as the solution of the wave equation. Thus, the superposition of photons gives the classical result.
- As r goes to infinity, the spherical wave becomes a plane wave.
- The double slit interference pattern is predicted.
- From the equation of a photon, the wave-particle duality arises naturally.
- The energy is always given by Planck's equation; yet, an interference pattern is observed when photons add over time or space.

Equations of the Free Electron

Mass Density Function of a Free Electron is a two dimensional disk having the mass density distribution in the xy(*p*)-plane

$$\rho_m(\rho,\phi,z)=\frac{m_e}{\frac{2}{3}\pi\rho_0{}^3}\sqrt{\rho_0{}^2-\rho^2}\,\delta(z)$$

Charge Density Distribution, $\rho_e(\rho,\phi,z)$, in the xy-plane

$$\rho_e(\rho,\phi,z)=\frac{e}{\frac{2}{3}\pi\rho_0{}^3}\sqrt{\rho_0{}^2-\rho^2}\,\delta(z)$$

The wave-particle duality arises naturally.

Consistent with scattering experiments.

The Free Electron

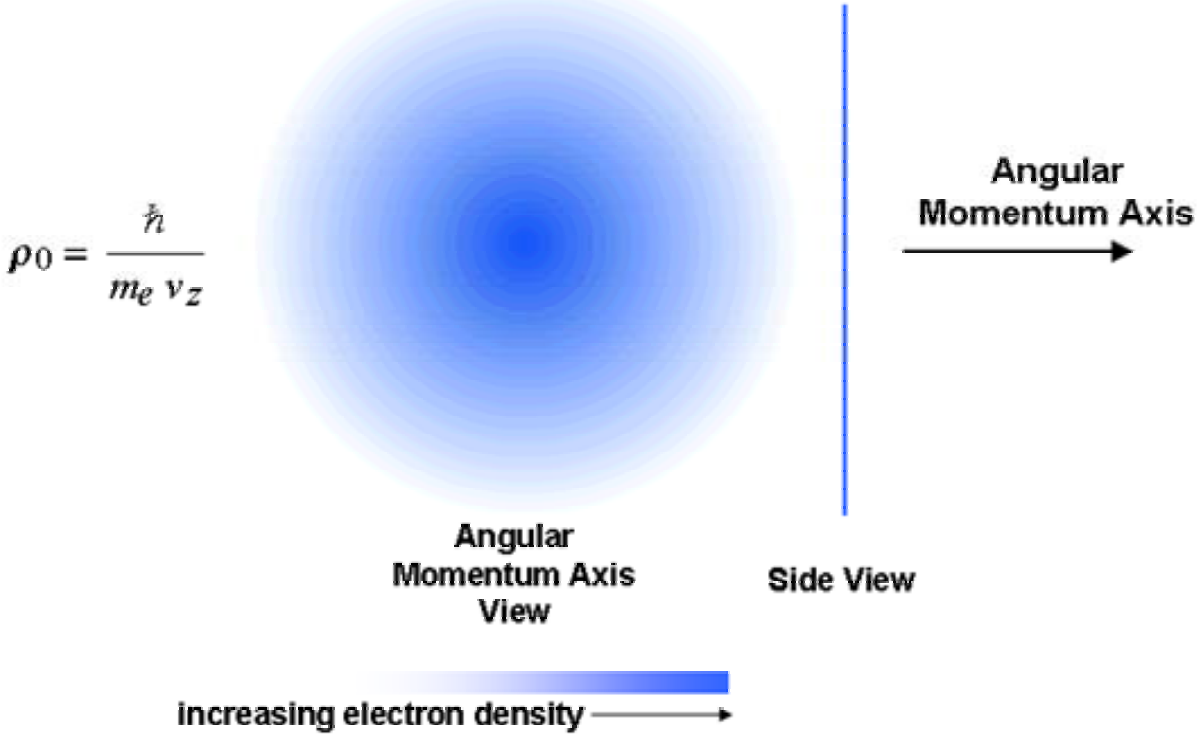

3-D View

Electron Ionization

Charge Density Function

(the size of the electron in the xy-plane centered about the origin as a function of its velocity is shown with the charge density plotted in on the z-axis)

The angular-momentum-axis view of the magnitude of the mass (charge) density function in the xy-plane of a polarized free electron; side-view of a free electron along the axis of propagation—z-axis.

Current-Density Function

$$\mathbf{J}(\rho,\phi,z,t)=\left[\frac{e}{\frac{2}{3}\pi\rho_0^3}\sqrt{\rho_0^2-\rho^2}\,\frac{5}{2}\frac{\hbar}{m_e\rho_0^2}\,\mathbf{i}_\phi\right]+\frac{e\hbar}{m_e\rho_0}\delta(z-\frac{\hbar}{m_e\rho_0}t)\mathbf{i}_z$$

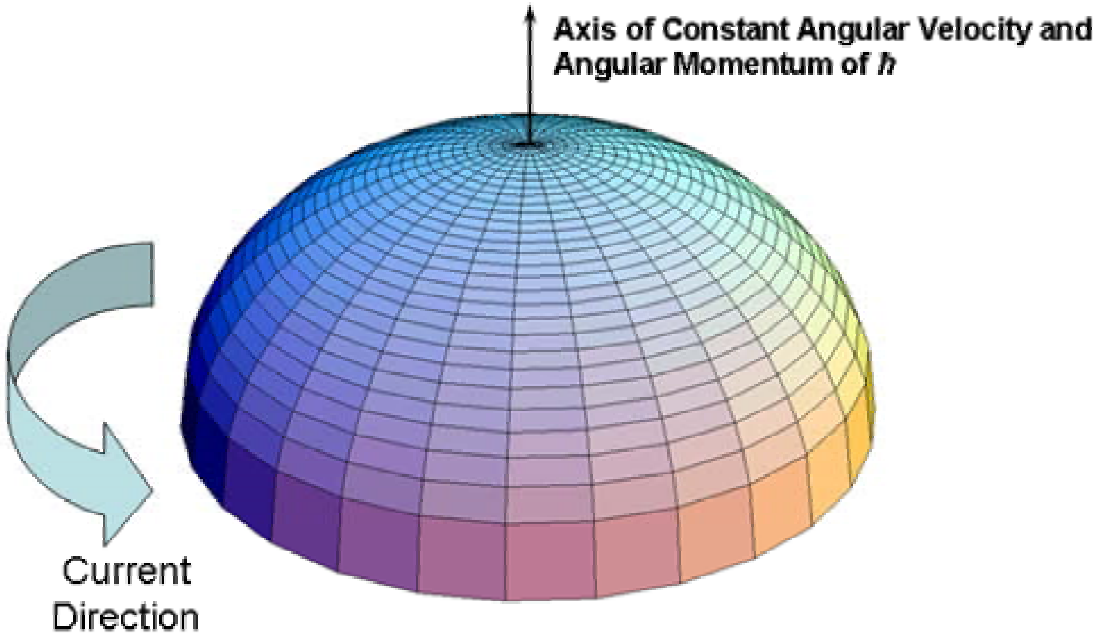

The magnitude plotted along the z-axis of the current-density function, J, of the free electron traveling at 10^5 ms^{-1} relative to the observer.

The radius of the xy-plane-lamina disc is 1.16×10^{-9} m.

The maximum current density at $\rho = 0$ is 1.23×10^{13} Am^{-2}.

Angular Momentum

$$\mathbf{Li}_z = \int_0^{2\pi} \int_0^{\rho_0} \frac{m_e}{\frac{2}{3}\pi\rho_0^3} \sqrt{\rho_0^2 - \rho^2}\, \frac{5}{2} \frac{\hbar}{m_e \rho_0^2}\, \rho^2 \rho d\rho d\phi$$

$$\mathbf{Li}_z = \hbar$$

Nonradiation Condition

$$\frac{e}{\frac{4}{3}\pi\rho_0{}^3}\frac{\hbar}{m_e}\operatorname{sinc}(2\pi\mathbf{s}\vec{\rho}_0)+2\pi e\frac{\hbar}{m_e\rho_0}\delta(\omega-\mathbf{k}_z\bullet\mathbf{v}_z)$$

$$\mathbf{J}_\perp\propto\operatorname{sinc}(\mathbf{s}\vec{\rho}_0)=\frac{\sin 2\pi\mathbf{s}\vec{\rho}_0}{2\pi\mathbf{s}\vec{\rho}_0}$$

$$2\pi\vec{\rho}_0=\lambda_0$$

Consider the wave vector of the sinc function. When the the velocity is *c* corresponding to a potentially emitted photon, $\mathbf{s}$ is the lightlike $\mathbf{s}^0$ wherein

$$\mathbf{s}\bullet\mathbf{v}=\mathbf{s}\bullet\mathbf{c}=\omega_0$$

The relativistically corrected wavelength is

$$\rho_0=\lambda_0$$

$$\lambda_0=\frac{h}{m_e v_z}=2\pi\rho_0$$

Spacetime harmonics of $\frac{\omega_n}{c}=k$ or $\frac{\omega_n}{c}\sqrt{\frac{\varepsilon}{\varepsilon_0}}=k$ for which the Fourier transform of the lightlike current-density function is nonzero do not exist corresponding to a nonradiative state.

Classical Physics of the de Broglie Relation

The linear velocity of the free electron can be considered to be due to absorption of photons that excite surface currents corresponding to a decreased de Broglie wavelength where the free electron is equivalent to a continuum excited state with conservation of the parameters of the bound electron.

The relationship between the electron wavelength and the linear velocity is

$$\frac{\lambda}{2\pi} = \rho_0 = \frac{\hbar}{m_e v_z} = k^{-1} = \frac{v_z}{\omega_z}$$

In this case, the angular frequency ω_z is given by

$$\omega_z = \frac{\hbar}{m_e \rho_0^2}$$

which conserves the photon's angular momentum of $\hbar$ with that of the electron.

Classical Physics of the de Broglie Relation cont'd

The total energy, E_T, is given by the sum of the change in the free-electron translational kinetic energy, T, the rotational energy, E_{rot}, corresponding to the current of the loops, and the potential energy, E_{mag}, due to the radiation reaction force $\mathbf{F}_{mag}$, the magnetic attractive force between the current loops due to the relative rotational or current motion:

$$\begin{aligned} E_T &= T + E_{rot} + E_{mag} \\ &= \frac{1}{2}\frac{\hbar^2}{m_e\rho_0^2} + \frac{5}{4}\frac{\hbar^2}{m_e\rho_0^2} - \frac{5}{4}\frac{\hbar^2}{m_e\rho_0^2} \\ &= \frac{1}{2}\frac{\hbar^2}{m_e\rho_0^2} \end{aligned}$$

Thus, the total energy, E_T, of the excitation of a free-electron transitional state by a photon having $\hbar$ of angular momentum and an energy given by Planck's equation of $\hbar\omega$ is

$$E_T = T = \frac{1}{2}m_e v_z^2 = \frac{1}{2}\frac{h^2}{m_e\lambda^2} = \frac{1}{2}\hbar\omega_z$$

where λ is the de Broglie wavelength.

Classical Physics of the de Broglie Relation cont'd

The angular momentum of the free electron of $\hbar$ is unchanged.

The energies in the currents in the plane lamina are balanced so that the total energy is unchanged.

The radius ρ_0 decreases to match the de Broglie wavelength and frequency at an increased velocity.

At this velocity, the kinetic energy matches the energy provided by the photon wherein the de Broglie frequency matches the photon frequency and both the electron-kinetic energy and the photon energy are given by Planck's equation.

Classical Physics of the de Broglie Relation cont'd

The correspondence principle is the basis of the de Broglie wavelength relationship.

The de Broglie relationship is not an independent fundamental property of matter in conflict with physical laws as formalized in the wave-particle-duality-related postulates of quantum mechanics and the corresponding Schrödinger wave equation.

The Stern-Gerlach experimental results and the double-slit interference pattern of electrons are also predicted classically.

The Central Mystery of Quantum Mechanics

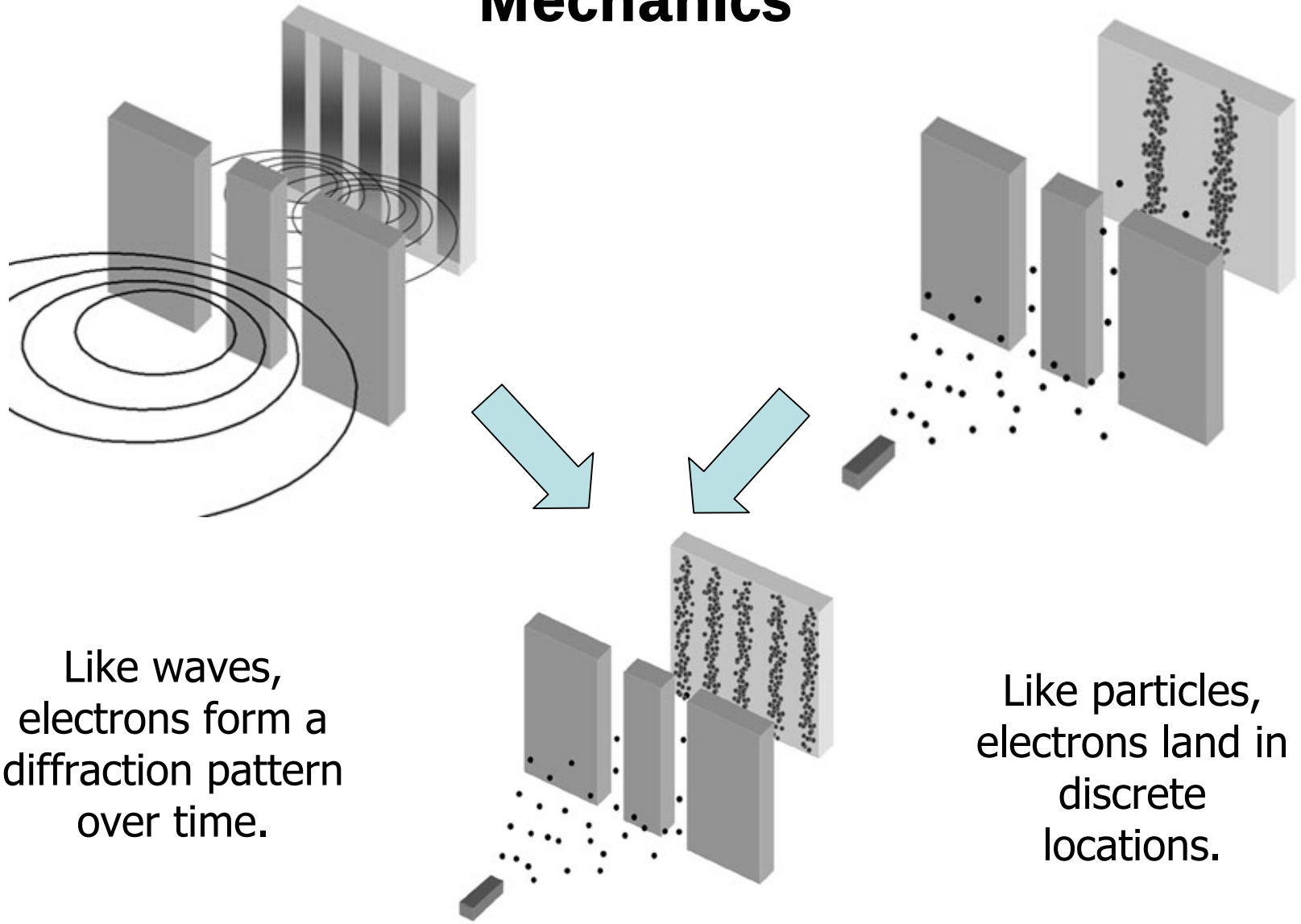

Like waves, electrons form a diffraction pattern over time.

Like particles, electrons land in discrete locations.

Classical Electron Diffraction

- The electron interacts with both slits via charge-induced photons.
- The angular momentum vector of the electron precesses about that of the absorbed photon.
- The photon-momentum distribution is imprinted onto that of the electrons such that transverse momentum distribution in the far-field is a result of this interaction.
- Rather than uncertainty in position and momentum according to the Uncertainty Principle:

$$\Delta x \Delta p \geq \frac{\hbar}{2}$$

- Δp is the *physical momentum change of the incident electron, and* Δx is the physical distance change from the incident direction such that the distribution in the far field is the Fourier transform of the slit pattern.

Animation of the Double Slit Exp

Top View

Spin of Free Electron

With the electron current in the counter clockwise direction, the Larmor precession of the angular momentum vector of the free electron is about two axes simultaneously, the (i_x, $0i_y$, i_z)-axis and the laboratory-frame z-axis defined by the direction of the applied magnetic field.

The motion generates CVFs equivalent to those of the bound electron.

Over one time period, the first motion sweeps out the equivalent of a BECVF, and the rotation about the z-axis sweeps out the equivalent of an OCVF.

Spin of Free Electron cont'd

The combined motions sweep out the equivalent of the convolution of the BECVF with the OCVF, a distribution and angular momentum equivalent to $Y_0^0(\theta,\phi)$ of the bound electron.

The electron may flip between the two states wherein the BECVF, OCVF, and $Y_0^0(\theta,\phi)$ precession distributions apply to both states, but the currents are opposite.

The rotation of a great circle in the xy-plane about the (i_x, $0i_y$, i_z)-axis by 2π generates a free electron BECVF corresponding to the precession motion with its resultant angular momentum of $\sqrt{2}\hbar$ along the (i_x, $0i_y$, i_z)-axis having components of $L_{xy} = \hbar$ and $L_z = \hbar$ corresponding to a magnetic moment of μ_B on the z-axis.

Spin of Free Electron cont'd

BECVF Matrices ($R_{(\mathbf{i_x},0\mathbf{i_y},\mathbf{i_z})}(\theta)$)

$$\begin{bmatrix} x' \\ y' \\ z' \end{bmatrix} = \begin{bmatrix} \frac{1}{2}+\frac{\cos\theta}{2} & \frac{\sin\theta}{\sqrt{2}} & \frac{1}{2}-\frac{\cos\theta}{2} \\ -\frac{\sin\theta}{\sqrt{2}} & \cos\theta & \frac{\sin\theta}{\sqrt{2}} \\ \frac{1}{2}-\frac{\cos\theta}{2} & -\frac{\sin\theta}{\sqrt{2}} & \frac{1}{2}+\frac{\cos\theta}{2} \end{bmatrix} \begin{bmatrix} \rho\cos\phi \\ \rho\sin\phi \\ 0 \end{bmatrix}$$

The infinite sum of great circles that constitute the BECVF:

$$BECVF = \lim_{\Delta\theta\to 0} \sum_{m=1}^{m=\frac{2\pi}{|\Delta\theta|}} \left[\left(R_{(\mathbf{i_x},0\mathbf{i_y},\mathbf{i_z})}(m\Delta\theta_M) \bullet GC^{basis}_{(\mathbf{i_x},\mathbf{i_y},0\mathbf{i_z})} \right) \right]$$

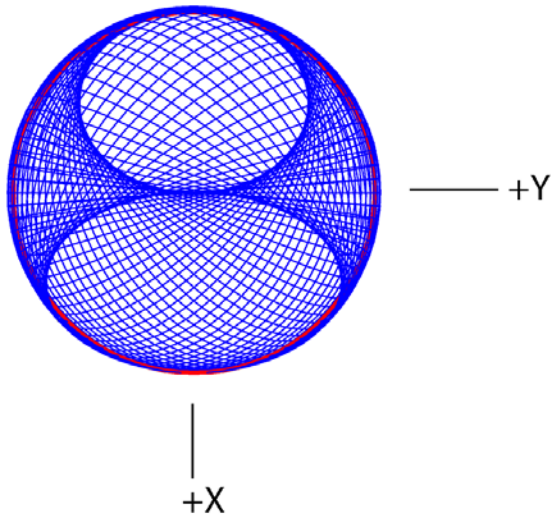

Conical Surfaces Formed by Variation of ρ

The rotation of the free-electron disc having a continuous progression of larger current loops along ρ forms two conical surfaces over a period that join at the origin and face in the opposite directions along the (i_x, $0i_y$, i_z)-axis, the axis of rotation.

At each position of $0 < \rho$, there exists a BECVF of that radius that is concentric to the one of infinitesimally larger radius to the limit at $\rho = \rho_0$.

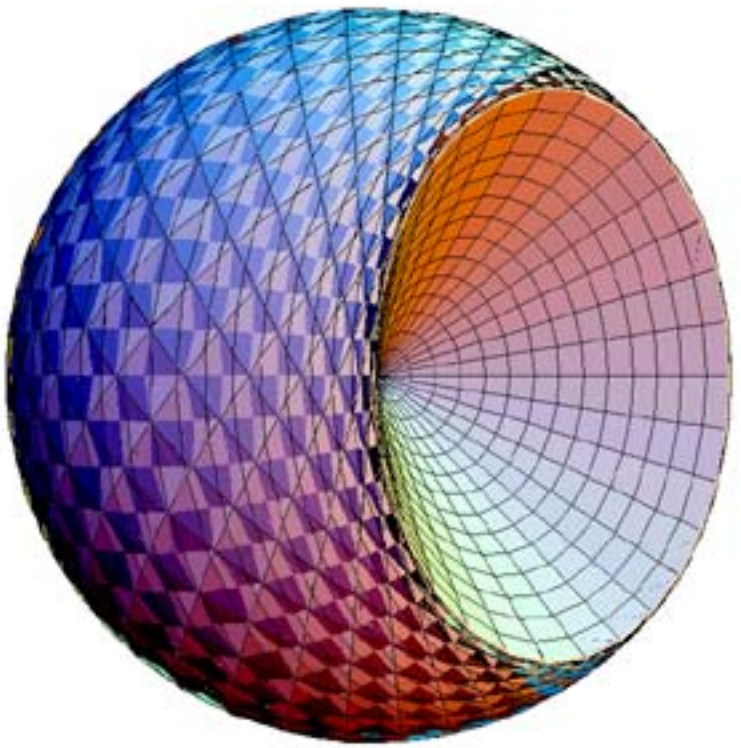

The $Y_0^0(\theta,\phi)$ Momentum-Density for the Combined Precession Motion of the Free Electron about the (i_x, $0i_y$, i_z)- Axis and Z-Axis

The combined precessional motion of the free electron about the (i_x, $0i_y$, i_z)-axis and z-axis having the magnetic moment of μ_B on the z-axis is the $Y_0^0(\theta,\phi)$ momentum-density distribution for each position ρ given by the convolution of the BECVF with the OCVF.

The OCVF is generated by rotating a basis-element great circle that is perpendicular to the (i_x, $0i_y$, i_z)- axis about the z-axis by 2π.

The $Y_0^0(\theta,\phi)$ Momentum-Density cont'd

OCVF Matrices ($R_z(\theta)$)

$$\begin{bmatrix} x' \\ y' \\ z' \end{bmatrix} = \begin{bmatrix} \cos(\theta) & \sin(\theta) & 0 \\ -\sin(\theta) & \cos(\theta) & 0 \\ 0 & 0 & 1 \end{bmatrix} \begin{bmatrix} \frac{\rho\cos\phi}{\sqrt{2}} \\ \rho\sin\phi \\ \frac{-\rho\cos\phi}{\sqrt{2}} \end{bmatrix}$$

The infinite sum of great circles representation of the OCVF:

$$OCVF = \lim_{\Delta\theta\to 0} \sum_{m=1}^{m=\frac{2\pi}{|\Delta\theta|}} \left[\left(R_z(m\Delta\theta_M) \bullet GC^{basis}_{\left(\frac{1}{\sqrt{2}}\mathbf{i_x}, \mathbf{i_y}, -\frac{1}{\sqrt{2}}\mathbf{i_z}\right)} \right) \right]$$

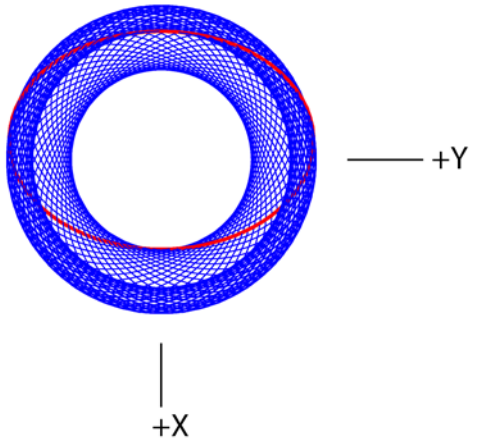

The $Y_0^0(\theta,\phi)$ Momentum-Density cont'd

The BECVF replaces the great circle basis element initially perpendicular to the (i_x, $0i_y$, i_z)- axis and matches its resultant angular momentum of $\sqrt{2}\hbar$ along the (i_x, $0i_y$, i_z)- axis having components of $L_{xy} = \hbar$ and $L_z = \hbar$.

$Y_0^0(\theta,\phi)$ is generated by rotation of the BECVF, about the z-axis by an infinite set of infinitesimal increments of the rotational angle over the 2π span such that coverage of the spherical surface is complete.

The Momentum-Density $Y_0^{\,0}(\theta,\phi)$ cont'd

The infinite double sum of great circles that constitute $Y_0^{\,0}(\theta,\phi)$:

$$Y_0^{\,0}(\theta,\phi) = \lim_{\Delta\theta\to 0}\sum_{m=1}^{m=\frac{2\pi}{|\Delta\theta|}}\left[R_z\left(m\Delta\theta_M^{OCVF}\right)\bullet\lim_{\Delta\theta\to 0}\sum_{n=1}^{n=\frac{2\pi}{|\Delta\theta|}}\left[R_{(\mathbf{i_x},0\mathbf{i_y},\mathbf{i_z})}\left(n\Delta\theta_N^{BECVF}\right)\bullet GC^{basis}_{(\mathbf{i_x},\mathbf{i_y},0\mathbf{i_z})}\right]\right]$$

A discrete representation of the current distribution $Y_0^{\,0}(\theta,\phi)$ can be generated from the continuous convolution of the BECVF with the OCVF as a superposition of *M* discrete incremental rotations of the position of the BECVF comprising *N* great circles about the z-axis such that the number of convolved BECVF elements is *M*.

The Momentum-Density $Y_0^{\,0}(\theta,\phi)$ cont'd

$$\begin{bmatrix} x' \\ y' \\ z' \end{bmatrix} = \sum_{m=1}^{m=M} \begin{bmatrix} \cos\left(\frac{m2\pi}{M}\right) & \sin\left(\frac{m2\pi}{M}\right) & 0 \\ -\sin\left(\frac{m2\pi}{M}\right) & \cos\left(\frac{m2\pi}{M}\right) & 0 \\ 0 & 0 & 1 \end{bmatrix}$$

$$\bullet \sum_{n=1}^{n=N} \begin{bmatrix} \frac{1}{2}+\frac{\cos\left(\frac{n2\pi}{N}\right)}{2} & \frac{\sin\left(\frac{n2\pi}{N}\right)}{\sqrt{2}} & \frac{1}{2}-\frac{\cos\left(\frac{n2\pi}{N}\right)}{2} \\ -\frac{\sin\left(\frac{n2\pi}{N}\right)}{\sqrt{2}} & \cos\left(\frac{n2\pi}{N}\right) & \frac{\sin\left(\frac{n2\pi}{N}\right)}{\sqrt{2}} \\ \frac{1}{2}-\frac{\cos\left(\frac{n2\pi}{N}\right)}{2} & -\frac{\sin\left(\frac{n2\pi}{N}\right)}{\sqrt{2}} & \frac{1}{2}+\frac{\cos\left(\frac{n2\pi}{N}\right)}{2} \end{bmatrix} \begin{bmatrix} \rho\cos\phi \\ \rho\sin\phi \\ 0 \end{bmatrix}$$

The Momentum-Density $Y_0^0(\theta,\phi)$ cont'd

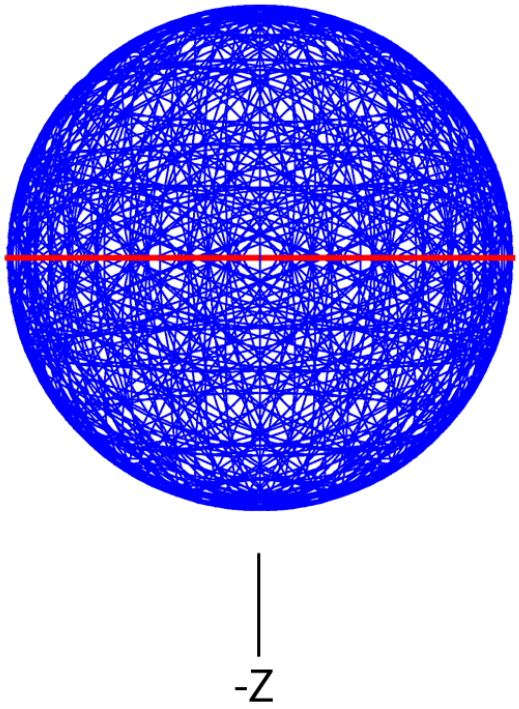

Discrete representations of the $Y_0^0(\theta,\phi)$ current distribution

(30 degree increments, $N = M = 12$) viewed along the x-axis.

The electron may flip between the two spin states having the magnetic moment parallel to the z-axis or antiparallel to the z-axis by a $\pm\pi$ rotation of the distribution $Y_0^0(\theta,\phi)$ about the x-axis with the application of a photon of the corresponding Larmor frequency energy with its angular momentum along this axis.

Stern-Gerlach Experiment

The Stern Gerlach experiment demonstrates that the magnetic moment of the electron can only be parallel or antiparallel to an applied magnetic field.

This implies a spin quantum number of 1/2 corresponding to an angular momentum on the z-axis of $\frac{\hbar}{2}$. However, the Zeeman splitting energy corresponds to a magnetic moment of a Bohr magneton μ_B and implies an electron angular momentum on the z-axis of $\hbar$—twice that expected.

Stern-Gerlach Experiment cont'd

The application of a magnetic field causes a resonant excitation of the Larmor precession wherein the corresponding photon has $\hbar$ of angular momentum on the x'-axis.

The corresponding torque causes the electron to precess about the (ix, 0iy, iz)-axis and the z-axsis to give the equivalent of the distribution $Y_0^0(\theta,\phi)$ at each radial position ρ of the free electron.

Stern-Gerlach Experiment cont'd

Free Electron Precession About the (i_x, $0i_y$, i_z)-Axis

Free Electron (i_x, $0i_y$, i_z)-Axis Precession About the Z-Axis Showing the ρ Dependency

Free Electron (i_x, $0i_y$, i_z)-Axis Precession About the Z-Axis Shown at a Fixed ρ

3-D View of the Uniform Distribution

Stern-Gerlach Experiment cont'd

The static projection of the resultant angular momentum onto the z-axis is $\hbar$ with a contribution of $\frac{\hbar}{2}$ from each of the intrinsic electron current and the photon.

The precessing electron can further interact with a resonant photon directed along the x-axis that rotates the z-axis-directed constant projection of the resultant of $\hbar$ such that it flips to the opposite direction.

The RF photon gives rise to Zeeman splitting—energy levels corresponding to flipping of the parallel or antiparallel alignment of the electron magnetic moment of a Bohr magneton with the magnetic field.

Stern-Gerlach Experiment cont'd

The spherical momentum density over a period interacts with the external applied magnetic field in a manner that is equivalent to that of orbitsphere function, $Y_0^0(\theta,\phi)$, having the momentum density on a spherical shell of radius ρ_0, a total integral of the magnitude of the angular momentum density on the orbitsphere of $\hbar$ and $\mathbf{L}_z = \frac{\hbar}{2}$.

Stern-Gerlach Experiment cont'd

Since the projection of the intrinsic free electron angular momentum and that of the resonant photon that excites the Larmor precession onto the z-axis are both $\frac{\hbar}{2}$, the Larmor-excited free electron behaves equivalently to the bound electron.

Flux must be linked in the same manner in units of the magnetic flux quantum,

$$\Phi_0 = \frac{h}{2e}$$

Consequently, the g factor for the free electron is the same as that of the bound electron, and the energy of the transition between these states is that of the resonant photon given by

$$\Delta E_{mag}^{spin} = g\mu_B B$$

Two Electron Atoms

Central Force Balance Equation with Nonradiation Condition

$$\frac{m_e}{4\pi r_2^2}\frac{v_2^2}{r_2} = \frac{e}{4\pi r_2^2}\frac{(Z-1)e}{4\pi\varepsilon_0 r_2^2} + \frac{1}{4\pi r_2^2}\frac{\hbar^2}{Zm_e r_2^3}\sqrt{s(s+1)}$$

$$r_2 = r_1 = a_0\left(\frac{1}{Z-1} - \frac{\sqrt{s(s+1)}}{Z(Z-1)}\right); s = \frac{1}{2}$$

Two Electron Atoms cont'd

Ionization Energies Calculated Using the Poynting Power Theorem

For helium, which has no electric field beyond r_1

$$Ionization\ Energy(He) = -E(electric) + E(magnetic)$$

where $$E(electric) = -\frac{(Z-1)e^2}{8\pi\varepsilon_o r_1}$$

$$E(magnetic) = \frac{2\pi\mu_0 e^2\hbar^2}{m_e^2 r_1^3}$$

Where

For $3 \le Z$

$$Ionization\ Energy\ = -Electric\ Energy - \frac{1}{Z}\,Magnetic\ Energy$$

The Calculated Energies for Some Two-Electron Atoms

Atom	r_1 (a_o)	Electric Energy (eV)	Magnetic Energy (eV)	Calculated Ionization Energy(eV)	Experimental Ionization Energy (eV)
He	0.567	-23.96	0.63	24.59	24.59
Li^{+}	0.356	-76.41	2.54	75.56	75.64
Be^{2+}	0.261	-156.08	6.42	154.48	153.89
B^{3+}	0.207	-262.94	12.96	260.35	259.37
C^{4+}	0.171	-396.98	22.83	393.18	392.08
N^{5+}	0.146	-558.20	36.74	552.95	552.06
O^{6+}	0.127	-746.59	55.35	739.67	739.32
F^{7+}	0.113	-962.17	79.37	953.35	953.89

Elastic Electron Scattering from Helium Atoms

Aperture distribution function, $a(\rho,\phi,z)$, for the scattering of an incident electron plane wave $\pi(z)$

by the He atom

$$\frac{2}{4\pi(0.567a_o)^2}[\delta(r-0.567a_o)]$$

is

$$a(\rho,\phi,z)=\pi(z)\otimes\frac{2}{4\pi(0.567a_o)^2}[\delta(r-0.567a_o)]$$

$$a(\rho,\phi,z)=\frac{2}{4\pi(0.567a_o)^2}\sqrt{(0.567a_o)^2-z^2}\,\delta(\rho-\sqrt{(0.567a_o)^2-z^2})$$

Far Field Scattering
(Circular Symmetry)

$$F(s) = \frac{2}{4\pi(0.567a_o)^2} 2\pi \int_0^{\infty} \int_{-\infty}^{\infty} \sqrt{(0.567a_o)^2 - z^2}\, \delta(\rho - \sqrt{(0.567a_o)^2 - z^2})\, J_o(s\rho) e^{-iwz}\, \rho d\rho dz$$

$$I_1^{ed} = F(s)^2$$

$$= I_e \left\{ \left[\frac{2\pi}{(z_o w)^2 + (z_o s)^2} \right]^{\frac{1}{2}} \left\{ 2\left[\frac{z_o s}{(z_o w)^2 + (z_o s)^2} \right] J_{3/2}\left[((z_o w)^2 + (z_o s)^2)^{1/2} \right] - \left[\frac{z_o s}{(z_o w)^2 + (z_o s)^2} \right]^2 J_{5/2}\left[((z_o w)^2 + (z_o s)^2)^{1/2} \right] \right\} \right\}^2$$

$$s = \frac{4\pi}{\lambda} \sin\frac{\theta}{2};\ w = 0\ (units\ of\ \mathring{A}^{-1})$$

Experimental Results
and Born Approximation

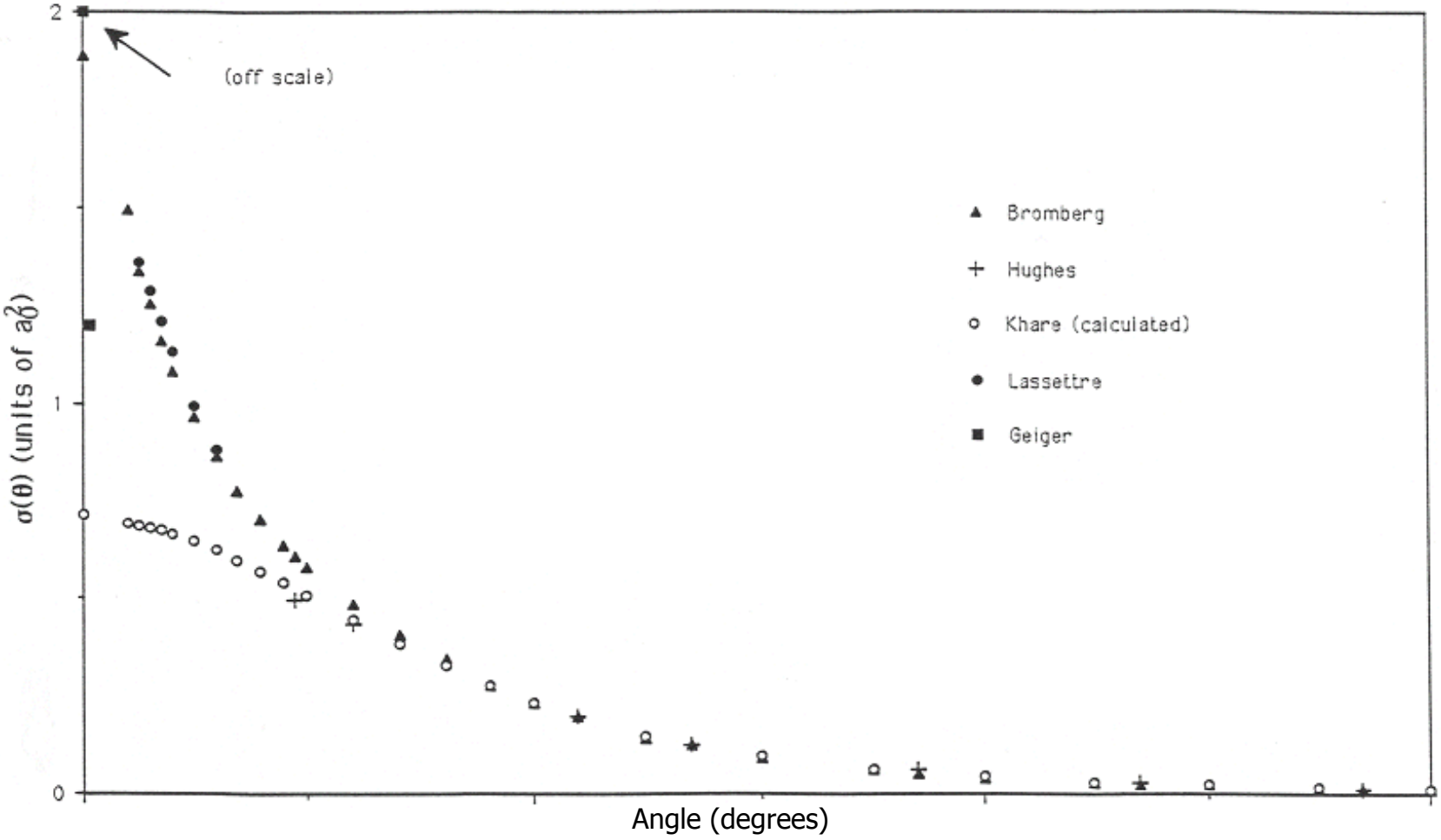

The experimental results of Bromberg, the extrapolated experimental data of Hughes, the small angle data of Geiger, and the semiexperimental results of Lassettre for the elastic differential cross section for the elastic scattering of electrons by helium atoms and the elastic differential cross section as a function of angle numerically calculated by Khare using the first Born approximation and first-order exchange approximation.

The Closed Form Function

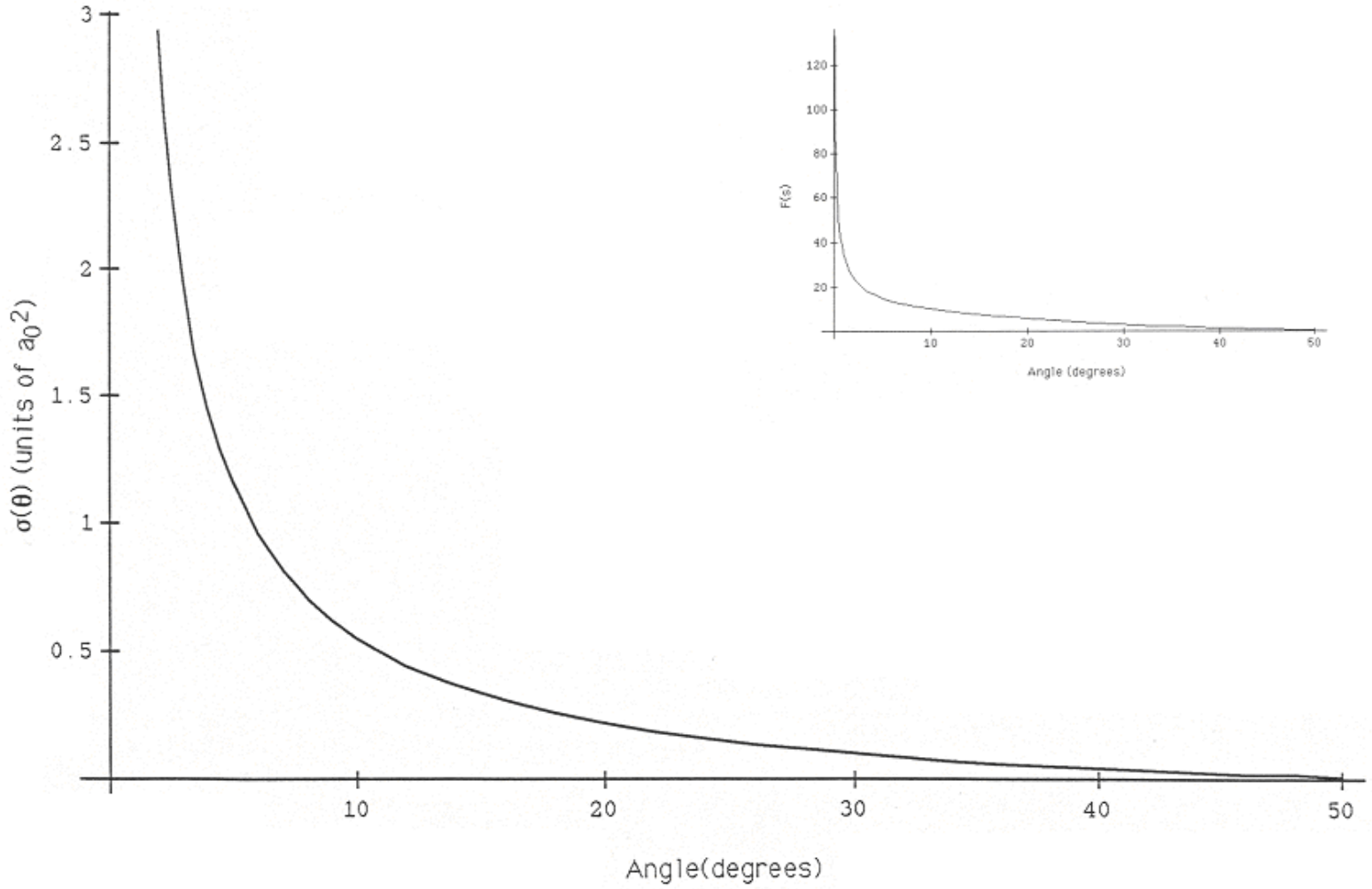

The closed form function for the elastic differential cross section for the elastic scattering of electrons by helium atoms. The scattering amplitude function, F(s), is shown as an insert.

One- Through Twenty-Electron Atoms

The physical approach based on Maxwell's equations was applied to multielectron atoms that were solved exactly.

The classical predictions of the ionization energies were solved for the physical electrons comprising concentric orbitspheres ("bubble-like" charge-density functions) that are electrostatic and magnetostatic corresponding to a constant charge distribution and a constant current corresponding to spin angular momentum.

Alternatively, the charge is a superposition of a constant and a dynamical component.

In the latter case, charge density waves on the surface are time and spherically harmonic and correspond additionally to electron orbital angular momentum that superimposes the spin angular momentum.

One- Through Twenty-Electron Atoms cont'd

Thus, the electrons of multielectron atoms all exist as orbitspheres of discrete radii which are given by r_n of the radial Dirac delta function, $\delta(r - r_n)$.

These electron orbitspheres may be spin paired or unpaired depending on the force balance which applies to each electron.

Ultimately, the electron configuration must be a minimum of energy. Minimum energy configurations are given by solutions to Laplace's equation.

Electrons of an atom with the same principal and ℓ quantum numbers align parallel until each of the m_ℓ levels are occupied, and then pairing occurs until each of the m_ℓ levels contain paired electrons.

The electron configuration for one through twenty-electron atoms that achieves an energy minimum is: 1s < 2s < 2p < 3s < 3p < 4s.

Into the K Atom

Sectional View of the Potassium (K) Atom

(Electrons shown at relative size scale, but nucleus not to scale.)

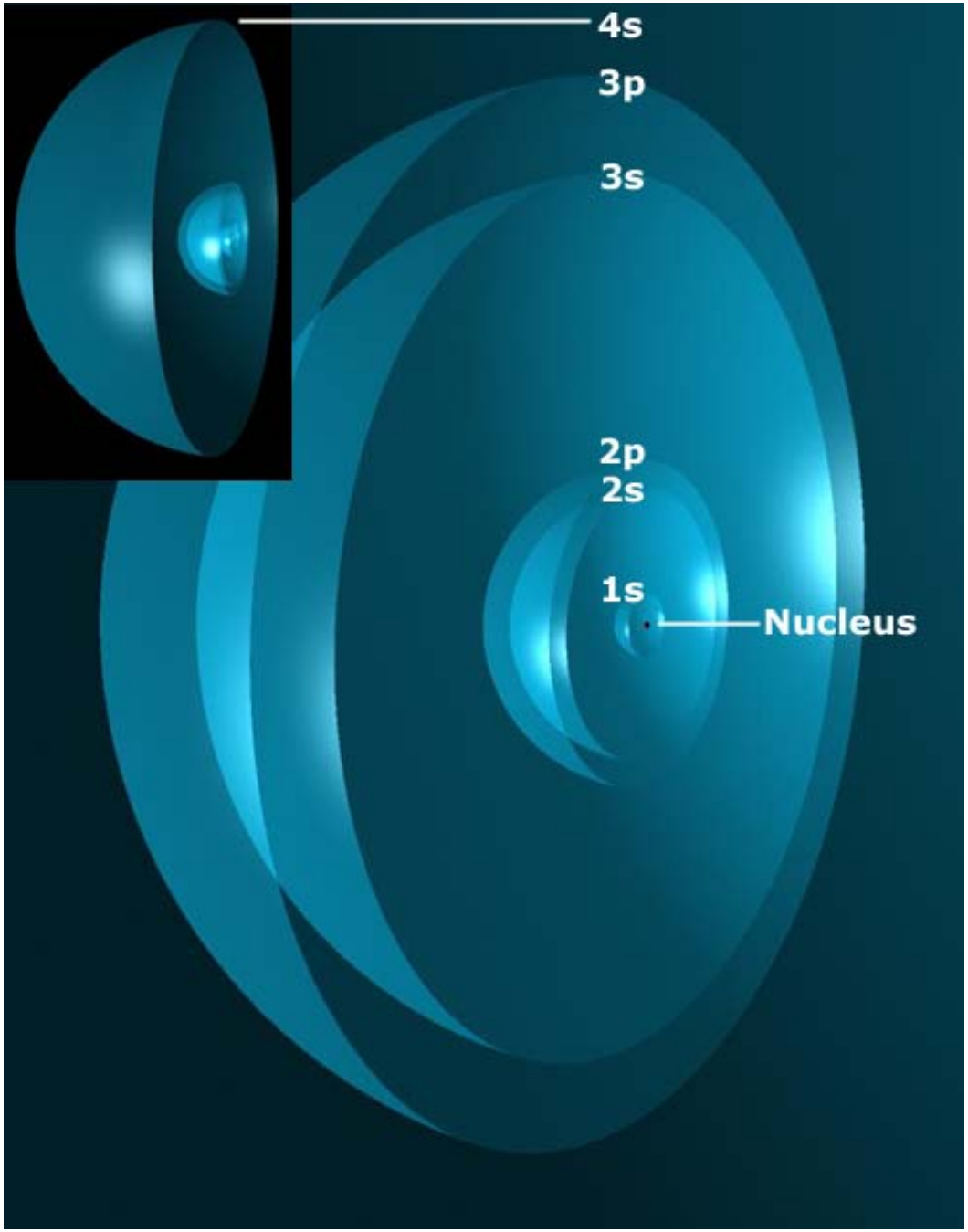

Visualization of the One-Through-Twenty Electron Atoms.

Color-Scaled Charge-Densities shown with relative-size-scale.

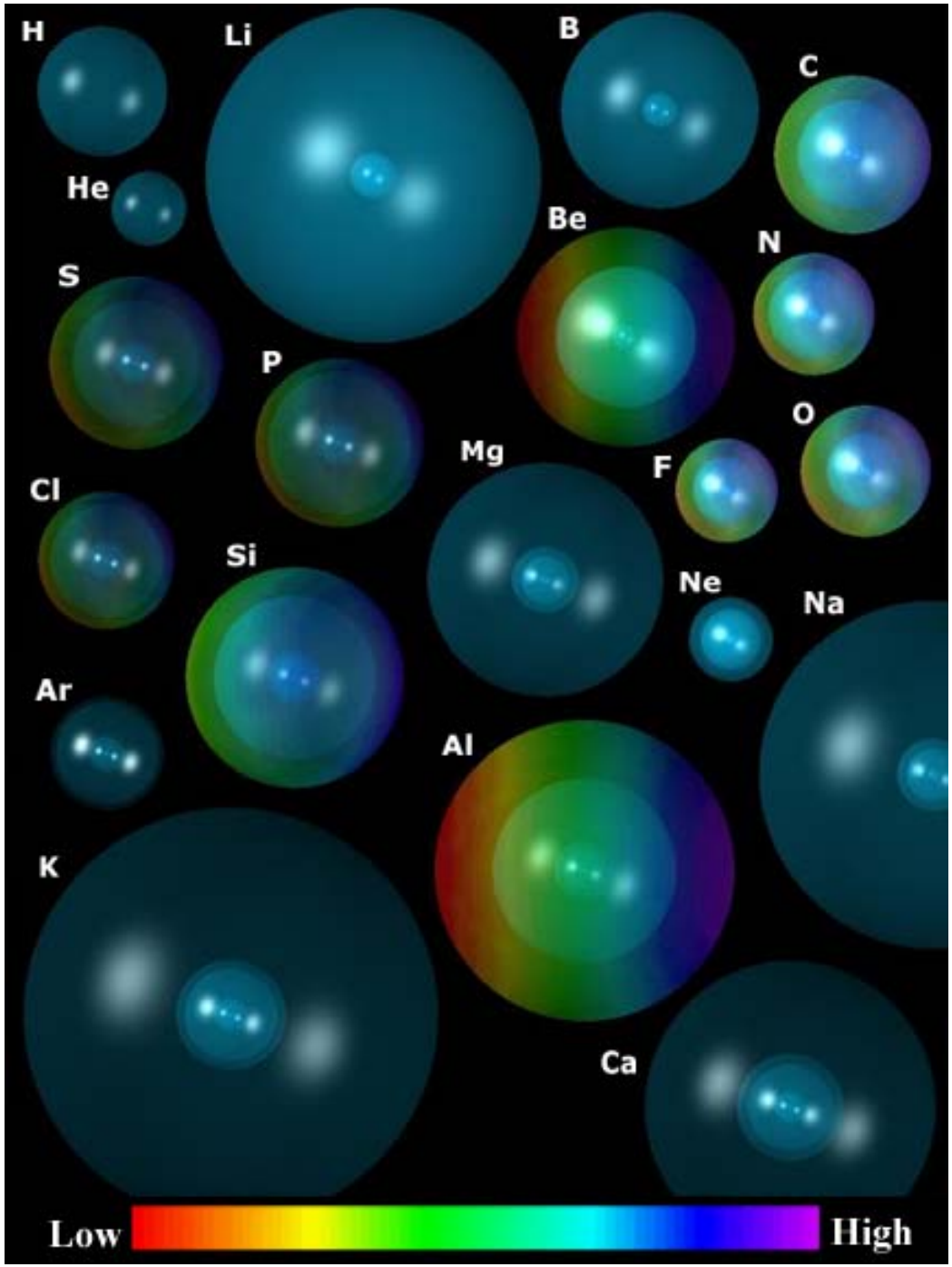

Visualization of the One-Through-Twenty Electron Ions

Color-Scaled Charge-Densities shown with relative-size-scale.

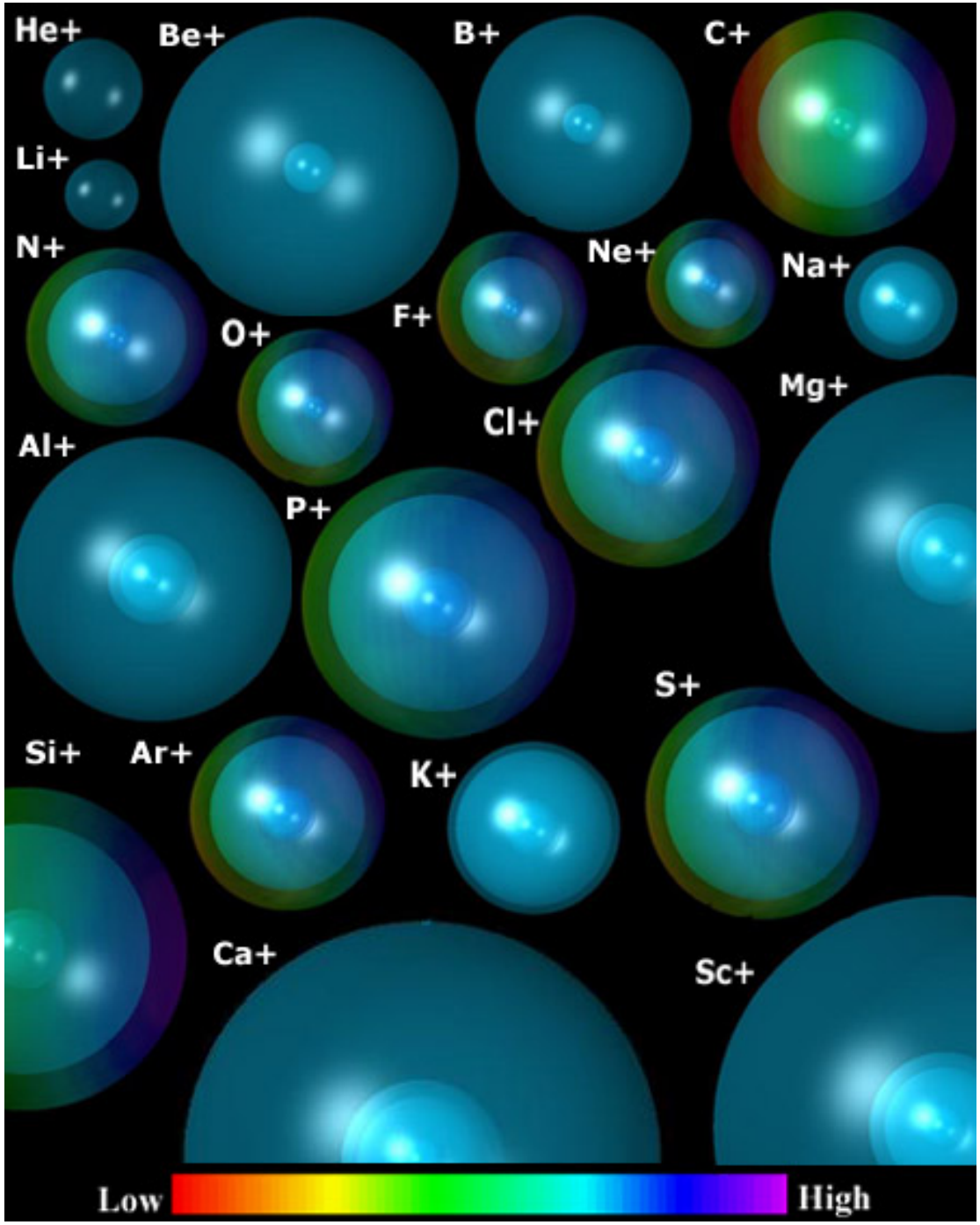

One- Through Twenty-Electron Atoms cont'd

In each case, the corresponding force balance of the central Coulombic, paramagnetic, and diamagnetic forces was derived for each n-electron atom that was solved for the radius of each electron.

The central Coulombic force was that of a point charge at the origin since the electron charge-density functions are spherically symmetrical with a time dependence that was nonradiative.

This feature eliminated the electron-electron repulsion terms and the intractable infinities of quantum mechanics and permitted general solutions.

The ionization energies were obtained using the calculated radii in the determination of the Coulombic and any magnetic energies.

The radii and ionization energies for all cases are given by equations having fundamental constants and each nuclear charge, Z, only.

The predicted ionization energies and electron configurations are in remarkable agreement with the experimental values known for 400 atoms and ions.

General Equation for the Ionization Energies of Five Through Ten-Electron Atoms

For example, for each n-electron atom having a central charge of Z times that of the proton and an electron configuration $1s^2 2s^2 2p^{n-4}$, there are two indistinguishable spin-paired electrons in an orbitsphere with radii r_1 and r_2 both given by:

$$r_1 = r_2 = a_o \left[\frac{1}{Z-1} - \frac{\sqrt{\frac{3}{4}}}{Z(Z-1)} \right]$$

two indistinguishable spin-paired electrons in an orbitsphere with radii r_3 and r_4 both given by:

$$r_4 = r_3 = \frac{\dfrac{a_0\left(1-\dfrac{\sqrt{\frac{3}{4}}}{Z}\right)}{\left((Z-3)-\left(\frac{1}{4}-\frac{1}{Z}\right)\frac{\sqrt{\frac{3}{4}}}{r_1}\right)} \pm a_o \sqrt{\dfrac{\left(1-\dfrac{\sqrt{\frac{3}{4}}}{Z}\right)^2}{\left((Z-3)-\left(\frac{1}{4}-\frac{1}{Z}\right)\frac{\sqrt{\frac{3}{4}}}{r_1}\right)^2} + 4\dfrac{\left[\frac{Z-3}{Z-2}\right] r_1 10\sqrt{\frac{3}{4}}}{\left((Z-3)-\left(\frac{1}{4}-\frac{1}{Z}\right)\frac{\sqrt{\frac{3}{4}}}{r_1}\right)}}}{2}$$

r_1 *in units of* a_o

Equation for the Ionization Energies of Five through Ten-Electron Atoms cont'd

and n - 4 electrons in an orbitsphere with radius r_n given by

$$r_n = \frac{\dfrac{a_0}{\left((Z-(n-1))-\left(\dfrac{A}{8}-\dfrac{B}{2Z}\right)\dfrac{\sqrt{3}}{r_3}\right)} \pm a_0\sqrt{\left(\dfrac{1}{\left((Z-(n-1))-\left(\dfrac{A}{8}-\dfrac{B}{2Z}\right)\dfrac{\sqrt{3}}{r_3}\right)}\right)^2 + \dfrac{20\sqrt{3}\left(\left[\dfrac{Z-n}{Z-(n-1)}\right]\left(1-\dfrac{\sqrt{2}}{2}\right)r_3\right)}{\left((Z-(n-1))-\left(\dfrac{A}{8}-\dfrac{B}{2Z}\right)\dfrac{\sqrt{3}}{r_3}\right)}}}{2}$$

r_3 *in units of* a_0

$1s^2 2s^2 2p^{n-4}$-Atom Ionization Energies cont'd

The parameter *A* corresponds to the diamagnetic force, $\mathbf{F}_{diamagnetic}$:

$$\mathbf{F}_{diamagnetic} = -\sum_m \frac{(\ell + |m|)!}{(2\ell+1)(\ell - |m|)!} \frac{\hbar^2}{4 m_e r_n^2 r_3} \sqrt{s(s+1)}\mathbf{i}_\mathbf{r}$$

The parameter *B* corresponds to the paramagnetic force, $\mathbf{F}_{mag2}$:

$$\mathbf{F}_{mag\,2} = \frac{1}{Z} \frac{\hbar^2}{m_e r_n^2 r_3} \sqrt{s(s+1)}\mathbf{i}_\mathbf{r}$$

or

$$\mathbf{F}_{mag\,2} = \frac{1}{Z} \frac{4\hbar^2}{m_e r_n^2 r_3} \sqrt{s(s+1)}\mathbf{i}_\mathbf{r}$$

depending on the positive or negative superposition of spin and orbital angular momentum.

The ionization energies for the n-electron atoms are given by the negative of the electric energy, *E(electric)*:

$$E(Ionization) = -Electric\ Energy = \frac{(Z - (n-1))e^2}{8\pi\varepsilon_o r_n}$$

Summary of the Parameters of Five through Ten-Electron Atoms

Atom Type	Electron Configuration	Ground State Term	Orbital Arrangement of 2p Electrons (2p state)	Diamagnetic Force Factor A	Paramagnetic Force Factor B
Neutral 5 e Atom *B*	$1s^2 2s^2 2p^1$	$^2P^0_{1/2}$	$\underline{\uparrow}\ \underline{\ }\ \underline{\ }$ (1, 0, -1)	1	0
Neutral 6 e Atom *C*	$1s^2 2s^2 2p^2$	$^3P_0$	$\underline{\uparrow}\ \underline{\uparrow}\ \underline{\ }$ (1, 0, -1)	$\frac{2}{3}$	0
Neutral 7 e Atom *N*	$1s^2 2s^2 2p^3$	$^4S^0_{3/2}$	$\underline{\uparrow}\ \underline{\uparrow}\ \underline{\uparrow}$ (1, 0, -1)	$\frac{1}{3}$	1
Neutral 8 e Atom *O*	$1s^2 2s^2 2p^4$	$^3P_2$	$\underline{\uparrow\downarrow}\ \underline{\uparrow}\ \underline{\uparrow}$ (1, 0, -1)	1	2
Neutral 9 e Atom *F*	$1s^2 2s^2 2p^5$	$^2P^0_{3/2}$	$\underline{\uparrow\downarrow}\ \underline{\uparrow\downarrow}\ \underline{\uparrow}$ (1, 0, -1)	$\frac{2}{3}$	3
Neutral 10 e Atom *Ne*	$1s^2 2s^2 2p^6$	$^1S_0$	$\underline{\uparrow\downarrow}\ \underline{\uparrow\downarrow}\ \underline{\uparrow\downarrow}$ (1, 0, -1)	0	3
5 e Ion	$1s^2 2s^2 2p^1$	$^2P^0_{1/2}$	$\underline{\uparrow}\ \underline{\ }\ \underline{\ }$ (1, 0, -1)	$\frac{5}{3}$	1
6 e Ion	$1s^2 2s^2 2p^2$	$^3P_0$	$\underline{\uparrow}\ \underline{\uparrow}\ \underline{\ }$ (1, 0, -1)	$\frac{5}{3}$	4
7 e Ion	$1s^2 2s^2 2p^3$	$^4S^0_{3/2}$	$\underline{\uparrow}\ \underline{\uparrow}\ \underline{\uparrow}$ (1, 0, -1)	$\frac{5}{3}$	6
8 e Ion	$1s^2 2s^2 2p^4$	$^3P_2$	$\underline{\uparrow\downarrow}\ \underline{\uparrow}\ \underline{\uparrow}$ (1, 0, -1)	$\frac{5}{3}$	6
9 e Ion	$1s^2 2s^2 2p^5$	$^2P^0_{3/2}$	$\underline{\uparrow\downarrow}\ \underline{\uparrow\downarrow}\ \underline{\uparrow}$ (1, 0, -1)	$\frac{5}{3}$	9
10 e Ion	$1s^2 2s^2 2p^6$	$^1S_0$	$\underline{\uparrow\downarrow}\ \underline{\uparrow\downarrow}\ \underline{\uparrow\downarrow}$ (1, 0, -1)	$\frac{5}{3}$	12

Ionization Energies for Some Five-Electron Atoms

5 e Atom	Z	r_1 (a_0)	r_3 (a_0)	r_5 (a_0)	Theoretical Ionization Energies (eV)	Experimental Ionization Energies (eV)	Relative Error
B	5	0.20670	1.07930	1.67000	8.30266	8.29803	-0.00056
C^{+}	6	0.17113	0.84317	1.12092	24.2762	24.38332	0.0044
N^{2+}	7	0.14605	0.69385	0.87858	46.4585	47.44924	0.0209
O^{3+}	8	0.12739	0.59020	0.71784	75.8154	77.41353	0.0206
F^{4+}	9	0.11297	0.51382	0.60636	112.1922	114.2428	0.0179
Ne^{5+}	10	0.10149	0.45511	0.52486	155.5373	157.93	0.0152
Na^{6+}	11	0.09213	0.40853	0.46272	205.8266	208.5	0.0128
Mg^{7+}	12	0.08435	0.37065	0.41379	263.0469	265.96	0.0110
Al^{8+}	13	0.07778	0.33923	0.37425	327.1901	330.13	0.0089
Si^{9+}	14	0.07216	0.31274	0.34164	398.2509	401.37	0.0078
P^{10+}	15	0.06730	0.29010	0.31427	476.2258	479.46	0.0067
S^{11+}	16	0.06306	0.27053	0.29097	561.1123	564.44	0.0059
Cl^{12+}	17	0.05932	0.25344	0.27090	652.9086	656.71	0.0058
Ar^{13+}	18	0.05599	0.23839	0.25343	751.6132	755.74	0.0055
K^{14+}	19	0.05302	0.22503	0.23808	857.2251	861.1	0.0045
Ca^{15+}	20	0.05035	0.21308	0.22448	969.7435	974	0.0044
Sc^{16+}	21	0.04794	0.20235	0.21236	1089.1678	1094	0.0044
Ti^{17+}	22	0.04574	0.19264	0.20148	1215.4975	1221	0.0045
V^{18+}	23	0.04374	0.18383	0.19167	1348.7321	1355	0.0046
Cr^{19+}	24	0.04191	0.17579	0.18277	1488.8713	1496	0.0048
Mn^{20+}	25	0.04022	0.16842	0.17466	1635.9148	1644	0.0049
Fe^{21+}	26	0.03867	0.16165	0.16724	1789.8624	1799	0.0051
Co^{22+}	27	0.03723	0.15540	0.16042	1950.7139	1962	0.0058
Ni^{23+}	28	0.03589	0.14961	0.15414	2118.4690	2131	0.0059
Cu^{24+}	29	0.03465	0.14424	0.14833	2293.1278	2308	0.0064

Ionization Energies for Some Six-Electron Atoms

6 e Atom	Z	r_1 (a_0)	r_3 (a_0)	r_6 (a_0)	Theoretical Ionization Energies (eV)	Experimental Ionization Energies (eV)	Relative Error
C	6	0.17113	0.84317	1.20654	11.27671	11.2603	-0.0015
N^{+}	7	0.14605	0.69385	0.90119	30.1950	29.6013	-0.0201
O^{2+}	8	0.12739	0.59020	0.74776	54.5863	54.9355	0.0064
F^{3+}	9	0.11297	0.51382	0.63032	86.3423	87.1398	0.0092
Ne^{4+}	10	0.10149	0.45511	0.54337	125.1986	126.21	0.0080
Na^{5+}	11	0.09213	0.40853	0.47720	171.0695	172.18	0.0064
Mg^{6+}	12	0.08435	0.37065	0.42534	223.9147	225.02	0.0049
Al^{7+}	13	0.07778	0.33923	0.38365	283.7121	284.66	0.0033
Si^{8+}	14	0.07216	0.31274	0.34942	350.4480	351.12	0.0019
P^{9+}	15	0.06730	0.29010	0.32081	424.1135	424.4	0.0007
S^{10+}	16	0.06306	0.27053	0.29654	504.7024	504.8	0.0002
Cl^{11+}	17	0.05932	0.25344	0.27570	592.2103	591.99	-0.0004
Ar^{12+}	18	0.05599	0.23839	0.25760	686.6340	686.1	-0.0008
K^{13+}	19	0.05302	0.22503	0.24174	787.9710	786.6	-0.0017
Ca^{14+}	20	0.05035	0.21308	0.22772	896.2196	894.5	-0.0019
Sc^{15+}	21	0.04794	0.20235	0.21524	1011.3782	1009	-0.0024
Ti^{16+}	22	0.04574	0.19264	0.20407	1133.4456	1131	-0.0022
V^{17+}	23	0.04374	0.18383	0.19400	1262.4210	1260	-0.0019
Cr^{18+}	24	0.04191	0.17579	0.18487	1398.3036	1396	-0.0017
Mn^{19+}	25	0.04022	0.16842	0.17657	1541.0927	1539	-0.0014
Fe^{20+}	26	0.03867	0.16165	0.16899	1690.7878	1689	-0.0011
Co^{21+}	27	0.03723	0.15540	0.16203	1847.3885	1846	-0.0008
Ni^{22+}	28	0.03589	0.14961	0.15562	2010.8944	2011	0.0001
Cu^{23+}	29	0.03465	0.14424	0.14970	2181.3053	2182	0.0003

Ionization Energies for Some Seven-Electron Atoms

7 e Atom	Z	r_1 (a_0)	r_3 (a_0)	r_7 (a_0)	Theoretical Ionization Energies (eV)	Experimental Ionization Energies (eV)	Relative Error
N	7	0.14605	0.69385	0.93084	14.61664	14.53414	-0.0057
O^{+}	8	0.12739	0.59020	0.78489	34.6694	35.1173	0.0128
F^{2+}	9	0.11297	0.51382	0.67084	60.8448	62.7084	0.0297
Ne^{3+}	10	0.10149	0.45511	0.57574	94.5279	97.12	0.0267
Na^{4+}	11	0.09213	0.40853	0.50250	135.3798	138.4	0.0218
Mg^{5+}	12	0.08435	0.37065	0.44539	183.2888	186.76	0.0186
Al^{6+}	13	0.07778	0.33923	0.39983	238.2017	241.76	0.0147
Si^{7+}	14	0.07216	0.31274	0.36271	300.0883	303.54	0.0114
P^{8+}	15	0.06730	0.29010	0.33191	368.9298	372.13	0.0086
S^{9+}	16	0.06306	0.27053	0.30595	444.7137	447.5	0.0062
Cl^{10+}	17	0.05932	0.25344	0.28376	527.4312	529.28	0.0035
Ar^{11+}	18	0.05599	0.23839	0.26459	617.0761	618.26	0.0019
K^{12+}	19	0.05302	0.22503	0.24785	713.6436	714.6	0.0013
Ca^{13+}	20	0.05035	0.21308	0.23311	817.1303	817.6	0.0006
Sc^{14+}	21	0.04794	0.20235	0.22003	927.5333	927.5	0.0000
Ti^{15+}	22	0.04574	0.19264	0.20835	1044.8504	1044	-0.0008
V^{16+}	23	0.04374	0.18383	0.19785	1169.0800	1168	-0.0009
Cr^{17+}	24	0.04191	0.17579	0.18836	1300.2206	1299	-0.0009
Mn^{18+}	25	0.04022	0.16842	0.17974	1438.2710	1437	-0.0009
Fe^{19+}	26	0.03867	0.16165	0.17187	1583.2303	1582	-0.0008
Co^{20+}	27	0.03723	0.15540	0.16467	1735.0978	1735	-0.0001
Ni^{21+}	28	0.03589	0.14961	0.15805	1893.8726	1894	0.0001
Cu^{22+}	29	0.03465	0.14424	0.15194	2059.5543	2060	0.0002

Ionization Energies for Some Eight-Electron Atoms

8 e Atom	Z	r_1 (a_0)	r_3 (a_0)	r_8 (a_0)	Theoretical Ionization Energies (eV)	Experimental Ionization Energies (eV)	Relative Error
O	8	0.12739	0.59020	1.00000	13.60580	13.6181	0.0009
F^{+}	9	0.11297	0.51382	0.7649	35.5773	34.9708	-0.0173
Ne^{2+}	10	0.10149	0.45511	0.6514	62.6611	63.45	0.0124
Na^{3+}	11	0.09213	0.40853	0.5592	97.3147	98.91	0.0161
Mg^{4+}	12	0.08435	0.37065	0.4887	139.1911	141.27	0.0147
Al^{5+}	13	0.07778	0.33923	0.4338	188.1652	190.49	0.0122
Si^{6+}	14	0.07216	0.31274	0.3901	244.1735	246.5	0.0094
P^{7+}	15	0.06730	0.29010	0.3543	307.1791	309.6	0.0078
S^{8+}	16	0.06306	0.27053	0.3247	377.1579	379.55	0.0063
Cl^{9+}	17	0.05932	0.25344	0.2996	454.0940	455.63	0.0034
Ar^{10+}	18	0.05599	0.23839	0.2782	537.9756	538.96	0.0018
K^{11+}	19	0.05302	0.22503	0.2597	628.7944	629.4	0.0010
Ca^{12+}	20	0.05035	0.21308	0.2434	726.5442	726.6	0.0001
Sc^{13+}	21	0.04794	0.20235	0.2292	831.2199	830.8	-0.0005
Ti^{14+}	22	0.04574	0.19264	0.2165	942.8179	941.9	-0.0010
V^{15+}	23	0.04374	0.18383	0.2051	1061.3351	1060	-0.0013
Cr^{16+}	24	0.04191	0.17579	0.1949	1186.7691	1185	-0.0015
Mn^{17+}	25	0.04022	0.16842	0.1857	1319.1179	1317	-0.0016
Fe^{18+}	26	0.03867	0.16165	0.1773	1458.3799	1456	-0.0016
Co^{19+}	27	0.03723	0.15540	0.1696	1604.5538	1603	-0.0010
Ni^{20+}	28	0.03589	0.14961	0.1626	1757.6383	1756	-0.0009
Cu^{21+}	29	0.03465	0.14424	0.1561	1917.6326	1916	-0.0009

Ionization Energies for Some Nine-Electron Atoms

9 e Atom	Z	r_1 (a_0)	r_3 (a_0)	r_9 (a_0)	Theoretical Ionization Energies (eV)	Experimental Ionization Energies (eV)	Relative Error
F	9	0.11297	0.51382	0.78069	17.42782	17.42282	-0.0003
Ne^{+}	10	0.10149	0.45511	0.64771	42.0121	40.96328	-0.0256
Na^{2+}	11	0.09213	0.40853	0.57282	71.2573	71.62	0.0051
Mg^{3+}	12	0.08435	0.37065	0.50274	108.2522	109.2655	0.0093
Al^{4+}	13	0.07778	0.33923	0.44595	152.5469	153.825	0.0083
Si^{5+}	14	0.07216	0.31274	0.40020	203.9865	205.27	0.0063
P^{6+}	15	0.06730	0.29010	0.36283	262.4940	263.57	0.0041
S^{7+}	16	0.06306	0.27053	0.33182	328.0238	328.75	0.0022
Cl^{8+}	17	0.05932	0.25344	0.30571	400.5466	400.06	-0.0012
Ar^{9+}	18	0.05599	0.23839	0.28343	480.0424	478.69	-0.0028
K^{10+}	19	0.05302	0.22503	0.26419	566.4968	564.7	-0.0032
Ca^{11+}	20	0.05035	0.21308	0.24742	659.8992	657.2	-0.0041
Sc^{12+}	21	0.04794	0.20235	0.23266	760.2415	756.7	-0.0047
Ti^{13+}	22	0.04574	0.19264	0.21957	867.5176	863.1	-0.0051
V^{14+}	23	0.04374	0.18383	0.20789	981.7224	976	-0.0059
Cr^{15+}	24	0.04191	0.17579	0.19739	1102.8523	1097	-0.0053
Mn^{16+}	25	0.04022	0.16842	0.18791	1230.9038	1224	-0.0056
Fe^{17+}	26	0.03867	0.16165	0.17930	1365.8746	1358	-0.0058
Co^{18+}	27	0.03723	0.15540	0.17145	1507.7624	1504.6	-0.0021
Ni^{19+}	28	0.03589	0.14961	0.16427	1656.5654	1648	-0.0052
Cu^{20+}	29	0.03465	0.14424	0.15766	1812.2821	1804	-0.0046

Ionization Energies for Some Ten-Electron Atoms

10 e Atom	Z	r_1 (a_0)	r_3 (a_0)	r_{10} (a_0)	Theoretical Ionization Energies (eV)	Experimental Ionization Energies (eV)	Relative Error
Ne	10	0.10149	0.45511	0.63659	21.37296	21.56454	0.00888
Na^{+}	11	0.09213	0.40853	0.560945	48.5103	47.2864	-0.0259
Mg^{2+}	12	0.08435	0.37065	0.510568	79.9451	80.1437	0.0025
Al^{3+}	13	0.07778	0.33923	0.456203	119.2960	119.992	0.0058
Si^{4+}	14	0.07216	0.31274	0.409776	166.0150	166.767	0.0045
P^{5+}	15	0.06730	0.29010	0.371201	219.9211	220.421	0.0023
S^{6+}	16	0.06306	0.27053	0.339025	280.9252	280.948	0.0001
Cl^{7+}	17	0.05932	0.25344	0.311903	348.9750	348.28	-0.0020
Ar^{8+}	18	0.05599	0.23839	0.288778	424.0365	422.45	-0.0038
K^{9+}	19	0.05302	0.22503	0.268844	506.0861	503.8	-0.0045
Ca^{10+}	20	0.05035	0.21308	0.251491	595.1070	591.9	-0.0054
Sc^{11+}	21	0.04794	0.20235	0.236251	691.0866	687.36	-0.0054
Ti^{12+}	22	0.04574	0.19264	0.222761	794.0151	787.84	-0.0078
V^{13+}	23	0.04374	0.18383	0.210736	903.8853	896	-0.0088
Cr^{14+}	24	0.04191	0.17579	0.19995	1020.6910	1010.6	-0.0100
Mn^{15+}	25	0.04022	0.16842	0.19022	1144.4276	1134.7	-0.0086
Fe^{16+}	26	0.03867	0.16165	0.181398	1275.0911	1266	-0.0072
Co^{17+}	27	0.03723	0.15540	0.173362	1412.6783	1397.2	-0.0111
Ni^{18+}	28	0.03589	0.14961	0.166011	1557.1867	1541	-0.0105
Cu^{19+}	29	0.03465	0.14424	0.159261	1708.6139	1697	-0.0068
Zn^{20+}	30	0.03349	0.13925	0.153041	1866.9581	1856	-0.0059

Proton and Neutron

The proton and neutron each comprise three charged fundamental particles called quarks and three massive photons called gluons.

Proton Parameters

$$\lambda_{C,p} = \lambda\!\!\!^{-}_{c,q} = \frac{2\pi a_o m_e}{\alpha^{-1} m_P} = 1.3\ X\ 10^{-15}\ m = r_p = r_q$$

$$m_P = m_q + m_g^{"} = m_q^{"}$$

$$m_q = \frac{m_P}{2\pi}$$

$$m_q^{"} = 2\pi m_q = 2\pi X \frac{m_P}{2\pi} = m_P$$

$$m_g^{"} = m_P - m_q = m_P\left[1 - \frac{1}{2\pi}\right]$$

$$E = m_q c^2 + m_g c^2 = \frac{m_p}{2\pi} c^2 + m_P\left[1 - \frac{1}{2\pi}\right]c^2 = m_P c^2$$

m_P proton rest mass

$\lambda_{C,p}$ is the Compton wavelength of the proton

$\lambda\!\!\!^{-}_{c,q}$ is the Compton wavelength bar of the quarks

r_p is the radius of the proton

r_q is the radius of the quarks

m_q is the rest mass of the quarks

$m_g^{"}$ is the relativistic mass of the gluons

$m_q^{"}$ is the relativistic mass of the quarks

Proton and Neutron cont'd

Neutron Parameters

$$\lambda_{C,n} = \lambda\!\!\!^{-}_{c,q} = \frac{2\pi a_o m_e}{\alpha^{-1} m_N} = 1.3214\ X\ 10^{-15}\ m = r_n = r_q$$

$$m_N = m_q + m_g^{"} = m_q^{"}$$

$$m_q = \frac{m_N}{2\pi}$$

$$m_q^{"} = 2\pi m_q = 2\pi X \frac{m_N}{2\pi} = m_N$$

$$m_g^{"} = m_N - m_q = m_N\left\lfloor 1 - \frac{1}{2\pi}\right\rfloor$$

$$E = m_q c^2 + m_g c^2 = \frac{m_N}{2\pi} c^2 + m_N\left\lfloor 1 - \frac{1}{2\pi}\right\rfloor c^2 = m_N c^2$$

m_N neutron rest mass

$\lambda\!\!\!^{-}_{c,p}$ is the Compton wavelength of the neutron

$\lambda\!\!\!^{-}_{c,q}$ is the Compton wavelength bar of the quarks

r_n is the radius of the neutron

r_q is the radius of the quarks

m_q is the rest mass of the quarks

$m_g^{"}$ is the relativistic mass of the gluons

$m_q^{"}$ is the relativistic mass of the quarks

Quark and Gluon Functions of the Proton

The proton functions can be viewed as a linear combination of three fundamental particles, three quarks, of charge $+\frac{2}{3}e$, $+\frac{2}{3}e$, and $-\frac{1}{3}e$. Each quark is associated with its gluon where the quark mass/charge function has the same angular dependence as the gluon mass/charge function.

The quark mass function of a proton is

$$\frac{m_P}{2\pi}\left\lfloor \frac{1}{3}(1+\sin\theta\sin\phi)+\frac{1}{3}(1+\sin\theta\cos\phi)+\frac{1}{3}(1+\cos\theta)\right\rfloor \delta(r-\lambda_{C,p})$$

The charge function of the quarks of a proton is

$$e\left\lfloor \frac{2}{3}(1+\sin\theta\sin\phi)+\frac{2}{3}(1+\sin\theta\cos\phi)-\frac{1}{3}(1+\cos\theta)\right\rfloor \delta(r-\lambda_{C,p})$$

The radial electric field of a proton is

$$E_r=\frac{-\alpha^{-1}e}{4\pi\varepsilon_o r^3}\frac{2\pi a_o}{\frac{m_N}{m_e}\alpha^{-1}}\left\lfloor \frac{3}{2}(1+\sin\theta\sin\phi)+\frac{3}{2}(1+\sin\theta\cos\phi)-3(1+\cos\theta)\right\rfloor \delta(r-\lambda_{C,p})$$

Quark and Gluon Functions of the Proton Cont…

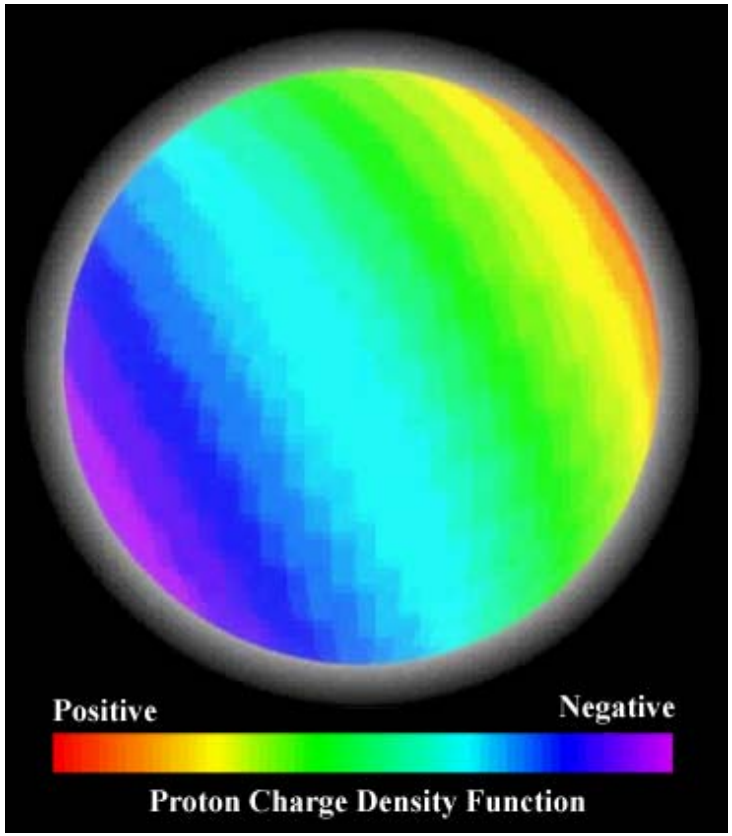

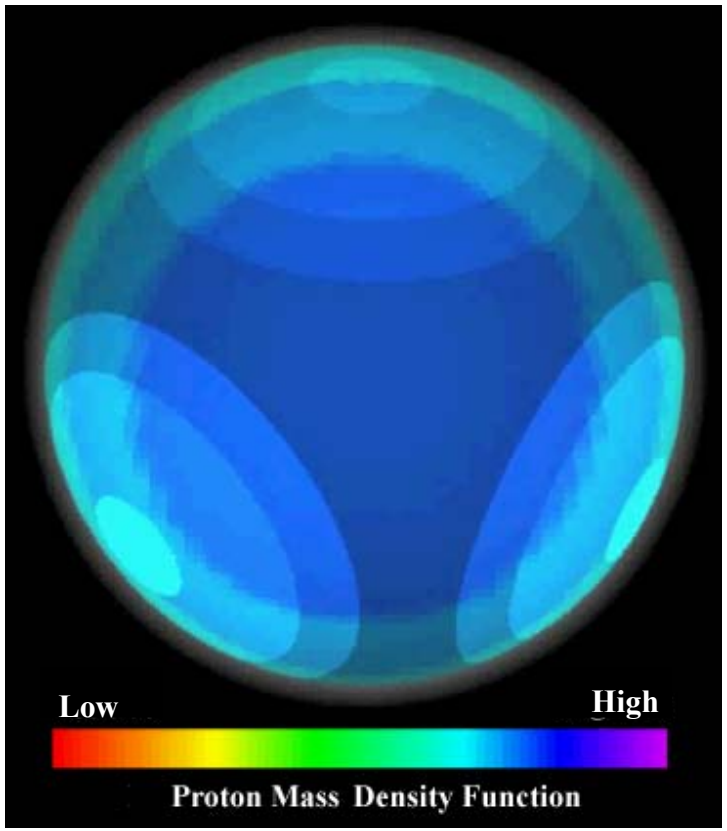

Quark and Gluon Functions of the Neutron

The neutron functions can be viewed as a linear combination of three fundamental particles, three quarks, of charge $+\frac{2}{3}e$, $-\frac{1}{3}e$, and $-\frac{1}{3}e$. Each quark is associated with its gluon where the quark mass/charge function has the same angular dependence as the gluon mass/charge function.

The quark mass function of a neutron is

$$\frac{m_N}{2\pi}\left[\frac{1}{3}(1+\sin\theta\sin\phi)+\frac{1}{3}(1+\sin\theta\cos\phi)+\frac{1}{3}(1+\cos\theta)\right]\delta(r-\lambda_{C,n})$$

The charge function of the quarks of a neutron is

$$e\left[\frac{2}{3}(1+\sin\theta\sin\phi)-\frac{1}{3}(1+\sin\theta\cos\phi)-\frac{1}{3}(1+\cos\theta)\right]\delta(r-\lambda_{C,n})$$

The radial electric field of a neutron is

$$E_r=\frac{-\alpha^{-1}e}{4\pi\varepsilon_o r^3}\frac{2\pi a_o}{\frac{m_N}{m_e}\alpha^{-1}}\left[\frac{3}{2}(1+\sin\theta\sin\phi)-3(1+\sin\theta\cos\phi)-3(1+\cos\theta)\right]\delta(r-\lambda_{C,n})$$

Quark and Gluon Functions of the Neutron Cont…

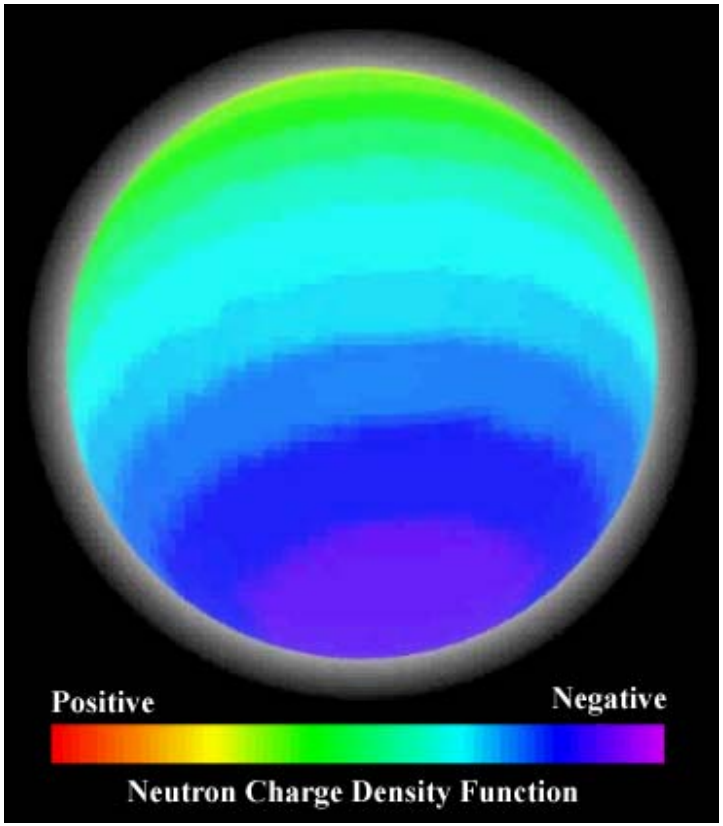

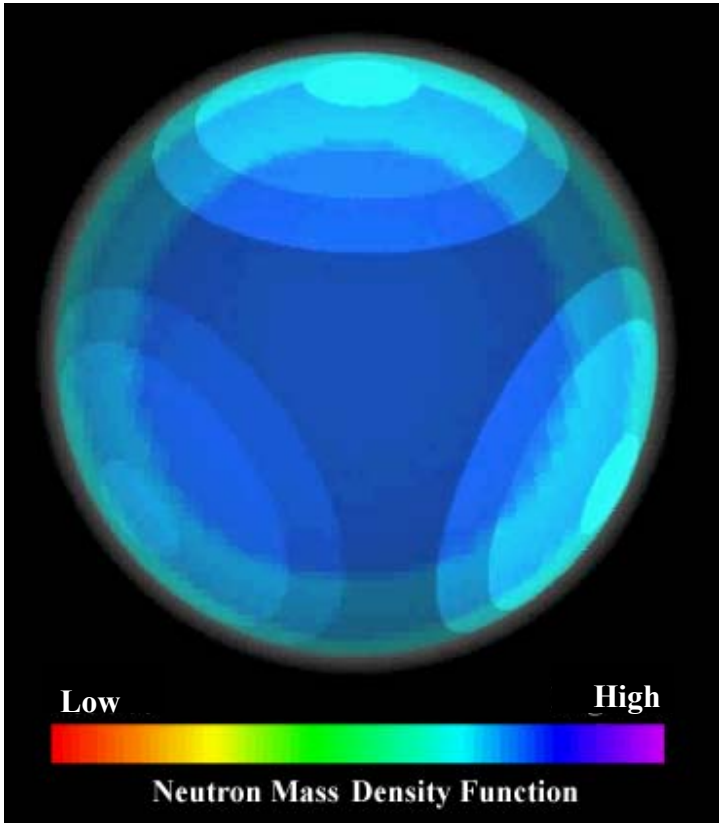

Magnetic Moments

Proton Magnetic Moment

$$\mu = \frac{\text{charge} \times \text{angular momentum}}{2 \times \text{mass}}$$

$$\mu_{proton} = \frac{\frac{2}{3} e \frac{2}{3} \hbar}{2 \frac{m_P}{2\pi}} = \frac{4}{9} 2\pi \frac{e\hbar}{2m_P} = 2.79253 \mu_N$$

where μ_N is the nuclear magneton $\frac{e\hbar}{2m_P}$

The experimental magnetic moment of the proton is 2.79268 μ_N

Neutron Magnetic Moment

The magnetic moment of the neutron, μ_n , is

$$\mu_n = \left[1 - \frac{4}{9} 2\pi - \frac{3}{25} \right] \mu_N = -1.91253 \mu_N$$

The experimental magnetic moment of the neutron is –1.91315 μ_n

The Weak Nuclear Force: Beta Decay of the Neutron

The nuclear reaction for the beta decay of a neutron is

$$^1n \rightarrow {}^1H + \beta + \bar{\nu}_e + 0.7824 MeV$$

where $\bar{\nu}_e$ is the electron antineutrino. The energy terms of the beta decay are

$$E_{mag} = m_p c^2 \frac{\alpha}{2\pi} = 1.089727 \times 10^6 \; eV \qquad E_{mag}(gluon) = \left[\frac{3}{25}\right]^2 E_{mag} = 1.569207 \times 10^4 \; eV$$

$$E_{ele} = \frac{e^2}{8\pi\varepsilon_o \lambda_{C,n}} = 5.456145 \times 10^5 \; eV \qquad E_\nu\left(\lambda_{C,n}, \lambda_{C,p}\right) = \frac{e^2}{4\pi\varepsilon_o}\left(\frac{1}{\lambda_{C,n}} - \frac{1}{\lambda_{C,p}}\right) = 1502.2 \, eV$$

$$T = \frac{1}{2} m v^2 = \frac{1}{2} \frac{m_e \hbar^2}{\left[\frac{m_N}{2\pi}\right]^2 \left(\frac{2\pi a_o m_e}{\alpha^{-1} m_N}\right)^2} = \frac{1}{2} m_e \left(\frac{\hbar}{m_e \lambda\!\!\!^{-}_C}\right)^2$$

$$= \frac{1}{2} m_e c^2 = 2.555017 \times 10^5 \; eV$$

The beta decay energy is

$$E_\beta = E_{mag} - E_{mag}(gluon) - E_{ele} - E_\nu\left(\lambda_{C,n}, \lambda_{C,p}\right) + T$$

$$E_\beta = 0.7824 \, MeV$$